

**Forebrain Acetylcholine in Action:
Dynamic Activities and Modulation on Target Areas**

by

Hao Zhang

Department of Neurobiology
Duke University

Date: _____

Approved:

Miguel A.L. Nicolelis, Supervisor

Sidney A. Simon, Dissertation Committee Chair

Dona M. Chikaraishi

Erich D. Jarvis

Warren H. Meck

Dissertation submitted in partial fulfillment of
the requirements for the degree of Doctor
of Philosophy in the Department of
Neurobiology in the Graduate School
of Duke University

2009

ABSTRACT

**Forebrain Acetylcholine in Action:
Dynamic Activities and Modulation on Target Areas**

by

Hao Zhang

Department of Neurobiology
Duke University

Date: _____

Approved:

Miguel A.L. Nicolelis, Supervisor

Sidney A. Simon, Dissertation Committee Chair

Dona M. Chikaraishi

Erich D. Jarvis

Warren H. Meck

An abstract of a dissertation submitted in partial
fulfillment of the requirements for the degree
of Doctor in the Department of
Neurobiology in the Graduate School
of Duke University

2009

Copyright by
Hao Zhang
2009

Abstract

Forebrain cholinergic projection systems innervate the entire cortex and hippocampus. These cholinergic systems are involved in a wide range of cognitive and behavioral functions, including learning and memory, attention, and sleep-waking modulation. However, the *in vivo* physiological mechanisms of cholinergic functions, particularly their fast dynamics and the consequent modulation on the hippocampus and cortex, are not well understood. In this dissertation, I investigated these issues using a number of convergent approaches.

First, to study fast acetylcholine (ACh) dynamics and its interaction with field potential theta oscillations, I developed a novel technique to acquire second-by-second electrophysiological and neurochemical information simultaneously with amperometry. Using this technique on anesthetized rats, I discovered for the first time the tight *in vivo* coupling between phasic ACh release and theta oscillations on fine spatiotemporal scales. In addition, with electrophysiological recording, putative cholinergic neurons in medial septal area (MS) were found with firing rate dynamics matching the phasic ACh release.

Second, to further elucidate the dynamic activities and physiological functions of cholinergic neurons, putative cholinergic MS neurons were identified in behaving rats. These neurons had much higher firing rates during rapid-eye-movement (REM) sleep, and brief responses to auditory stimuli. Interestingly, their firing promoted theta/gamma oscillations, or small-amplitude irregular activities (SIA) in a state-dependent manner. These results suggest that putative MS cholinergic neurons may be a generalized hippocampal activation/arousal network.

Third, I investigated the hypothesis that ACh enhances cortical and hippocampal immediate-early gene (IEG) expression induced by novel sensory experience. Cholinergic transmission was manipulated with pharmacology or lesion. The resultant cholinergic impairment suppressed the induction of *arc*, a representative IEG, suggesting that ACh promotes IEG induction.

In conclusion, my results have revealed that the firing of putative cholinergic neurons promotes hippocampal activation, and the consequent phasic ACh release is tightly coupled to theta oscillations. These fast cholinergic activities may provide exceptional opportunities to dynamically modulate neural activity and plasticity on much finer temporal scales than traditionally assumed. By the subsequent promotion of IEG induction, ACh may further substantiate its function in neural plasticity and memory consolidation.

To my late loving grandparents:

ZHANG, Meng-Bai,

GU, Nian-Chun,

XU, Jin-Xian

And

RU, Zheng-Wei.

Contents

Abstract	iv
List of Figures	xiv
List of Abbreviations	xvi
Acknowledgements	xviii
Chapter 1 Introduction	1
1.1 Overview	1
1.2 Acetylcholine as a neurotransmitter	2
1.2.1 ACh discovery and metabolism in central nervous system.....	2
1.2.2 Mode of transmission	3
1.2.3 Cholinergic receptors.....	3
1.3 Forebrain cholinergic projection systems.....	4
1.3.1 MSvDB - septohippocampal projection	5
1.3.2 Basal forebrain – basalocortical projection	6
1.4 Functions of forebrain cholinergic systems	7
1.4.1 Cognitive and behavioral functions: attention, learning and memory	7
1.4.2 Potential mechanisms of cholinergic functions.....	8
1.4.2.1 Dynamic regulation of acetylcholine release.....	9
1.4.2.2 Selective enhancement of neuronal pathways	10
1.4.2.3 Interaction with theta oscillations	10
1.4.2.4 Promoting neural plasticity.....	12

1.5	Overarching questions: what are the properties of fast dynamics of cholinergic activities <i>in vivo</i> , and how do they interact with and influence the activities in their target areas?.....	13
1.6	Methodological considerations in cholinergic studies	14
1.6.1	Pharmacological and lesion studies.....	15
1.6.2	Chemical measurement of acetylcholine	16
1.6.3	Recording from cholinergic neurons <i>in vivo</i>	17
Chapter 2	Fine spatiotemporal coupling between hippocampal acetylcholine release and theta oscillations <i>in vivo</i>	23
2.1	Introduction.....	23
2.1.1	Interaction between acetylcholine and theta oscillations	23
2.1.2	Simultaneous acquisition of fast dynamics of neurochemicals and LFP information.....	25
2.2	Material and methods	27
2.2.1	Animals.....	27
2.2.2	Chemicals and drugs	27
2.2.3	Amperometric probes and choline sensor preparation	27
2.2.4	Simultaneous <i>in vivo</i> recording in urethane-anesthetized rats	29
2.2.4.1	Simultaneous acquisition using both amperometry and electrophysiology.....	29
2.2.4.2	Tail-pinch.....	30
2.2.4.3	MS Carbachol injection.....	30
2.2.4.4	Theta depth profile.....	30

2.2.4.5	Recording choline concentration and LFP theta information with amperometry alone.....	31
2.2.5	Single unit recording in anesthetized rats.....	31
2.2.6	Surgery and <i>in vivo</i> recordings in freely-moving rats.....	32
2.2.6.1	Sleep/wake recordings.....	32
2.2.6.2	Amphetamine injection.....	33
2.2.7	Data Analyses.....	33
2.2.7.1	Pre-processing of simultaneous amperometric and LFP signals.....	33
2.2.7.2	HFC calculation, amperometric HFC amplitude and oxidation current.	33
2.2.7.3	Spectral analysis.....	34
2.2.7.4	Theta depth profile in HFC.....	35
2.2.7.5	Acquiring theta information in amperometry HFC.....	35
2.2.7.6	Choline signals and noise reduction.....	36
2.2.7.7	Estimation of choline or theta rising time.....	37
2.2.7.8	Single unit activities.....	37
2.3	Results.....	38
2.3.1	Technical advancement –simultaneous acquisition of electrophysiological and neurochemical information.....	38
2.3.1.1	Implementation of simultaneous electrophysiology and amperometry – similarity between LFP and amperometric signals.....	38
2.3.1.2	Acquiring local field potential information from amperometric neurochemical recordings.....	40
2.3.2	Fine-scale acetylcholine release coupled to theta oscillation.....	44

2.3.2.1	Choline increase coupled to theta oscillations on the time scale of tens of seconds.....	44
2.3.2.2	Maximal choline increase around CA1 pyramidal layer	45
2.3.3	Phasic acetylcholine release lagging theta initiation.....	46
2.3.3.1	Choline increase slower than theta initiation	46
2.3.3.2	Activities of a subpopulation of low-frequency neurons in medial septal area matching the slow choline increase.....	47
2.4	Conclusion	49
2.5	Discussion.....	50
2.5.1	Acetylcholine and theta oscillations	50
2.5.2	Temporally- and spatially-refined ACh action	52
2.5.3	Putative cholinergic neurons in MSvDB recorded from anesthetized rats... 54	
Chapter 3	Putative medial septal cholinergic neurons promote hippocampal arousal and theta oscillations	79
3.1	Introduction.....	79
3.2	Material and methods	81
3.2.1	Electrodes, animals and surgery	81
3.2.2	Behavior task, auditory stimuli and electrophysiological recording.....	83
3.2.2.1	Undisturbed sleep-waking.....	83
3.2.2.2	Behavioral task and auditory stimuli	83
3.2.2.3	Electrophysiological recording	84
3.2.3	Data analysis.....	84
3.2.3.1	Single unit isolation (spike sorting)	84

3.2.3.2	Sleep-waking analysis and SIA definition	84
3.2.3.3	Firing property indices for individual neurons	85
3.2.3.4	Spectral analysis.....	86
3.2.3.5	Theta related analysis	87
3.3	Results	87
3.3.1	Slow-firing ¹ neurons often have higher firing rate in REM sleep	87
3.3.2	Some slow-firing neurons have transient auditory responses	88
3.3.3	Activities of REM+/Aud+ neurons coupled to SIA epochs in SW sleep.....	89
3.3.4	A distinctive population of MSvDB neurons bearing all three firing properties - putative cholinergic neurons.....	90
3.3.5	Putative MSvDB cholinergic neurons promote hippocampal activation in a state-dependent manner.....	91
3.3.6	Putative MSvDB cholinergic neurons are not rhythmic-firing, and have mild phase-locking to theta oscillations	92
3.4	Conclusion	92
3.5	Discussion.....	93
3.5.1	Evidence that support the putative cholinergic neuron hypothesis	93
3.5.2	A distinctive subpopulation of neurons in MSvDB	95
3.5.3	New insights on the function of MSvDB cholinergic neurons.	96
Chapter 4	Cholinergic modulation promotes immediate-early-gene upregulation induced by novel sensory experience: implication for learning and memory	115
4.1	Introduction.....	115
4.2	Material and methods.....	117

4.2.1	Chemicals and materials	117
4.2.2	Novel enriched environment exploration and drug treatment in mice	117
4.2.3	Immunolesion of rats and novel enriched environment	119
4.2.4	<i>In situ</i> hybridization and immunohistochemistry	119
4.3	Results	121
4.3.1	Novel sensory experience induced <i>arc</i> upregulation in both somatosensory cortex and hippocampus	121
4.3.2	Central but not peripheral scopolamine suppressed <i>arc</i> induction	122
4.3.3	Specific lesion of basal forebrain cholinergic neurons constrains <i>arc</i> induction in somatosensory cortex	123
4.4	Conclusion	124
4.5	Discussion	125
4.5.1	Site of action: direct (local) or indirect?	125
4.5.2	Intracellular mechanism of local cholinergic modulation on <i>arc</i> expression 128	
4.5.3	Molecular mechanism underlying cholinergic modulation of neural plasticity <i>in vivo</i> : implications for learning and memory	129
Chapter 5	General discussions.....	139
5.1	Conclusions	139
5.2	Cholinergic neurons in the medial septal area	141
5.3	Acetylcholine and theta oscillations	142
5.4	The role of acetylcholine in learning and memory functions.....	142
5.4.1	Enhancement but not required?	142

5.4.2	Acetylcholine and sleep-dependent memory consolidation.....	144
5.5	Forebrain acetylcholine functioning and common theme of the functioning of neuromodulatory systems.....	145
5.5.1	Cholinergic modulation of plasticity.....	145
5.5.2	A global network.....	146
5.5.3	Comparison to other neuromodulatory systems.....	147
5.6	A novel neurophysiology method and its potential applications	148
5.6.1	A hidden property of voltammetry method never describe before.....	148
5.6.2	Further improvements to use amperometry HFC as an LFP substitute	149
5.6.3	Separating chemical signals from electrical signals and the validity of chemical information obtained from amperometry	151
5.6.4	Potential applications	154
5.7	Limitation and Future directions	155
5.7.1	Choline measurement in free-moving animals.....	155
5.7.2	Chemical identity of neurons recorded <i>in vivo</i>	157
5.7.3	General future directions	158
	References	159
	Biography.....	185

List of Figures

Figure 1. Acetylcholine synthesis, release and metabolism.....	20
Figure 2. Cholinergic systems in the brain.	22
Figure 3. Simultaneous recording with amperometry and electrophysiology.	58
Figure 4. Simultaneous recordings reveal similarity between high frequency LFP and amperometric signals (>1Hz).	60
Figure 5. Similar spectral information can be obtained from either LFP or high frequency amperometric signals.	62
Figure 6. Physiological and pharmacologically-induced frequency signatures preserved in amperometry HFC signals recorded in free-moving rats.....	64
Figure 7. Amperometry HFC not affected by sensor modifications intended for neurochemical detection.	66
Figure 8. Noise reduction and LOD improvement for <i>in vivo</i> amperometric signals, and sensor response time <i>in vitro</i>	68
Figure 9. Phasic choline increase coupled to theta oscillations induced by tail pinch.....	70
Figure 10. Phasic choline increase coupled to spontaneous theta oscillations.....	72
Figure 11. Maximal phasic choline increase observed around CA1 pyramidal layer.....	74
Figure 12. Phasic choline increase often lags theta initiation.....	76
Figure 13. A subpopulation of low-frequency MSvDB neurons has slow firing rate increase matching the slow choline increase.	78
Figure 14. Recording site and neuronal spike sorting	100
Figure 15. Slow-firing neurons often have higher firing rate in REM sleep.....	102
Figure 16. Many slow-firing neurons have transient auditory responses.	104
Figure 17. Activities of REM+/Aud+ neurons coupled to SIA epochs in SW sleep.	106

Figure 18. Putative cholinergic neurons are distinctive from other neurons.	108
Figure 19. Putative cholinergic neurons promote hippocampal activation (example)...	110
Figure 20. Putative cholinergic neurons promote hippocampal activation (population).	112
Figure 21. Firing properties of putative cholinergic neurons	114
Figure 22. Schematics of mice experiments with pharmacology	132
Figure 23. Novel sensory experience induces <i>arc</i> upregulation in both somatosensory cortex and hippocampus.....	134
Figure 24. Central but not peripheral scopolamine suppresses <i>arc</i> induction.	136
Figure 25. Specific lesion of basal forebrain cholinergic neurons constrains <i>arc</i> induction in ipsilateral somatosensory cortex.	138

List of Abbreviations

ACh	acetylcholine
BF	basal forebrain area
CA1	cornus ammonis 1 of hippocampus
CA3	cornus ammonis 3 of hippocampus
ChAT	choline acetyltransferase
DG	dentate gyrus
ERK	extracellular regulated protein kinase
GABA	gamma-aminobutyric acid
HDB	the horizontal limb of the diagonal band of Broca
HFC	high frequency component
IEG	immediate-early gene
LDT	laterodorsal tagmental nucleus
LFP	local field potential
LTP	long-term potentiation
LIA	large-amplitude irregular activity
MCPO	magnocellular preoptic nucleus
MS	medial septum
MSvDB	medial septum and the vertical limb of the diagonal band of Broca
NBM	nucleus basalis magnocellularis
NGF	nerve growth factor
PPT	pedunculopontine tegmental nucleus
REM	rapid-eye-movement

S1BF	primary somatosensory cortex, barrel field
S2	secondary somatosensory cortex
SI	substantia innominata
SIA	small-amplitude irregular activity
SW	slow-wave
vAChT	vesicular acetylcholine transporter

Acknowledgements

This work would not have been possible without the guidance, support and help from many important people during the six years of my graduate life.

First of all, I own my sincere and deepest gratitude to Miguel, who has encouraged, inspired and guided me in my research, who has supported me even during the hard times, and who has created a wonderful lab and let me explore various directions. I would like to say special thanks to my committee members, Sid, Dona, Erich and Warren, who have been through the ups and downs of my research with me, and given me tremendous help in my studies. Many thanks to Sidarta Ribeiro, who brought me to the Nicolelis Lab, and mentored me in the first two years of my research here. Your enthusiasm has always been very encouraging. Many thanks to Shih-Chieh Lin, who mentored me in the last few years, explored a lot of possibilities with me, and guided me in various aspects of neuroscience research. I am also indebted to Gary Lehew and Jim Meloy, two wonderful colleagues who has given me tremendous technical support and built powerful electrodes for me, and to Laura, Susan, Gayle and Terry for all the administrative assistance.

I deeply appreciate all the help and intellectual inspirations from all the friends and colleagues in Nicolelis Lab, as well as those from other labs in the department, especially the Jarvis Lab, Hall Lab and Feng Lab, who I have bothered a lot. Particularly, I'd like to thank Yangzhong Huang, who mentored me in my first rotation, and continued to guide me in my graduate life.

Most importantly, I want to thank my parents, the most loving parents in the world. I feel really sorry that I have been away for these years. When I was studying, you

endured my absence; when I had to have back surgery, you took me back and cared for me with all the love till I recovered and left again. Your love supports me through all my life.

Chapter 1 Introduction

1.1 Overview

In this dissertation, I will focus on the forebrain cholinergic projection systems. Most of my studies were carried out in the septohippocampal system, and part of the studies in the last part also included the basalocortical system.

In the introduction (Chapter 1), I will briefly review acetylcholine (ACh), the cholinergic systems and the current understanding of their functions. I will then raise the overarching question of my dissertation: what are the properties of fast dynamics of cholinergic activities *in vivo*, and how do they interact with and influence the activities in their target areas. These issues on *in vivo* cholinergic mechanisms have rarely been studied, largely limited by experimental techniques. I will also briefly comment on the traditional approaches and their limitations, and introduce the approaches I used in my studies to investigate these issues.

In Chapters 2-4, I will present three studies that addressed the following detailed questions: 1) whether and how fast ACh dynamics interact with theta oscillations in the hippocampus; 2) how putative cholinergic neurons behave and what is the consequent impact on hippocampal activity; 3) whether ACh modulates immediate-early gene (IEG) upregulation induced by novel sensory experience. Almost all the experiments and analysis were carried out by myself, with initial guidance and help from Shih-Chieh Lin and Sidarta Ribeiro. Dr. Erich Jarvis and his colleagues kindly taught me the *in situ* hybridization and immunostaining techniques, and let me do some of those experiments in Jarvis Lab. Jin Young “Jimmy” Kim assisted in some of the histology,

immunohistochemistry and the blind data quantification for *arc* expression. Part of the results in Chapter 2 and discussion in section 5.6 (acquiring LFP information from amperometric neurochemical recording) have been published (Zhang, Lin et al. 2009).

In Chapter 5, I will discuss in general what my findings contribute to the current understanding of cholinergic function and the mechanisms underlying these functions. In addition, I will discuss the general application of the novel neurophysiology methods I developed in Chapter 2. In the end, I will point out the limitation of my studies and potential follow-up research directions.

1.2 Acetylcholine as a neurotransmitter

1.2.1 ACh discovery and metabolism in central nervous system.

Acetylcholine is the first neurotransmitter discovered in the nervous system, discovered by Otto Loewi in 1921 (Nicholls and Fuchs 2001). Although it was discovered as a universal neurotransmitter in the peripheral nervous system, being used at the neuromuscular junction to cause muscle contraction, it was later discovered to exist in central nervous system (CNS) as well.

In the central nervous system, neurons communicate with each other using a variety of transmitters, such as glutamate, GABA, etc. The neurons that specifically produce and use acetylcholine as a transmitter are referred to as cholinergic neurons. In these neurons, acetylcholine is produced by a specific enzyme, choline acetyltransferase (ChAT), which transfers the acetyl group from acetyl coenzyme A (AcCoA) to choline to make ACh molecules (Figure 1). After ACh molecules are made, they are loaded into the (presynaptic) vesicles of cholinergic neurons, by an enzyme called vesicular acetylcholine transferase (vAChT). Upon excitation, cholinergic neurons

fire action potentials and the ACh molecules are released. Once outside the neuron, ACh will bind to their receptors to produce consequent actions. The unbounded ACh molecules will soon be degraded by an enzyme called acetylcholine esterase (AChE), and turn into choline and acetate. Choline will be re-uptaken by specific transporters on cholinergic neurons to be reused to make ACh (Figure 1). Besides being reused, choline is also provided from diet (Lockman and Allen 2002).

1.2.2 Mode of transmission

The axons of cholinergic neurons do not make a lot of synaptic contacts in their target areas. In CA1 area of the hippocampus, only 7% of cholinergic axon terminals make synaptic contacts with postsynaptic neurons. In cortex, the ratio is about 14% (Descarries 1998). As a result, the mode of forebrain cholinergic transmission is generally considered as volume transmission, but not wired, synaptic transmission (Descarries 1998). The effect of ACh is considered mostly modulatory, affecting specific information conveyed by other neurotransmitters.

1.2.3 Cholinergic receptors

There are various types of receptors that ACh acts on. Two general categories, nicotinic and muscarinic receptors, are defined based on their structure and the functional consequence after receptor activation (Purves, Augustine et al. 2004).

Nicotinic receptors are ionotropic receptors, which open an ion channel upon receptor activation, with nicotine as a typical agonist. Each receptor protein is composed of 5 subunits, which form the ion channel (Gotti and Clementi 2004). Neuronal nicotinic

receptors are involved in a wide range of physiological functions, and are the target of nicotine, the most widespread substance of abuse.

Muscarinic receptors are metabotropic receptors whose activation leads to activation of receptor-coupled G proteins, which further activates second messengers and signaling pathways (Purves, Augustine et al. 2004). Muscarinic receptors have 5 major subtypes, M1-M5. M1, M3 and M5 are associated with G_q proteins, while M2 and M4 are associated with $G_{i/o}$ proteins. M1, M3 and M5 are often found on target neurons (post-synaptic), while M2 are often considered as an autoreceptor that exist on the presynaptic terminals of cholinergic neurons to regulate ACh release (Lanzafame, Christopoulos et al. 2003). The distribution and functions of individual subtypes have been studied with specific agonists/antagonists, and receptor knock-out mice (Volpicelli and Levey 2004; Wess 2004).

1.3 Forebrain cholinergic projection systems

Cholinergic systems, or major nuclei containing cholinergic neurons, are distributed along the rostral-caudal axis of the central nervous system. They are usually projection nuclei that send out cholinergic projections to innervate other brain areas, including other cholinergic nuclei (Woolf 1991). For example, cholinergic neurons in the brainstem, specifically, pedunculopontine tegmental (PPT) and laterodorsal tegmental (LDT) nuclei, project mainly to the thalamus, and also to the basal forebrain nuclei, and are generally considered to be an essential component of the arousal system (Woolf 1991). There are also local cholinergic interneurons, such as the ones in striatum and the insular cortex (Woolf 1991).

In my studies, I focused on the cholinergic projection systems in the forebrain, since these cholinergic systems are involved more in cognitive processes than the other ones (discussed in section 1.4). These subcortical nuclei form a seemingly rostral-caudal continuum, and project to the cortical mantle and some subcortical structures (Figure 2). At the rostral end is the medial septum and the vertical limb of the diagonal band of Broca (MSvDB); the horizontal limb of the diagonal band of Broca (HDB) sits in the middle of this continuum; at the caudal end resides substantia innominata (SI), magnocellular preoptic nucleus (MCPO) and nucleus basalis magnocellularis (NBM), which are generally referred to as the basal forebrain (BF) areas. Some authors refer to the whole continuum from MSvDB to the caudal nuclei as basal forebrain. Here I will use BF areas as specifically the caudal nuclei, which project to the entire neocortical mantle (Woolf 1991).

1.3.1 MSvDB - septohippocampal projection

Cholinergic neurons in MSvDB project to hippocampus, subicular, cingulate, retrosplenial, and entorhinal cortices (Woolf 1991). Except for some local cholinergic interneurons whose existence in hippocampus is still controversial, MSvDB is the sole source of ACh in the hippocampus (Lewis, Shute et al. 1967; Mesulam, Mufson et al. 1983; Dutar, Bassant et al. 1995). In MSvDB, there are also non-cholinergic projection neurons, such as GABAergic, and recently described glutamatergic neurons (Kohler, Chan-Palay et al. 1984; Kiss, Patel et al. 1990; Hajszan, Alreja et al. 2004; Gritti, Henny et al. 2006). These projection neurons send out their axons, which travel through the fornix, to innervate hippocampal neurons. Septohippocampal cholinergic neurons are said to innervate both pyramidal and interneurons in the hippocampus, while GABAergic

projection neurons are said to innervate preferentially hippocampal interneurons (Buzsaki 2002). These projection neurons also send out axon collaterals locally to innervate other neurons in MSvDB, and there may also be cholinergic and GABAergic local neurons in MSvDB (Woolf 1991; Dutar, Bassant et al. 1995).

1.3.2 Basal forebrain – basalocortical projection

Cholinergic neurons are dispersed in the BF nuclei (SI, MCPO and NBM) and also sparsely in the internal capsule and ventral pallidum, but as a whole they project to the entire neocortical mantle with some possible topographical organization (Zaborszky 2002). They, like their counterparts in MSvDB, also project with GABAergic and glutamatergic neurons (Zaborszky, Buhl et al. 2005; Henny and Jones 2008).

Cholinergic neurons in BF also send out some projections to MSvDB, amygdala and other subcortical structures (Woolf 1991).

One interesting and useful feature of the cholinergic neurons in MSvDB, BF and HDB is that these hippocampal or cortical projecting cholinergic neurons express a receptor, p75, which is a weak receptor for a neurotrophic factor, nerve growth factor (NGF). In early 1990s, a novel cell-type specific targeting technique was invented (Heckers, Ohtake et al. 1994; Jouvenceau, Billard et al. 1994), which used this p75 receptor as the target protein (discussed later in 1.6.1).

1.4 Functions of forebrain cholinergic systems

1.4.1 Cognitive and behavioral functions: attention, learning and memory

It has been known for a long time that the cholinergic systems are critical for many cognitive and behavioral functions, such as sleep/arousal, attention and memory, and maybe even consciousness (Everitt and Robbins 1997; Perry, Walker et al. 1999). Patients with impairment in their cholinergic system, such as patients with Alzheimer's disease (AD), have profound memory problems (Coyle, Price et al. 1983; Mesulam 2004). Early studies have shown that cholinergic antagonists produce memory deficits, hallucination and other cognitive deficits, suggesting that disturbance of cholinergic systems severely affects normal brain functioning (Pazzagli and Pepeu 1965; Safer and Allen 1971; Gillin, Sitaram et al. 1982; Jones 1993). However, these studies with systemic administration of cholinergic drugs may affect cholinergic systems in the forebrain as well as those in caudal areas. It was necessary to disambiguate the contribution of specific cholinergic systems. Studies, especially on animals, have revealed that the forebrain cholinergic projection systems are mainly involved in attention and memory functions, and sleep/arousal regulation to some extent (Jones 1993; Blokland 1995; Woolf 1997; Sarter and Bruno 2000; Sarter, Givens et al. 2001).

The involvement of cholinergic mechanism in attention has been studied for decades (Everitt and Robbins 1997). It is generally believed that the BF cholinergic system is part of the attention mechanism in the cortex (Everitt and Robbins 1997; Sarter, Hasselmo et al. 2005). In visual attention tasks, one of the best studied attention models, it has been shown that impairment of BF cholinergic system could affect visual attention (McGaughy, Dalley et al. 2002).

Another type of vital functions, learning and memory functions, also involves the cholinergic systems in both MSvDB and BF (Everitt and Robbins 1997; Parent and Baxter 2004). Early pharmacological studies have demonstrated that local administration of cholinergic antagonists in hippocampus, cortex and MSvDB disrupts learning and memory (Izquierdo, da Cunha et al. 1992; Warburton, Koder et al. 2003), and boosting ACh level or cholinergic signaling may enhance learning/memory functions (Izquierdo, da Cunha et al. 1992), or reverse learning/memory deficits produced by other manipulations (Davis and Mohs 1982; Levy, Kong et al. 1991; Hersi, Rowe et al. 1995). MSvDB lesion recapitulates many memory deficits shown in hippocampal lesion (Mahut 1972; Winson 1978; Mitchell, Rawlins et al. 1982; Gray and McNaughton 1983; Parent and Baxter 2004), suggesting that septohippocampal system is an integral system that has very important role in learning and memory functions. However, more recent studies specifically targeting cholinergic neurons in MSvDB could not recapitulate most of the deficits shown in complete lesion of MSvDB, leading to questions on the importance and the exact role of MSvDB cholinergic system in hippocampal dependent learning/memory (Blokland 1995; Parent and Baxter 2004). I will address this controversy in the methodological considerations (1.6.1) and later discussions (4.5.3 and 5.4.1).

1.4.2 Potential mechanisms of cholinergic functions

Although intervention of cholinergic systems, such as pharmacological manipulations and lesion, reveals their participation in cognitive functions, the exact mechanisms by which the cholinergic systems fulfill these functions are not well understood. Based on insights gained from *in vitro* studies and some *in vivo* studies, theories and postulations have been proposed (Woolf 1997; Kimura 2000; Gold 2003;

Weinberger 2003; Hasselmo and Giocomo 2006), and they mainly fall into the following categories.

1.4.2.1 Dynamic regulation of acetylcholine release

The first level of participation of forebrain cholinergic systems in these cognitive processes is the dynamic release of ACh (Pepeu and Giovannini 2004). Dynamic ACh release has been studied with microdialysis in the last two decades. ACh release in both cortex and hippocampus is associated with general arousal states (Jones 1993). Learning tasks, or simply novel information, can induce ACh release in hippocampus and/or cortex (Aloisi, Casamenti et al. 1997; Giovannini, Rakovska et al. 2001). Attention-requiring tasks also induce ACh release in cortex (Himmelheber, Sarter et al. 2000; Passetti, Dalley et al. 2000). Even though the baseline ACh level may be needed to ensure the normal brain functions under baseline conditions, the existence of dynamic recruitment of cholinergic systems suggests that ACh functioning probably relies more on these temporally-tuned ACh effluxes, and less likely on the action of constitutive baseline ACh level.

Other than temporally-tuned ACh release, spatially differential ACh release may also participate in cognitive processes. BF corticopedal or septohippocampal cholinergic projection may have some rough topographic organization (Bigl, Woolf et al. 1982; Luiten, Gaykema et al. 1987; Nyakas, Luiten et al. 1987; Gaykema, Luiten et al. 1990; Zaborszky, Buhl et al. 2005), and cortical ACh release may be differentially regulated, depending on the specific domain involved in information processing (Butt, Testylier et al. 1997; Jimenez-Capdeville, Dykes et al. 1997). This also seems to be true when different cortical or subcortical structures are involved in the task (Pych, Chang et al.

2005). Consequently, during learning tasks in which different memories are formed depending on hippocampal or amygdaloidal pathway, ACh in either structure seems to promote the memory consolidation in that specific pathway (Calandreau, Trifilieff et al. 2006).

1.4.2.2 Selective enhancement of neuronal pathways

The released ACh seems to have a general excitatory effect on cortical and hippocampal neurons (Hasselmo 2006). *In vitro* studies showed that ACh can promote persistent spiking (Hasselmo and Fehlau 2001). It has been suggested that ACh release may selectively enhance information processing on feedforward pathway through nicotinic enhancement, and inhibit feedback pathway through muscarinic presynaptic inhibition (Hasselmo 2006). Such differential effects in a local region are presumably mediated by different receptor distribution.

1.4.2.3 Interaction with theta oscillations

Theta activity is the best characterized rhythmic activity in the brain. Discovered in rodent hippocampus probably in the 1930s, theta oscillations are large sinusoidal activities that can be recorded in many areas of the brain, particularly the limbic system (Buzsaki, Leung et al. 1983; Bland 1986; Vertes and Kocsis 1997). Theta oscillations appear more often during voluntary behaviors (or Type I behaviors, such as exploration, locomotion, etc) and also rapid-eye-movement (REM) sleep, but less likely with automatic behaviors (or Type II behaviors, such as drinking, eating and grooming) (Vanderwolf 1969). Theta oscillations associated with Type I behaviors or REM sleep

are termed Type I theta, while the ones associated with Type II behaviors, or theta under urethane anesthesia, are termed Type II theta (Vanderwolf 1969; Buzsaki 2002).

Theta oscillations seem to be tightly linked to the spatial information processing in the hippocampus, and the function of theta oscillations is often considered to be related to learning and memory (Vertes and Kocsis 1997; Kahana, Seelig et al. 2001; Buzsaki 2002). Evidence supporting this notion includes studies on long-term potentiation (LTP), which is considered one of the major cellular mechanisms underlying memory consolidation (Morris 2003; Whitlock, Heynen et al. 2006). Stimulation in theta frequency, compared to other frequencies, seems to be the favorite in inducing LTP (Larson, Wong et al. 1986; Pavlides, Greenstein et al. 1988; Vertes 2005).

Interaction between theta oscillations and cholinergic system has been studied for decades (Vanderwolf 1975; Konopacki, MacIver et al. 1987; Colom, Nassif-Caudarella et al. 1991). MSvDB is thought to be the key pacemaker of theta oscillations, since many neurons in MSvDB fire rhythmically and phase-lock to hippocampal theta (Stumpf, Petsche et al. 1962; Morales, Roig et al. 1971; Feder and Ranck 1973; Apostol and Creutzfeldt 1974; Gaztelu and Buno 1982; Ford, Colom et al. 1989; Stewart and Fox 1989), while inactivation or lesion of MSvDB eliminate theta oscillations in the hippocampus (Winson 1978; Andersen, Bland et al. 1979; Mitchell, Rawlins et al. 1982; Monmaur 1982; Buzsaki, Leung et al. 1983). Cholinergic muscarinic antagonist, such as atropine, eliminates Type II theta (Vanderwolf 1975; Buzsaki, Kellenyi et al. 1980), which is therefore also called atropine-sensitive theta. Type I theta is less affected by atropine (Vanderwolf 1975), which is also called atropine-resistant theta. Specific lesion of MSvDB cholinergic neurons seems to eliminate Type II theta too, and severely affects the amplitude and stability of the remaining Type I theta (Lee, Chrobak et al. 1994;

Bassant, Apartis et al. 1995). In contrast, cholinergic activation, such as agonist, or AChE inhibitors, can induce prolonged theta oscillations (Vanderwolf 1975; Bland 1986; Golebiewski, Eckersdorf et al. 1992), in addition to enhancing learning/memory or reversing memory deficits I mentioned above in 1.4.1.

Besides pharmacological intervention or lesion, microdialysis studies in normal animals have shown that ACh release seem to be associated with theta-dominant behavioral states. For example, exploration of a novel environment induces strong ACh release as well as theta oscillations (Crouzier, Baubichon et al. 2006).

1.4.2.4 Promoting neural plasticity

Many studies have suggested that synaptic plasticity including LTP, and regulation of signaling molecules as well as immediate-early genes (IEG), as cellular and molecular mechanisms underlying memory consolidation (example of reviews in Bliss and Collingridge 1993; Milner, Squire et al. 1998; Martin, Grimwood et al. 2000; Miyamoto 2006; Miyashita, Kubik et al. 2008). ACh seems to participate in these processes as well.

Studies showed that ACh is able to modulate classical LTP formation, both *in vitro* and *in vivo* (Jerusalinsky, Kornisiuk et al. 1997; Leung, Shen et al. 2003; Power AE 2003; Hasselmo 2006). Such modulation seems to be mediated by muscarinic receptors mostly, but involvement of nicotinic receptors in LTP has also been described (Buccafusco, Letchworth et al. 2005). Beyond LTP, ACh mechanism is also involved in cortical reorganization, one type of neural plasticity. Trimming whiskers can cause sensory map reorganization, such that cortical sensory areas used to represent the trimmed whiskers would be shifted to represent adjacent, remaining whiskers (Sachdev,

Lu et al. 1998). Pairing with auditory stimuli at a certain frequency (tone) with an artificial electrical stimulation of BF, would facilitate behavioral response of the animal to that tone, and reorganize the representation of that tone in auditory cortex (Kilgard and Merzenich 1998; Weinberger 2003) . These cortical reorganization events rely on cholinergic mechanisms, since muscarinic antagonist or cholinergic-specific lesion disrupts such plasticity (Weinberger 2003; Ramanathan, Tuszynski et al. 2009) (but see Kamke, Brown et al. 2005). The cholinergic system is also considered to be essential for cortical plasticity following brain injury (Conner, Chiba et al. 2005).

As molecular mechanisms underlying neural plasticity and memory consolidation, participation of ACh in regulating signaling molecules and immediate-early genes (IEG) has been studied, mostly with *in vitro* models (Trejo and Brown 1991; Ding, Larsson et al. 1998; Hirabayashi and Saffen 2000). Studies suggest that cholinergic modulation can affect signaling molecules such as extracellular regulated protein kinase (ERK) (Giovannini, Pazzagli et al. 2005), and subsequently regulate expression of IEGs such as *c-fos*, *zif-268* and *arc* (Trejo and Brown 1991; Hirabayashi and Saffen 2000; Teber, Kohling et al. 2004). Studies *in vivo* have been rare (Hughes and Dragunow 1994), but suggest a consistent scheme.

1.5 Overarching questions: what are the properties of fast dynamics of cholinergic activities in vivo, and how do they interact with and influence the activities in their target areas?

Although the cholinergic system has been intensively studied, its *in vivo* functioning and mechanisms are still not well understood, and many fundamental questions remain unanswered.

For example, what is the time scale of forebrain ACh operation? ACh is known to be modulated across behavioral states, but finer (faster) dynamics is almost not known, except that it may exist (Parikh, Kozak et al. 2007). The time scale ACh operates on can give us a clue and suggest new schemes of ACh functioning.

Second, how do forebrain cholinergic neurons behave (firing pattern) in normal, behaving animals? Understanding their individual behavior and their behavior as an ensemble would shed light on their functions, but there are almost no studies that directly addressed this question (King, Recce et al. 1998; Simon, Poindessous-Jazat et al. 2006).

Last but not least, if fine-scale behavior of cholinergic system exists, what is its influence on the target areas? How would they modulate neural activities in the target areas? How would they influence the intracellular molecular signaling in the target areas?

In my research, I tried to address these questions to better understand the *in vivo* functioning of cholinergic system. First I looked at the fine-scale behavior of the cholinergic system, by monitoring ACh release with a technique that has greatly improved temporal and spatial resolution. Then I asked how the fine-scale activities of putative cholinergic neurons in MSvDB affected the activities of its target, the hippocampus, and further asked what the impact of the ACh release was, on IEG expressions in cortical and hippocampal areas in behaving animals.

1.6 Methodological considerations in cholinergic studies

Some attention should be paid to the approaches and techniques when studying the cholinergic systems *in vivo*, since individual techniques/methods have their

advantages and limitations. To study the questions I raised above, I used a number of approaches, including some novel techniques that I developed during the course.

1.6.1 Pharmacological and lesion studies

Studies of cholinergic systems, as other systems, often began with large scale interventions, such as using systemic drugs that affect cholinergic transmission. Early studies often use cholinergic antagonists which were available at that time, to investigate how these drugs would affect normal functions, in humans and in animals (Pazzagli and Pepeu 1965; Safer and Allen 1971). Later studies tried to refine the spatial specificity of cholinergic action, by applying cholinergic drugs locally into individual brain areas (Izquierdo, da Cunha et al. 1992). With better knowledge of the cholinergic receptors and their subtypes, more receptor-type specific drugs are used to further dissect the function of individual receptor and pathways that ACh acts on (Golebiewski, Eckersdorf et al. 1993; Ma, Seager et al. 2009). More recently, receptor subtype specific knock-out mice were generated to better understand the intricacy of cholinergic receptors (Granon, Faure et al. 2003; Wess 2004).

With the cholinergic nuclei mapped out, lesion studies were performed as a complementary way to study individual cholinergic systems, often with electrolytic or excitatory lesion which eliminates all the neurons in a particular region (Winson 1978; Mitchell, Rawlins et al. 1982) (more examples reviewed in Everitt and Robbins 1997; Parent and Baxter 2004). The interpretation of cholinergic function by these studies may be confounded by the nonspecificity of the lesion. Later, a cell-type specific toxin provided better resolution for the lesion studies, in which a toxin (saporin) was conjugated to p75 receptor antibody to specifically target the forebrain cholinergic

projecting neurons in MSvDB and BF regions (Wiley, Oeltmann et al. 1991; Book, Wiley et al. 1992; Book, Wiley et al. 1994; Heckers, Ohtake et al. 1994; Jouvenceau, Billard et al. 1994). This approach provided more insights on the function of cholinergic system, as it minimized the non-specific lesion to other neurons in the same nuclei. However, the completeness and specificity should still be carefully examined before interpreting the results with these specific lesions (Waite and Chen 2001).

1.6.2 Chemical measurement of acetylcholine

Chemical measurement of ACh evolved with the technical developments. Early studies used “cup” method to collect ACh release at the cortical surface, or used indirect measurement such as high-affinity choline uptake assay (Brioni, Decker et al. 1990; Pepeu and Giovannini 2004). These crude methods were replaced after microdialysis methods matured in the 1980s. Microdialysis, with circulation of dialysis solution to directly collect chemicals from the extracellular space, is able to measure multiple neurochemicals with specificity and precision ensured by the analytical power of chemistry (Pepeu and Giovannini 2004). However, it takes time to accumulate enough sample for signal detection (instrument limit-of-detection, LOD), and the microdialysis probes by which chemicals are exchanged through have to be big enough, usually >200µm in diameter, and 1mm in length (Kawagoe, Zimmerman et al. 1993). These factors limit the temporal and spatial resolution of microdialysis method. Furthermore, since extracellular ACh is quickly broken down by the potent AChE enzyme, inhibitors of AChE had to be added in the microdialysis to prevent the degradation of ACh, until most recently (Chang, Savage et al. 2006). Using such AChE inhibitors accumulates ACh artificially, which might have interfered with normal physiological ACh release, and

confounded the results in most microdialysis studies on ACh (Chang, Savage et al. 2006).

A relatively new method, amperometry, has been applied very recently to measure cholinergic activities *in vivo* (Burmeister, Palmer et al. 2003). This method relies on electrochemical principals, and uses an enzyme-coated micro-electrode to detect choline (and/or ACh) level fluctuations. It has greatly improved temporal resolution, as well as finer spatial resolution, compared to microdialysis method (Burmeister, Palmer et al. 2003; Parikh, Pomerleau et al. 2004). This new method enables the study of fast ACh dynamics, and suggested that ACh release may be regulated on time scale of seconds (Parikh and Sarter 2006).

1.6.3 Recording from cholinergic neurons *in vivo*

An alternative approach to study the cholinergic activity is to record from cholinergic neurons and study how they behave under different conditions, and what are the consequences of their firing. This, of course, assumes that cholinergic neurons in a nuclei form a fairly homogeneous group in terms of their firing pattern. Although this is not really known, it is a reasonable assumption to begin with.

The major difficulty in this approach is the identification of cholinergic neurons. Earlier studies, based on pharmacological responses and spike waveforms obtained *in vitro*, suggested that certain rhythmic firing MSvDB neurons, with wide spike waveform and long after hyperpolarization (AHP), might be cholinergic neurons (Lamour, Dutar et al. 1984; Stewart and Fox 1989; Brazhnik and Fox 1997; Brazhnik and Fox 1999). These assumptions may not hold true. Indeed, a recent study contradicts these notions and suggests that cholinergic neurons *in vivo* do not fire at high rate, and they have no

apparent relationship with theta oscillations (Simon, Poindessous-Jazat et al. 2006). This study used juxtacellular recording technique and labeled the recorded neurons, whose chemical identities were later revealed by immunohistochemistry. Such recording-labeling technique is more reliable, but unfortunately, a very low-yield approach mostly suited for anesthetized recording. On unanesthetized animals, it currently seems to be limited to head-fixed preparations.

Given such reality, extracellular multi-electrode recording is still a good complementary technique. With simultaneous recording of multiple neurons, not only the firing behavior of individual neurons can be revealed, characteristics of ensemble activity may also be studied (Nicolelis, Ghazanfar et al. 1997). With this recording technique, firing properties are still the only choice to identify specific cell types. Since identification based on the spike waveform and pharmacological responses may not hold true, new presumptive properties should be used, and the results can be later verified with other techniques, including juxtacellular recording-labeling.

Figure 1. Acetylcholine synthesis, release and metabolism

in cholinergic neurons Acetylcholine is synthesized by choline acetyltransferase (ChAT), and packed into vesicles to be released. After exocytosis, ACh can bind to cholinergic receptors, or hydrolyzed by acetylcholine esterase (AChE) (Figure adapted from Nicholls and Fuchs 2001, figure 13.5).

Figure 1

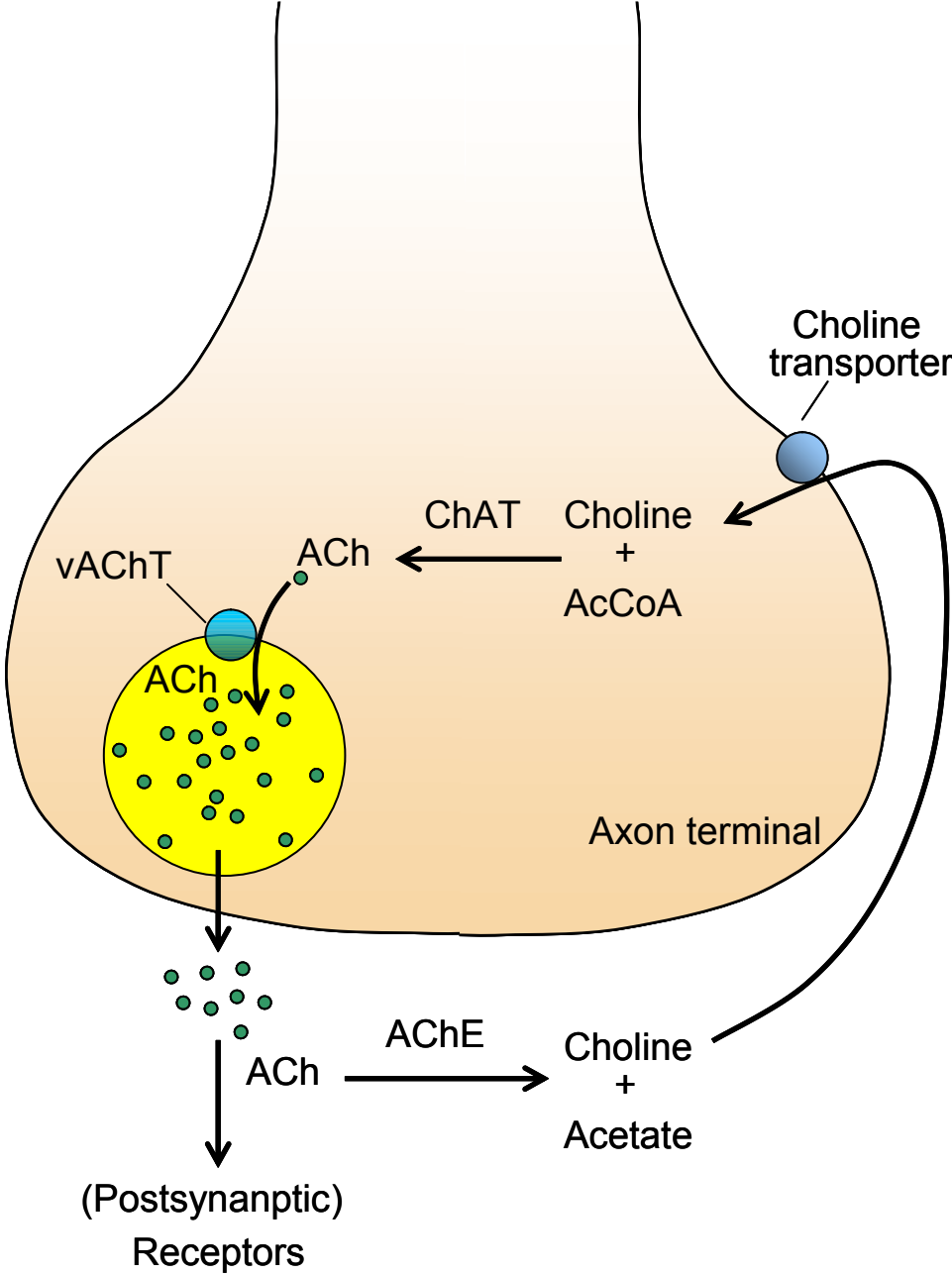
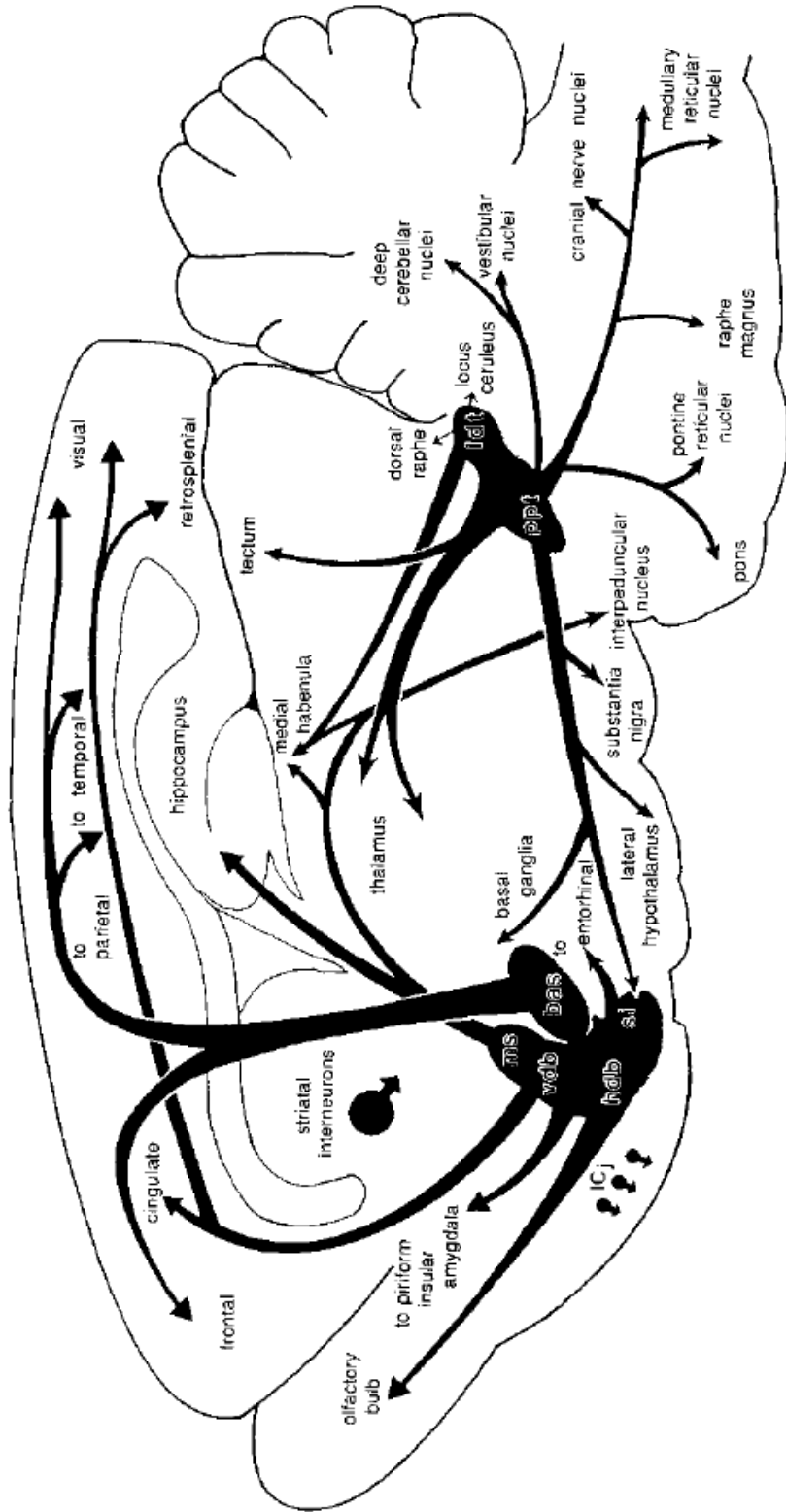


Figure 2. Cholinergic systems in the brain.

Cholinergic nuclei are distributed and interlinked across the rostral-caudal axis of the brain (Figure from Woolf 1991). ms, medial septum; vdb, the vertical limb of the diagonal band of Broca; hdb, the horizontal limb of the diagonal band of Broca; si, substantia innominata; bas, nucleus basalis. Cholinergic neurons in the medial septal – basal forebrain areas form the cholinergic projection systems, which innervate and provide ACh for the entire hippocampus and cortical mantle. The cholinergic nuclei pedunculopontine tegmental nucleus (ppt) and laterodorsal tagmental nucleus (ldt) mainly project to thalamus, basal forebrain and some caudal areas.

Figure 2 Central cholinergic systems



Chapter 2 Fine spatiotemporal coupling between hippocampal acetylcholine release and theta oscillations *in vivo*

2.1 Introduction

2.1.1 Interaction between acetylcholine and theta oscillations

Both acetylcholine (ACh) and theta oscillations in the hippocampus are important in learning and memory functions. Numerous studies on human and animals have shown that cholinergic system is important in many types of learning and memory tasks, in part by promoting neural plasticity (see reviews in Hasselmo and Bower 1993; Jerusalinsky, Kornisiuk et al. 1997; Gold 2003; Power, Vazdarjanova et al. 2003; Parent and Baxter 2004; Hasselmo 2006). Similarly, theta oscillations are also involved in learning and memory functions (see reviews in Vertes and Kocsis 1997; Kahana, Seelig et al. 2001; Buzsaki 2002), partly via promoting LTP and neural plasticity (Larson, Wong et al. 1986; Pavlides, Greenstein et al. 1988; Vertes 2005). These two processes appear to be tightly coupled, since septohippocampal cholinergic projection is one integral part of the theta generation system (Petsche, Stumpf et al. 1962; Kohler, Chan-Palay et al. 1984; Bland 1986). Indeed, lesion or pharmacological impairment of normal cholinergic activities dampens theta oscillations (Vanderwolf 1975; Buzsaki, Kellenyi et al. 1980; Lee, Chrobak et al. 1994), suggesting that at least a tonic level of ACh is essential for normal theta oscillations.

However, functioning of either ACh or theta oscillations under *in vivo* physiological conditions depends on their dynamics and the spatiotemporal scales they

operate on. Theta oscillations can appear on time scale as fast as seconds (Vanderwolf 1969; Bland, Declerck et al. 2007; DeCoteau, Thorn et al. 2007). On the other hand, in contrast to the traditional view of slow ACh functioning, one recent study has shed light on fast ACh dynamics (Parikh, Kozak et al. 2007). Therefore, it is plausible that ACh release and theta oscillations under physiological conditions are coupled on fine temporal scales. Nevertheless, this hypothesis has never been tested, largely due to technical difficulties in monitoring cholinergic activities on fine scales. Microdialysis, the prevalent method to directly monitor ACh concentrations, cannot provide ACh dynamics below 5-10 min (Pepeu and Giovannini 2004). Despite being slow, some microdialysis results did support the above hypothesis remotely, by showing that higher ACh level is associated with theta-dominant behavioral states, such as active waking (exploration of novel environment etc), REM sleep (Marrosu, Portas et al. 1995; Bianchi, Ballini et al. 2003), or during learning tasks (Stancampiano, Cocco et al. 1999; McIntyre, Marriott et al. 2003). Theta-related ACh dynamics on temporal scales finer than these behavioral states have not been revealed by microdialysis.

A related yet indirect approach that may provide insights on this issue is to monitor the activities of cholinergic neurons in MSvDB, which are arguably the sole source of hippocampal ACh (Lewis, Shute et al. 1967; Mesulam, Mufson et al. 1983; Dutar, Bassant et al. 1995). However, most *in vivo* neuronal recording studies could not unequivocally identify cholinergic cells, and they have not revealed the exact relationship between cholinergic activities and theta oscillations. One additional question, often debated in these studies, was whether MSvDB cholinergic neurons could pace theta oscillations (Markram and Segal 1990; Brazhnik and Fox 1997; Apartis, Poindessous-Jazat et al. 1998; Sotty, Danik et al. 2003; Simon, Poindessous-Jazat et al. 2006). If they

do, ACh release should precede or at least be as fast as the initiation of theta oscillations, which of course, has never been tested either.

To circumvent the limitation of traditional methods, and to simultaneously monitor ACh and theta on fine temporal (and spatial) scales, we used amperometry to acquire ACh dynamics on the level of seconds with a choline sensor (Burmeister, Palmer et al. 2003; Parikh, Pomerleau et al. 2004; Parikh, Kozak et al. 2007). In order to obtain LFP information, an electrophysiological system had to be implemented simultaneously.

2.1.2 Simultaneous acquisition of fast dynamics of neurochemicals and LFP information

Neurons communicate with each other using electrical and chemical signals. To characterize these signals, *in vivo* neurophysiology has made substantial progress in the last few decades by introducing a variety of methods for extracellular electrophysiology and voltammetric neurochemistry (Kissinger, Hart et al. 1973; Nicoletis, Ghazanfar et al. 1997; Dale, Hatz et al. 2005; Wightman 2006). Following the more recent emergence of real-time *in vivo* neurochemical studies (on the time scale of seconds or even faster), a promising research direction is to simultaneously acquire both types of information, i.e. electrophysiological and neurochemical, in the same preparation. Clearly, such a new experimental approach could greatly facilitate our understanding of the dynamic interactions between diencephalic neural circuits and neuromodulatory systems, such as acetylcholine and dopamine. Moreover, this approach would also allow better mapping of these broad neural interactions during normal and pathological brain states, exemplified by the pioneering studies done by Dr. Wightman and colleagues (e.g. Cheer et al., 2005). Unfortunately, due to considerable technical challenges, attempts to obtain

simultaneous *in vivo* electrophysiology and voltammetry have been rare. Furthermore, until now two independent recording systems have always been required to obtain such data sets (Ewing, Alloway et al. 1983; Hefti and Felix 1983; Kuhr, Wightman et al. 1987; Sammut, Park et al. 2007; Viswanathan and Freeman 2007; Johnson, Franklin et al. 2008).

Given this reality, the purpose of this part of the study was to demonstrate that a simple instrumentation approach, based on a single amperometry system, can simultaneously capture both electrophysiological (local field potentials or LFPs) and neurochemical information during the same experiment. This rather inexpensive technical solution was proposed based on the distinctive but related principles of extracellular electrophysiology and voltammetric neurochemistry. Extracellular electrophysiology, including LFPs and neuronal action potential (spike) recordings, studies the activities of neuronal populations or individual neurons by measuring extracellular voltage fluctuations with microelectrodes (Robinson 1968). On the other hand, voltammetric neurochemistry, including amperometry, detects dynamics of extracellular neurochemical concentration by measuring the faradic current resulting from chemical oxidation/reduction, when a voltage is applied to the same microelectrode that is used to measure the current (Stamford 1985; Kawagoe, Zimmerman et al. 1993). The similarity in the two recording principles led us to believe that, in theory, the current measurement in the voltammetric methods could concomitantly capture endogenous electrical signals in the brain, such as LFPs.

With such technique, we were then able to investigate a few fundamental issues regarding theta-related ACh release on fine scales: whether phasic ACh release could

accompany the appearance of theta oscillations on fine temporal scale; and whether ACh release is spatially modulated across hippocampal layers. In urethane-anesthetized rats, we observe for the first time a tight coupling between phasic ACh releases and theta oscillations on the time scale of tens of seconds. We therefore further asked whether such phasic ACh release was required for the initiation of theta activity.

2.2 Material and methods

2.2.1 Animals

Animal use and procedures were approved by the Duke IACUC and performed in accordance with NIH guidelines. Twenty-seven adult male Long-Evans rats (3-9 months old) were used in the experiments.

2.2.2 Chemicals and drugs

Choline oxidase (CO; EC 1.1.3.17), bovine serum albumin (BSA), glutaraldehyde (25% in water), ascorbic acid (AA), choline, meta-phenylenediamine dihydrochloride (mPD), carbachol and urethane were all obtained from Sigma Chemical Co. (St Louis, MO, USA).

2.2.3 Amperometric probes and choline sensor preparation

Amperometric probes were either ceramic-base multi-site microelectrodes ("R2" design, 4 sites, 50 μm X150 μm per site with 50 μm space between sites) purchased from CenMeT (University of Kentucky, KY, USA), or in-house-made four-channel probes

with platinum-iridium wires assembled onto 8-pin IC socket (DIGI-KEY, MN, USA ; only 4 pins out of 8 were used).

Choline sensors were constructed by coating choline oxidase and applying exclusion layer (mPD) to the probes (Burmeister, Palmer et al. 2003; Burmeister, Pomerleau et al. 2008). Before each coating, the probes were cleaned with 70% isopropyl alcohol and distilled water, and then dried. Two sites of the probe were coated with ~0.01 μ l of choline oxidase solution (1U of CO, 1% BSA and 0.125% glutaraldehyde in 5 μ l distilled water) for 3 times with a 1 μ l microsyringe (Hamilton, NV, USA). The two remaining sites were coated with BSA solution omitting the CO (~0.01 μ l X 3times), serving as self-reference sites. Enzyme-coated probes were allowed to dry for 30min in desiccator before stored at 4°C. After at least 2 days, mPD was applied to the probe sites by employing cyclic voltammetry between +0.2 and +0.7 V versus an Ag/AgCl reference electrode in the mPD solution (5mM, in 0.05mM argon-bubbled phosphor-buffered saline solution/PBS) using a scan rate of 50 mV/sec (Burmeister, Pomerleau et al. 2008). After the plating was completed, the choline sensors were stored at 4°C for at least 24hr before calibration.

Sensors were calibrated *in vitro* both before *in vivo* use and also after acute recordings. They were connected to a FAST-16 electrochemical recording system (Quanteon, LLC, Nicholesville, KY, USA) with the sensor sites immersed in PBS (0.05mM, pH 7.4, 37°C, continuous stirring). A constant potential (+0.7V) was applied to sensor sites, versus an Ag/AgCl reference electrode. After a stable baseline was established, standard solutions including ascorbic acid (100 μ M), choline (20 μ M X 3 times) and hydrogen peroxide (8.8 μ M) were added to the PBS in order, and the corresponding currents were measured. The sensitivity, limit-of-detection (LOD) and

selectivity of the choline sensors were calculated based on linear regression by the FAST-16 software (Quanteon, LLC, Nicholasville, KY, USA).

Choline sensors were calibrated *in vitro* before and after acute recordings. Sensitivity, selectivity and limit-of-detection (LOD) were calculated based on regression. Sensitivity, 27.0 ± 2.0 ; selectivity, 301 ± 63 , average \pm SEM. The *in vivo* noise level was actually lower than that *in vitro*, thus LOD (or 3x standard deviation) *in vivo* could be improved and reached 100nM and lower (more details in *Choline signal and noise reduction*). In the analysis, we only included the experiments performed with sensors showing satisfactory properties in post-calibration.

2.2.4 Simultaneous *in vivo* recording in urethane-anesthetized rats

2.2.4.1 Simultaneous acquisition using both amperometry and electrophysiology

Male rats (3-6 months, n=16) were anesthetized with urethane (1.25-1.5g/kg body weight, I.P.) and positioned in a stereotaxic frame. A miniature Ag/AgCl reference electrode for amperometry was secured in the frontal cortex. Stainless steel screws were secured above frontal cortex and cerebellum, serving as grounds for electrophysiology. Craniotomies were opened above the hippocampus bilaterally at AP -4.0mm, ML 2.5mm relative to Bregma (Paxinos and Watson 2005). A multi-electrode array (MEA) was lowered into one hemisphere, recording electrophysiological signals from CA1 (-2.2mm below dura) and dentate gyrus (DG, -2.9mm below dura). A calibrated choline sensor or a bare probe was lowered into the contralateral CA1 to record amperometric signals.

During the experiment, electrophysiological signals (LFPs and spikes) were recorded with Plexon Neurosurgery WorkStation (Plexon Inc, Dallas, TX), using a 1000

Hz sampling frequency for LFPs. Amperometric signals were recorded with the FAST-16 electrochemical recording system, using a 40 Hz sampling frequency (maximum in the system). For temporal synchronization, marker events in the two systems were simultaneously logged bi-manually, and the signals from the two systems were aligned by these events during off-line processing (alignment SD: 29 ± 8 ms). After the amperometric signals stabilized (~15-30min), a baseline was recorded for at least 15 min.

2.2.4.2 Tail-pinch.

Animals received a series of tail pinches to elicit transient hippocampal theta activity. The inter-trial interval was set at 5-10 min so that LFPs could return to baseline delta activity.

2.2.4.3 MS Carbachol injection.

A guiding tube (23 gauge) was implanted above medial septum (MS) with a 15° angle (entry point: AP +0.7, ML 1.5, mm). A cannula (30 gauge) was inserted through the guiding tube for injecting cholinergic agonist (carbachol, 4 μ g in 1 μ l DI water, 30 sec) into MS (target: AP +0.7, ML 0.0, DV -6.0, mm).

2.2.4.4 Theta depth profile.

For some animals, an amperometric sensor or probe was lowered step-by-step through the hippocampus with 200 μ m intervals, while theta activity was induced by tail pinches.

2.2.4.5 Recording choline concentration and LFP theta information with amperometry alone.

For choline recording in the hippocampus, a miniature Ag/AgCl reference electrode was secured above the frontal cortex. A choline sensor was then lowered into the hippocampus and signals were recorded with FAST-16 electrochemical recording system (Quanteon, LLC, Nicholesville, KY, USA). After 30-60min when baseline stabilized, data acquisition started. Choline sensor was lowered from -1.8mm to -3.4mm (below dura) at 0.2mm increments, and tail-pinches (30-120 sec) were applied at each depth to induce theta activity and potential choline increase. Five-ten min were set between trials for LFP and choline signal to return to baseline.

At the end of the acute experiment, choline sensors were removed for post-experiment calibration. Animals received an overdose of pentobarbital for euthanasia.

2.2.5 Single unit recording in anesthetized rats.

For single unit recordings, stainless steel screws were secured above frontal and parietal cortex as grounds. A 4x4 multielectrode array (35 μ m tungsten wires, 250 μ m spacing) was inserted at a 15° angle targeting MSvDB. Single units were searched for as the array was lowered between 5.8-7.5mm from dura. Activities were sampled at every 0.2-0.3mm where maximal number of single units were found. Tail pinches were applied similarly as in amperometry recordings and the activities of single units were recorded with Plexon Neurosurgery WorkStation (Plexon Inc, Dallas, TX).

2.2.6 Surgery and *in vivo* recordings in freely-moving rats

Male rats (3-6 months, n=8) were anesthetized with ketamine (100mg/kg) and xylazine (5mg/kg). Atropine (0.02mg) was used to reduce airway secretion. Choline sensor (3 rats) or MEA (5 rats) were implanted stereotaxically as described for the acute experiments (One rat had both implants, and the simultaneous recordings are shown in Figure 6A.) A miniature Ag/AgCl reference electrode and stainless steel screws were secured above frontal cortex and cerebellum as reference (amperometry) and ground (electrophysiology) electrodes, respectively. A choline sensor (CA1, -2.2mm, below dura) or MEA (CA1, -2.2mm, DG, -2.9, mm, below dura) was implanted into the dorsal hippocampus (AP -4.0, ML 2.5 mm). Dental acrylic was used to cover and secure the implant with the help of anchoring screws. Rats were allowed to recover for at least 7 days after surgery.

2.2.6.1 Sleep/wake recordings.

Either amperometry (FAST-16 system) or electrophysiological data (Multichannel Acquisition processor, MAP, Plexon Inc, Dallas, TX) was recorded while rats moved freely around or went to sleep. Animal behavior was monitored on-line with a camera and recorded on video tapes. The time of major sleep and waking states were registered for subsequent analysis. Waking state was characterized by a standing posture, sometimes actively moving and/or exploring the cage. Sleep states were characterized as described elsewhere (Gervasoni, Lin et al. 2004).

2.2.6.2 Amphetamine injection.

Two rats implanted with choline sensor received an injection of amphetamine (4mg/kg, intraperitoneal/I.P.) during the amperometric recording.

2.2.7 Data Analyses

Recordings from the two systems were analyzed in MATLAB (The MathWorks, Natick, MA). Statistics were performed with SPSS software (SPSS Inc., Chicago, IL, USA).

2.2.7.1 Pre-processing of simultaneous amperometric and LFP signals.

For simultaneous recordings, signals were aligned by synchronization marker events. Before comparing the signals from the two systems, recordings were pre-processed to the same sampling frequency. Even though the FAST-16 hardware could acquire data at 250kHz/channel, its software allowed a maximal sampling rate at 40Hz, and each data point was an average of 6125 data points (250,000/40). To match this averaging process, LFP signals were also re-sampled at 40Hz by averaging from the 1000Hz sampling rate.

2.2.7.2 HFC calculation, amperometric HFC amplitude and oxidation current.

High frequency component (HFC) of the amperometric signals were calculated by high-pass filtering the original signals in MATLAB. The cut-off frequency was arbitrarily set at 1 Hz, assuming that evoked chemical dynamics did not fluctuate beyond

this faster time-scale (but see Robinson et al. 2003). HFC of the pre-processed LFP signals were calculated in the same way as the amperometric signals.

For a baseline of 120 sec of amperometric signals, HFC amplitude was calculated as the root mean square of the HFC. Oxidation current was the average of the residual low-frequency component of the amperometric signal during the baseline period.

2.2.7.3 Spectral analysis.

Spectral and coherence analyses of HFC were performed using multitaper spectral methods with the Chronux package (Dr. Partha Mitra and www.chronux.org). In urethane-anesthetized rats, baseline (120 sec) and pinch (30-120sec) periods were defined as the time before and during pinch. Each baseline period ended with a 20-sec period with the clamp touching the tail without pinching. Power spectral density (PSD) was calculated by averaging the spectrogram over time during each individual period, and then normalized to the total power of the particular PSD. Theta/delta spectral indices for baseline and pinch periods were calculated as the ratio between the power values in theta and delta bands (2.2-5Hz, 1-2.2Hz respectively).

For free-moving animals, spectral analysis was performed for selected sleep-wake episodes, whose time was registered during online behavior monitoring. The sleep periods started with slow-wave (SW) sleep, and ended with a REM sleep. For amphetamine injection experiments, the PSD after injection was normalized to the pre-injection PSD power.

2.2.7.4 Theta depth profile in HFC.

For theta depth profile in anesthetized rats, amperometry HFC was filtered for theta frequency (2-5Hz). Theta amplitude and phase were estimated with the Hilbert transform of the filtered HFC. Amplitudes were corrected for differences in the effective electrode area using the proportional correlation obtained for the baseline periods during the whole recording (Figure 7B). For phase calculation, since there was no fixed electrode to provide a phase reference, phase values on site 4 were used as reference (phase=0 degree) until the phase difference between site 2 and site 4 was bigger than 90 degrees, suggesting a phase reversal had occurred on site 1 and 2. Starting from this depth, site 1 was used for phase reference (phase=180 degree). To account for the variance of depth in individual experiments, we aligned the depth profile of multiple experiments by the midpoint of the phase reversal (defined as 0 in Figure 11B). This alignment produced sharper transitions and smaller variance in the averaged depth profile.

2.2.7.5 Acquiring theta information in amperometry HFC.

After we establish that amperometric signals contain both chemical signals and reflected LFPs (Zhang, Lin et al. 2009), we high-pass filtered the raw signal (>0.5Hz), and used this high frequency component (HFC) as reflected LFPs. Power spectrograms were calculated using multitaper spectral methods (Chronux package, www.chronux.org, and Mitra 2007).

Theta oscillations were recognized when a band between 2.2-5Hz appeared as the dominant band. These oscillations were confirmed as theta because they reversed their phases as the sensor electrodes reached deeper layers of hippocampus. We

calculated the depth profile of amplitude and phase and determined the depth that theta phase reversed from the phase in stratum oriens, and used this depth as depth “0” for calculating depth profile in each experiment (Zhang, Lin et al. 2009). Relative theta power (theta index) was calculated as the ratio between power in theta band and theta+delta bands (delta, defined as 0.5Hz – low end of theta) with a moving window (8sec, 0.5 sec step). Occasionally, breathing would induce an artifact around 1Hz. If this artifact was visible in the power spectrum, the power from this band was excluded.

2.2.7.6 Choline signals and noise reduction.

After HFC extraction, the remaining amperometric signal ($\leq 0.5\text{Hz}$) was further processed to obtain choline signal (Figure 8A). First, data pieces that contained pinch trials (5~15min) were separated out. Very slow decay of baseline, approximated as a linear decay, was removed from all channels for each data piece, which aligned the signal to 0 during baseline delta periods. Then we further removed noise using self-referencing, and took into account the effective electrode area which may vary between channels (Zhang, Lin et al. 2009). Specifically, we obtained the relative area for all four channels in each experiment, with normalizations factors based on the averaged HFC amplitude for all the baseline delta period. Using these factors, we performed corrected self-referencing on choline channels to generate de-noised choline channel signals. The two reference channels were referenced to each other to generate de-noised sentinel channel signals. These signals were finally converted to choline/sentinel signal based on the *in vitro* choline channel sensitivity. This de-noise / self-referencing procedure produced signals with low noise and could achieve limit-of-detection (LOD) usually lower than 100 nM (Figure 8B). For each pinch trial, signals were displayed for 60 sec before

to 240 sec after pinch start, and baseline values were calculated for 30 sec before pinch start. ACh release was calculated as the average of choline signal 0-120 sec after pinch start, with baseline subtracted.

2.2.7.7 Estimation of choline or theta rising time

Upon pinch, theta index and choline signal rose to a maximum and then decayed. In order to estimate the speed of such rise, we calculated the rise time and slope. Before this calculation, choline signal was first smoothed using a local-fit algorithm (Chronux) to remove residual transient artifacts. Maximal values (baseline subtracted) were found for choline signal or theta index between 0-180sec after pinch start, and rise time (T_{80}) was defined as the time the signal reached 80% of its maximal. The slope was defined as the reverse of the time between 30% and 70% of the maximal, multiplied by 0.4.

We also used an alternative way to estimate the lag between theta and choline rise. Cross-correlation was calculated between the two signals for each trial, and lag time corresponding to the correlation maximum between -100 and +180 sec was found.

2.2.7.8 Single unit activities

Electrophysiological recordings were off-line processed to obtain single unit data using offline sorter (Plexon Inc, Dallas, TX, more details in 3.2.3.1). Timestamps of spikes were further analyzed in Matlab. Firing rate were calculated by binning spikes with 0.5 sec bins and smoothed for 2 sec windows. Overall firing rate was calculated as the average of the whole recording session for each neuron. Rising time (T_{80}) was

defined similarly as for choline signal or theta index, and slope was calculated between 0 and 70% of maximum (baseline subtracted).

2.3 Results

2.3.1 Technical advancement –simultaneous acquisition of electrophysiological and neurochemical information

2.3.1.1 Implementation of simultaneous electrophysiology and amperometry – similarity between LFP and amperometric signals

To directly compare electrophysiological and amperometric signals, we first obtained simultaneous measurements of both signals in urethane anesthetized rats using two independent recording systems (Figure 4A). In order to have both systems functioning without interfering with each other, it was essential to isolate the grounds of the two systems. This was achieved by running the electrophysiology system on a battery-powered laptop to record the LFP signals without being grounded to the earth. In parallel, a constant voltage was applied across the amperometric sensor and an Ag/AgCl reference electrode to oxidize neurochemicals of interest and to measure the resultant faradic current.

To test whether LFP and amperometric signals were similar, we employed two manipulations known to elicit LFP theta oscillations under urethane anesthesia, i.e. tail pinch and carbachol injection in the medial septum (MS) (Kramis, Vanderwolf et al. 1975; Monmaur and Breton 1991). During baseline periods, LFP signals were dominated by large-amplitude slow fluctuations in the delta range (1-2Hz) characteristic of urethane anesthesia (Kramis, Vanderwolf et al. 1975). Upon pinch or carbachol injection, LFP shifted to smaller-amplitude regular theta oscillations (3-6Hz, Figure 4). These changes

in LFP oscillation patterns were grossly mirrored in amperometric signals (Figure 4A). This similarity suggested to us that a certain component of the amperometric signal reflects the LFP signal.

To quantitatively determine the extent to which the amperometric signals resembled LFPs, and more importantly, what LFP-like information could be retrieved from amperometric measurements, we compared the spectral content of both signals, particularly for the 1-20 Hz frequency range. As plotted in Figure 4B, the spectrograms generated from the two signals were highly similar, with spectral peaks shifted from high power delta band during baseline, to ~3Hz theta band upon tail pinches, and a strong 5-6 Hz theta band after MS carbachol injection. Indeed, the oscillations at these dominant frequency bands were highly coherent between the two signals (Figure 4C).

Furthermore, the temporal fluctuations of spectral power in individual frequency bins were highly correlated between the LFP and the amperometric signals (Figure 5A), although the strength of correlation tended to be smaller as the frequency increased (to be discussed later). Besides the temporal domain correlation, it is known that LFP spectral features in the frequency domain are characteristic of distinct brain states (Gervasoni, Lin et al. 2004). Accordingly, normalized power spectral density (PSD) calculated from the two signals for individual episodes (baseline, pinch and carbachol-induced theta) showed similar characteristics for those states (Figure 5B). Particularly, the theta/delta power ratios derived from LFP and amperometric signals were similarly effective in distinguishing pinch from baseline states (Figure 5C, paired t-tests, both $p < 0.001$). Together, these results suggest that the LFP and the amperometric signals contain highly similar spectral information.

The evidence mentioned so far was obtained from anesthetized animals. Yet, for many studies, it is often critical, albeit technically challenging, to investigate the release of neuromodulators and its relationship to neurophysiological events in freely-moving animals. To extend our method to freely-moving animals, we implanted sensors into the rat hippocampus for chronic amperometric recordings to compare with LFP signals. Like what we observed in anesthetized rats, LFP and amperometry HFC shared similar spectral characteristics. Specifically, the LFP spectral features, characteristic of different sleep-wake states, were similarly represented in the amperometry HFC (Figure 6A), including prominent theta oscillations during waking period (WK) and rapid-eye-movement sleep (REM), and delta range oscillations during slow-wave sleep. The normalized PSDs, calculated using data obtained from the two recording techniques, were virtually identical for each corresponding sleep-wake state (Figure 6B).

Furthermore, in order to investigate the feasibility of obtaining quantitative LFP information from amperometry recordings, in two rats we also tested the effect of amphetamine, which is known to induce robust high-power theta oscillations (Vanderwolf, Kramis et al. 1977). As expected, theta power calculated from the amperometry HFC increased 2-3 fold (Figure 6C, D), and lasted more than 2 hours.

2.3.1.2 Acquiring local field potential information from amperometric neurochemical recordings

Since high frequency amperometric signals (>1Hz) resemble simultaneously recorded LFPs, we next tested the hypothesis that this high frequency component (HFC) of amperometric signals directly originated from LFPs and not from any chemical reaction on the sensor. A direct prediction of this hypothesis is that amperometry HFC

should not be disturbed by manipulations affecting chemical reactions, including sensor modifications for achieving chemical specificity, such as enzyme immobilization and exclusion layer application (Burmeister, Palmer et al. 2003; Burmeister, Pomerleau et al. 2008).

To show that the amperometry HFC does not have a chemical origin, first we recorded amperometric signals with a choline sensor, composed of choline-sensitive sites coated with choline oxidase, and choline-insensitive self-reference sites (within 400 μ m from the choline-sensitive sites). Previous studies took the differential signal between the choline-sensitive site and the self-reference site as the choline signal (Burmeister, Palmer et al. 2003). As shown in Figure 7A, the raw signals were quite different – the current on the choline site had a large increase upon tail pinch, which was absent on the self-reference site. This differential response, suggestive of an acetylcholine release (Parikh, Pomerleau et al. 2004), was captured by signals below 1Hz (Figure 7B, lower). In contrast, high frequency amperometric signals (>1Hz) on the two sites were almost proportionally correlated (Figure 7B, upper). Such proportionality existed between any two sites from the same sensor (data not shown). Therefore, the amperometry HFC above 1Hz carries information that seems to be independent of the specific chemical (choline) signal.

Although the HFC was not a choline signal, it could still have a chemical origin, resulting from the oxidation of interferents, i.e. oxidizable molecules such as ascorbic acid and dopamine, leaking through the exclusion layer on both choline and self-reference sites. To rule out this possibility, we recorded amperometric signals with bare probes which had neither exclusion layer nor enzyme coating. As a result, all interferents could freely contribute to and generate an oxidation current much larger than that on

sensors with an exclusion layer. Indeed, baseline oxidation current was about 1-3 nA on bare probes (Figure 7C), much larger than the 0.1-0.2 nA on choline sensors with exclusion layers (Figure 7A). If the HFC originated from oxidation of interferents, the HFC amplitude on the bare probes should also increase accordingly. Contrary to this prediction, the HFC amplitude on bare probes remained comparable to that on choline sensors (compare Figure 7C with A, summarized in D) -- even though baseline current varied by more than an order of magnitude (One-way ANOVA, $F=31.8$, $p<0.001$), the HFC amplitude remained relatively stable (One-way ANOVA, $F=2.57$, $p=0.093$). This allowed us to conclude that the amperometry HFC did not originate from the chemical reactions of interferents.

To further rule out the possibility that HFC originated from any chemical reaction, we applied various voltages to the sensor, ranging from +0.7V to 0.0V. As the applied voltage was lowered, fewer oxidation reactions should occur. However, the HFC amplitude again remained relatively stable (Figure 7E, four experiments, repeated measure ANOVA, $F=1.3$, $p=0.33$), suggesting that the HFC does not originate from any chemical reaction.

Together, all the above results support the notion that the amperometry HFC is generated by electrical signals in the brain, rather than chemical reactions on the sensor. In contrast, the residual low-frequency amperometric component contains chemical information.

Although the amperometry HFC described above evidently reflected LFP signals, it remained possible that the amperometry HFC might originate only from signals captured on the amperometric reference electrode, so the LFP-like HFC signals on individual sensor sites (working electrodes) would be identical to each other. To rule out

this possibility and to demonstrate differential HFC signals on individual sensor sites, we investigated the well-described phenomenon of hippocampal theta depth profile (Bland and Whishaw 1976; Scarlett, Dypvik et al. 2004), in which the amplitude and phase of theta oscillations change in characteristic ways across different layers of the hippocampus.

In urethane-anesthetized rats, we induced theta oscillations while lowering the sensor through the hippocampal layers, and observed a typical theta depth profile in the amperometry HFC (Figure 11 A and C). The HFC theta amplitude and phase were calculated from the signals on the four vertically arranged sites located at different depth (200 μ m center-to-center distance between sites, Figure 11A). Every time the sensor was lowered 200 μ m, HFC theta amplitude and phase changed systematically, such that HFC theta on sites 2-4 assumed the HFC theta that had existed on their immediate neighboring sites 1-3 before being lowered (Figure 11A). Single experiment (Figure 11C, left) and the averaged results from five experiments (Figure 11B) showed that the amperometry HFC theta depth profile was highly consistent with the LFP counterpart in urethane-anesthetized rats (Bland and Whishaw 1976; Scarlett, Dypvik et al. 2004). The amplitude profile had both a small and a large local maxima at stratum oriens and the hippocampal fissure, respectively, and a local minimum at stratum radiatum. The phase profile exhibited a rapid phase reversal around the same level of the amplitude local minimum. The amperometry HFC did not have an amplitude “null zone” described in the literature (Bland and Whishaw 1976; Scarlett, Dypvik et al. 2004), but had instead a local minimum. This difference was likely attributable to the larger size of the sensor site (150 μ m vertical length) compared to traditional LFP recording electrodes. Conceivably, this larger size may have smoothed the sharper transitions in the amplitude profile.

Altogether, the existence of a theta depth profile further supports the hypothesis that the amperometry HFC originates from LFP signals on the sensor sites.

The above results demonstrate that amperometric recordings in both anesthetized and freely-moving animals also yield signals similar to LFPs. Thus, we concluded that amperometric recording alone offers a feasible and technical simple solution to obtain both electrophysiological and neurochemical information in both anesthetized and freely-moving animals.

2.3.2 Fine-scale acetylcholine release coupled to theta oscillation

2.3.2.1 Choline increase coupled to theta oscillations on the time scale of tens of seconds

To study theta-related ACh release on fine temporal scales, we first tested whether phasic ACh release co-occurs with theta oscillations induced by tail-pinch (Whishaw 1976). As shown in Figure 9A, pinch induced a clear switch from baseline delta activity to theta oscillations, and a concomitant increase of choline concentration, peaking around 100nM and lasting about 200 sec. This increase indicated a phasic ACh release tightly accompanying the appearance of theta on time scale of tens of seconds. We observed such release in 10 out of 14 rats in which theta oscillations were induced. (The other four had large noise *in vivo*, making the detection of potential choline release impossible.) We pooled trials from individual rats at a depth that had largest choline increase in each rat (more depth-related analysis in next section), and summarized results for all the trials with choline increases exceeding 3 times standard deviation in baseline (Figure 9B, 29 out of 42 trials). To confirm that the “choline” increases were indeed choline signal, but not non-specific signals that occurred in those trials, or when

those channels were at that particular depth, we had two types of sentinel signals: the sentinel channels either at the same time, or at the same depth as the choline increase was observed. Signals on sentinel channels confirmed that such increase was not from non-specific chemical signals, nor was it reflecting very slow LFP signals. Quantification of these ACh releases (average choline signal for the first 120 sec after pinch start) showed that they were significantly different from the signals on sentinel channels (Figure 9C, Mann-Whitney Test, both $p < 0.001$).

Although occurring together, the phasic ACh release and theta oscillations shown above could have been independent and coincidental, only brought together because of the pinch. Alternatively, the two phenomena could have a shared mechanism, and could occur without external stimulus. We looked for spontaneously occurring theta activities, and asked if the fluctuations of the choline signal would be tightly coupled to the appearance of spontaneous theta. This was indeed the case in 3 out of 4 rats when spontaneous theta occurred without any external stimulation. As the example shown in Figure 10D, these choline fluctuations had similar or slightly smaller amplitude compared to pinch-induced ones, and could happen as fast as every 10-20 sec, tightly matching the rise and ebb of spontaneous theta oscillations. These results suggest that phasic ACh release could accompany theta oscillations on time scale of tens of seconds, whether theta was spontaneous or induced.

2.3.2.2 Maximal choline increase around CA1 pyramidal layer

Cholinergic axons and varicosities in hippocampus showed layer specific distributions (Mechawar, Cozzari et al. 2000), suggesting differential ACh release across layers. Our results above implied that phasic choline increase was not observed equally

at all depth in CA1, but had some depth-related distribution. We quantified phasic choline increases at different depths in the dorsal CA1 area, which has been divided into layers based on morphology and cell distribution (Andersen, Amaral et al. 1996). In an example shown in Figure 11C-E, we observed maximal choline increase 0.3mm above the depth of theta phase reversal. Aligned to the phase reversal point in individual rats, choline increases were summarized in histograms at every 0.2mm in depth, which showed the largest choline increase at 0.3-0.6mm above the phase reversal point (Figure 11F, Kruskal Wallis Test, $p < 0.001$). The release at 0.3-0.4mm were marginally larger than 0.5-0.6mm (Mann-Whitney Test, $p = 0.08$, two tails). The median values at each depth similarly demonstrated such depth-related variation. The depth 0.3-0.4mm above phase reversal, based on anatomy and the theta amplitude profile (Bland and Whishaw 1976; Winson 1976; Scarlett, Dypvik et al. 2004), corresponds to the CA1 pyramidal layer and/or slightly above. These results suggest that maximal phasic ACh release in CA1 occurs around or slightly above the pyramidal layer.

2.3.3 Phasic acetylcholine release lagging theta initiation

2.3.3.1 Choline increase slower than theta initiation

Earlier studies hypothesized that MSvDB cholinergic neurons could pace theta oscillations (Smythe, Colom et al. 1992; Brazhnik and Fox 1997), implying that ACh should be released before or at least as fast as theta is initiated. However, other studies suggest that intrinsic properties limit MSvDB cholinergic neurons to discharge at high frequency (Griffith and Matthews 1986), which would not support very fast ACh release in hippocampus when theta is initiated. The issue of whether cholinergic neurons directly participate in theta initiation has not been resolved. Since we observed a phasic ACh

release tightly coupled to theta appearance, we asked whether such phasic ACh participate in theta initiation. In our experiments (example in Figure 12A), phasic choline increase was often very slow, ramping up over a few tens of seconds, while theta onset was very fast (usually <5sec), quantified by the jump of theta power index. Over all trials, theta index rose much faster than the choline signal, reflected by either the rise time, or the rise slope (Figure 12B, Wilcoxon Signed Ranks Test, both $p < 0.001$). Alternatively, we estimated the difference of rise time between the two signals with cross-correlogram (Figure 12C), and the result was consistent with the rise time quantification (Figure 12D, H_0 : lag time = 0, Wilcoxon Signed Ranks Test, $p < 0.001$). Such time lag could not be attributed to a delay caused by the choline sensor (data not shown). All these results indicate that there was a genuine lag between the slow rise of ACh release and the rapid theta initiation, suggesting that the phasic ACh release we observed do not participate in the initiation of theta oscillations.

2.3.3.2 Activities of a subpopulation of low-frequency¹ neurons in medial septal area matching the slow choline increase

Since phasic ACh release did occur during theta oscillations, we predicted that the septohippocampal cholinergic neurons should increase their firing rate with a similar slow speed, which resulted in the slow ramping of choline signal. To test this prediction, we looked for neurons in MSvDB that increased firing during theta, particularly those increased their firing slowly during the theta oscillations. Since recent studies suggested

¹ In Chapter 2, “low-frequency neuron” is used to describe the MSvDB neurons with average firing rates below 4Hz, to avoid potential confusion with the description of “slow firing rate change” during tail pinch. In the rest of the dissertation (especially in Chapter 3), “slow-firing neuron” is used to refer to MSvDB neurons with firing rate below 4Hz.

that MSvDB cholinergic neurons *in vivo* have low discharging rate (Simon, Poindessous-Jazat et al. 2006), we included the low-frequency ones that have not been of focus in most MSvDB neuronal studies.

In experiments, simultaneous implementation of amperometry and extracellular recording was difficult. The online detection of choline increase was very difficult (signals dominated by HFC), and the yield of low-frequency, slow-ramping MSvDB neurons was pretty low too. These factors made it very difficult to capture these neurons with simultaneous choline recording. Despite such difficulty, we managed to obtain a few of them, and one of such neurons is shown Figure 13A. In this example, the neuron was virtually silent during the baseline period, only fired after theta started, and slowly changed its firing rate matching the simultaneous choline signal. For most of the extracellular recordings, we did not implement simultaneous choline recordings, but recorded multiple single neurons from MSvDB with the same pinch stimulation. Two distinct patterns of firing rate change were discovered in these MSvDB neurons. High-frequency neurons (overall firing rate >4Hz) often had a rapid increase in firing at pinch onset, while some low-frequency neurons (<4Hz) increased their firing rate over tens of seconds during the theta period (an example of 6 neurons in a single trial shown in Figure 13B). We similarly quantified the rise time and slope for these neurons (Figure 13C), and grouped the results according to the overall firing rate of the neurons (>4Hz or <4Hz). These two groups were significantly different for both rise time (Mann-Whitney Test, $p=0.001$) and slope ($p=0.001$). The majority of the high-frequency neurons increased their firing rapidly at theta onset (70%, rise time <10 sec), most likely pacing the theta oscillations. In contrast, a substantial proportion of the low-frequency neurons increased their firing slowly (51%, rise time > 20sec, compared to 21% for high-

frequency neurons), matching the slow increase of choline signal in Figure 12. These results demonstrated that a subpopulation of MSvDB low-frequency neurons change their firing rate in a way characteristic to the choline change, suggesting that these neurons may be septohippocampal cholinergic neurons.

2.4 Conclusion

First, we demonstrated that amperometry recordings alone can simultaneously capture both electrophysiological (LFP) and neurochemical information. We showed that the high frequency fluctuations (1-20 Hz range) in amperometric recordings are qualitatively and quantitatively similar to simultaneously recorded LFP signals in anesthetized rats under several experimental manipulations (Figure 4). The amperometry HFC showed similar spectral features as LFPs, and was as informative as regular LFPs about distinct brain states (Figure 5). The similarities were extended to free-moving animals (Figure 6). Using amperometry HFC, we were able to uncover a well-established LFP feature - theta depth profile in the hippocampus (Figure 11 A-C). Importantly, the HFC did not depend on the chemical reactions on the amperometric sensors, and it seemed to be unaffected by sensor modification intended for specific chemical detection (Figure 7). All these results indicate that the high frequency component in amperometric signals reflects LFPs, and it is feasible to obtain LFP information from any amperometric recording, regardless of the target neurochemical.

In the second part of the study, we demonstrated for the first time the existence of theta-coupled phasic ACh release *in vivo*, using amperometric techniques capable of revealing ACh dynamics on much finer spatiotemporal resolutions than microdialysis. In the dorsal CA1 area of the hippocampus in urethane anesthetized rats, these phasic

releases were maximal around or slightly above the pyramidal layer (Figure 11). The temporal dynamics of these releases were on the level of tens of seconds, co-fluctuating with the appearance of spontaneous or induced theta oscillations (Figure 9 and Figure 10). These phasic releases were not required for the initiation of theta oscillations, because they ramped up slowly, trailing the onset of theta oscillations by tens of seconds (Figure 12). Such dynamics matched the firing rate change of a subpopulation of MSvDB low-frequency neurons (Figure 13), which may be cholinergic neurons and the source of the phasic ACh release. Demonstration of such fine-scale ACh dynamics in hippocampus suggests new schemes of its relationship with theta oscillations, and new insights on ACh function.

2.5 Discussion

2.5.1 Acetylcholine and theta oscillations

ACh is shown to be involved in theta oscillations in numerous studies, which mostly focused on how ACh participates in the generation and modulation of theta oscillations (reviews in Bland 1986; Vanderwolf 1988; Bland and Colom 1993; Vertes and Kocsis 1997; Buzsaki 2002). Specifically, Type II theta (e.g. theta under urethane) is atropine-sensitive and can be abolished by muscarinic antagonists such as atropine (Kramis, Vanderwolf et al. 1975; Vanderwolf 1988). Besides antagonists, specific lesion of cholinergic cells in MSvDB also abolishes atropine-sensitive theta, and greatly diminishes the power of atropine-resistant theta (Type I) in freely-moving rats (Lee, Chrobak et al. 1994; Bassant, Apartis et al. 1995). Conversely, cholinergic agonists, or drugs that increases ACh action (such as AChE inhibitors) would induce theta or

enhance theta power (Vanderwolf 1975; Bland 1986; Golebiewski, Eckersdorf et al. 1992).

Although these lesion/pharmacological studies suggest that Type II theta and the power of Type I theta require an intact cholinergic system, they could not reveal whether or not cholinergic activities and the fast dynamics of theta oscillations are related, which could determine the mechanisms underlying ACh/theta functions. Here we have shown that ACh release tightly accompanies the appearance of theta oscillations under urethane anesthesia (Figure 9, Figure 10). Our results revealed yet another level of the tight connection between ACh and theta in the hippocampus, on much finer temporal scales.

The function of such phasic ACh release is not known yet. One possibility could be that such phasic ACh directly contributes to theta generation. This does not seem to be the case, at least not for the initial generation, because the theta index in our experiments usually rose much faster than the choline signal (Figure 12). Our estimation of theta onset was quite conservative, because we calculated a power index of theta with a window of 8 sec, which smoothed out the faster jump of the actual theta power index. In fact, based on original LFP (or amperometry HFC) waveforms, theta onset was most often less than one sec, in other words, almost instantaneous (data not shown). On the other hand, the slow choline increase was not caused by measurement delay, because choline sensors could respond to choline in a few seconds (data not shown) and ACh hydrolysis is very fast too (Parikh, Pomerleau et al. 2004). Therefore, the initiation of theta oscillations happened much faster than the phasic ACh release we observed, which suggests that such phasic ACh is not required for theta initiation. Of

course, our observation cannot rule out the possibility that a tonic baseline level of ACh is required for theta initiation.

Although not contributing to theta initiation, these phasic releases may hypothetically contribute to the power and/or duration of theta. Two microdialysis studies supported this hypothesis, and showed that across rats, hippocampal ACh level is weakly correlated with the spontaneous theta power and/or frequency under urethane anesthesia (Monmaur, Collet et al. 1997; Keita, Frankel-Kohn et al. 2000). Unfortunately, we were not able to test the hypothesis that phasic ACh release dynamically regulate the power and/or duration of theta in individual rats, since theta power/duration is influenced by anesthesia depth (Bland, Declerck et al. 2007; Musizza, Stefanovska et al. 2007), which was not systematically controlled in our experiments.

A more intriguing possibility concerns the role of ACh in neural plasticity. These phasic ACh releases, working synergistically or sequentially with theta oscillations, may provide exceptional opportunities to dynamically modulate neural plasticity on much finer temporal windows than traditionally assumed. Therefore, these phasic ACh may substantiate other functions, such as promoting LTPs and memory formation, which are often associated with theta oscillations in unanesthetized, behaving animals (Kahana, Seelig et al. 2001; Buzsaki 2002; Leung, Shen et al. 2003; Hasselmo 2005). This time course is also suitable to promote immediate-early gene (IEG) expression I studied in Chapter 4.

2.5.2 Temporally- and spatially-refined ACh action

More generally, elucidating the functions of the cholinergic systems requires the understanding of the temporal and spatial characteristics of ACh release. Based on

microdialysis results and because of the lack of experimental evidence on finer temporal scales, ACh dynamics are often assumed to be very slow, essentially as tonic levels changing according to behavioral states. These assumptions have been incorporated into modeling and theoretical framework (Woolf 1996; Cartling 2001; Hasselmo, Hay et al. 2002), limiting the consideration of ACh functions most often to large time scales. In experiments, only one study has demonstrated that phasic ACh release exists and is associated with particular behavior, suggesting that cortical ACh dynamics can act as fast as in seconds (Parikh, Kozak et al. 2007). Although our results are relatively slower, and with smaller peak amplitude, they provide the first evidence for ACh and theta interaction on the level of tens of seconds. The effects of acetylcholine on its targets, particularly through muscarinic receptors, are on the level of ten seconds or more (Cole and Nicoll 1984; Hasselmo and Fehlau 2001). These relatively slow effects suggest that in turn, the release of ACh on a similar or slightly faster time scale is enough to substantiate these functions. Intrinsic differences in fast-firing ability between cholinergic neurons in MSvDB and basal forebrain may cause the different speed of ACh release in cortex and hippocampus (Lee, Hassani et al. 2005; Simon, Poindessous-Jazat et al. 2006). Alternatively, phasic ACh releases may have faster onset and dynamics in unanesthetized rats in general. Whether faster (and bigger) theta-related ACh dynamics in hippocampus exist in free-behaving animals warrants further study.

The functioning of ACh also depends on the spatial distribution of its release. Although the mode of ACh transmission in the forebrain is most often considered as diffuse transmission (Descarries, Gisiger et al. 1997), local spatial heterogeneity may exist. This possibility is supported by studies on the spatial distributions of various cholinergic component, such as cholinergic axons and varicosities, with staining for

AChE (Lysakowski, Wainer et al. 1989), ChAT (Mechawar, Cozzari et al. 2000; Aznavour, Mechawar et al. 2002), or vAChT (Arvidsson, Riedl et al. 1997). These histological studies showed that cholinergic innervation in CA1 is higher in the strata oriens and pyramidale. This is consistent with our observation of layer-distribution of phasic ACh release. Since different layers of CA1 substantiate different input-output functions (Andersen, Amaral et al. 1996; Freund and Buzsaki 1996; Megias, Emri et al. 2001), higher ACh release at the strata pyramidale and oriens suggests that the phasic ACh is in a good position to directly or indirectly act on the soma and modulate the output of CA1. The spatial distribution of phasic ACh release in CA3, dentate gyrus, and along the longitudinal axis of hippocampus, needs further investigation.

Together, our results have revealed that phasic ACh releases in CA1 are able to act on the time scale of tens of seconds, and preferentially occur around or slightly above the pyramidal layer. Associated with the appearance of theta oscillations, these phasic ACh releases may be able to modulate hippocampal functioning on very fine spatiotemporal scales, including plastic changes of the network. These results provide experimental bases for future theoretical framework and modeling regarding the functions of ACh and theta oscillations in the hippocampus.

2.5.3 Putative cholinergic neurons in MSvDB recorded from anesthetized rats

In our single unit recordings, we found that most high-frequency (>4Hz) neurons and part of the low-frequency (<4Hz) neurons increased their firing very fast with theta onset, while a substantial proportion of low-frequency neurons ramped up their firing

over tens of seconds (Figure 13). The distinct physiological properties of these neuronal groups may reflect the different types of neurotransmitter they use.

Since cholinergic and GABAergic neurons in MSvDB are critical for theta generation (Mizumori, Barnes et al. 1989; Lee, Chrobak et al. 1994; Leung, Martin et al. 1994; Yoder and Pang 2005), a lot of interest and debate have been devoted to the chemical identity of the neurons that researchers recorded from MSvDB *in vivo*, especially in urethane-anesthetized animals. Neurons producing different neurotransmitters are assumed to form distinct populations which have characteristic action potential waveforms and/or responses to pharmacological agents (Lamour, Dutar et al. 1984; Stewart and Fox 1989; Brazhnik and Fox 1997; Brazhnik and Fox 1999). Earlier studies speculated that both cholinergic and GABAergic neurons can fire at high frequency and fire rhythmically during theta oscillations, which paces theta (Stewart and Fox 1989; Smythe, Colom et al. 1992; Brazhnik and Fox 1997; Apartis, Poindessous-Jazat et al. 1998; Brazhnik and Fox 1999). However, more recent studies seem to be reaching a consensus that fast firing GABAergic neurons in MSvDB fire rhythmically and pace theta (Serafin, Williams et al. 1996; Borhegyi, Varga et al. 2004; Hangya, Borhegyi et al. 2009), while cholinergic neurons probably discharge at a low rate (Markram and Segal 1990; Sotty, Danik et al. 2003; Simon, Poindessous-Jazat et al. 2006). Given the difficulty in determining the chemical identities of the *in vivo*-recorded neurons, only one study has identified cholinergic neurons *in vivo*, and concluded that the few cholinergic neurons (ChAT+) in their study were all low-discharging and could not rhythmically-burst in relation with theta (Simon, Poindessous-Jazat et al. 2006). Their sample number, nevertheless, was too low for making other conclusions about the temporal interaction between cholinergic activity and theta oscillations. Our results here are consistent with

the idea that a subpopulation of low-firing-rate neurons are cholinergic. Those neurons we observed had a slow increase during the pinch-induced theta period, matching the slow choline increase (Figure 13), suggesting that they may be the cholinergic neurons responsible for the observed ACh release. On the other hand, the majority of the high-frequency neurons increased their firing almost instantaneously, consistent with the GABAergic neurons described to pace the theta oscillations.

Figure 3. Simultaneous recording with amperometry and electrophysiology.

A. Schematics and example of simultaneous recording. *Upper right*, LFPs and neuronal activities recorded with an MEA in the hippocampus; *lower right*, amperometry recording with a four-channel choline sensor in the contralateral hippocampus. **B.**

Schematics, amperometric signal from an individual channel can be separated into low and high frequency components, reflecting chemical and LFP signals, respectively.

Figure 3

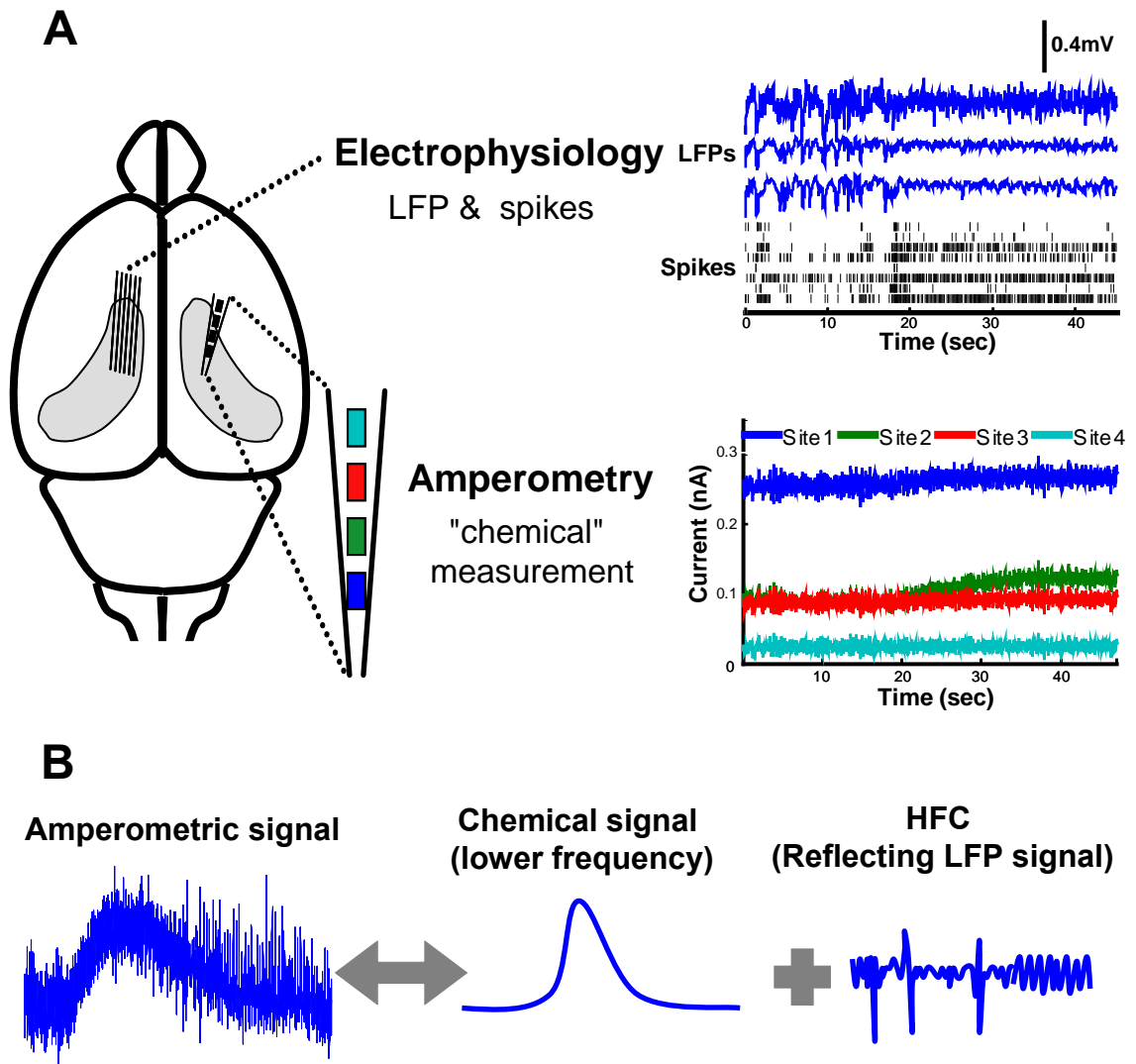


Figure 4. Simultaneous recordings reveal similarity between high frequency LFP and amperometric signals (>1Hz).

A. An example of simultaneously recorded LFP (upper traces) and amperometric signals (lower traces) from contralateral hippocampi (shaded area in the schematic) in urethane-anesthetized rats. Three tail-pinches (*, delimited by purple lines), followed by carbachol injection into the medial septum (grey lines), were applied to modulate LFP and amperometric signals. The top expanded traces show signals at a finer temporal resolution upon pinch (left, purple arrow) and after carbachol injection (right). **B.** High similarity between power spectrograms of the LFP (upper) and amperometric signals (lower). Log power values are color-coded with matched color scales (original signal unit, mV and nA, respectively). **C.** High coherence at dominant frequency bands in different states between the example LFP and amperometric signals in (A). Only significant coherence is plotted (non-significant coherence in white).

Figure 4

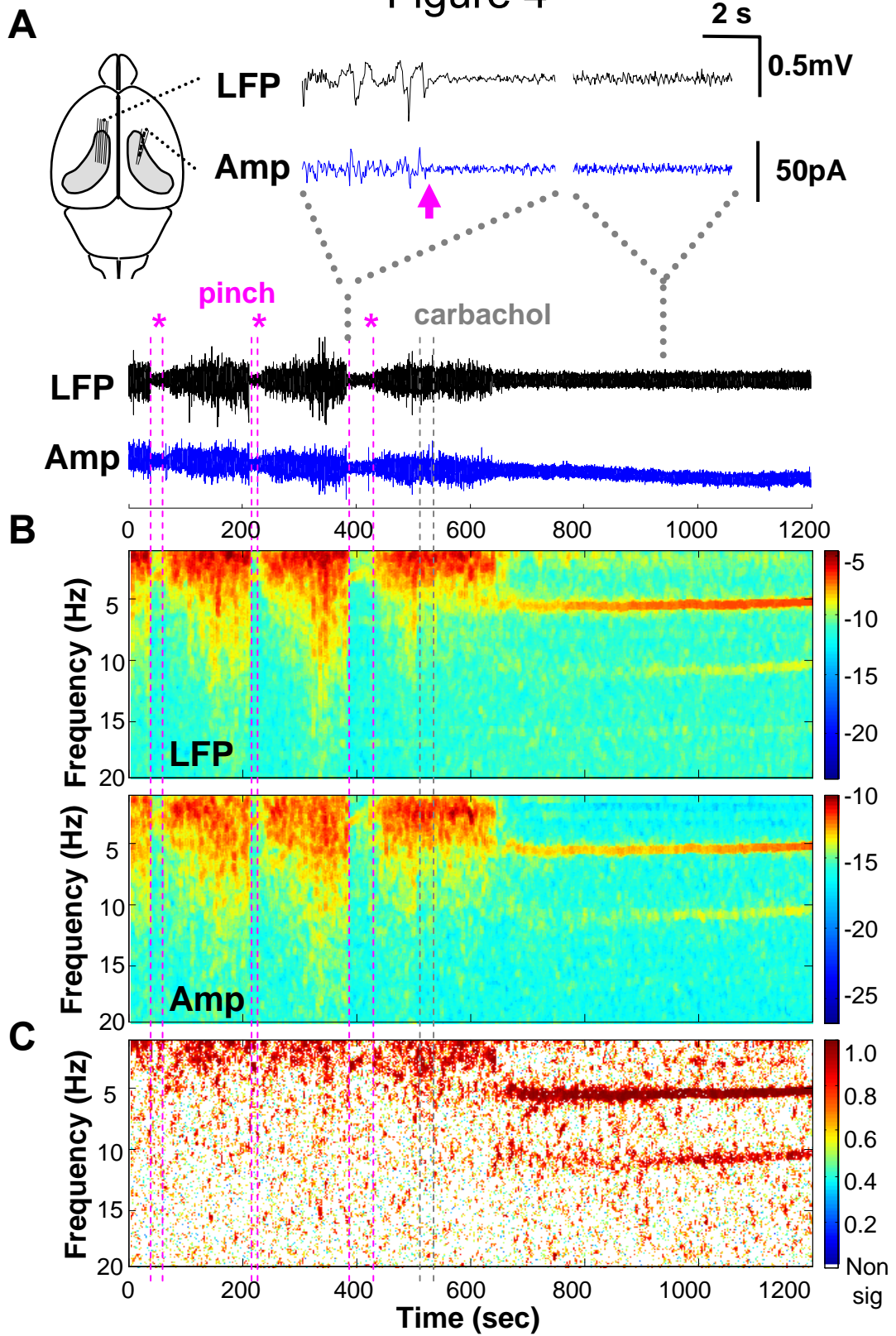


Figure 5. Similar spectral information can be obtained from either LFP or high frequency amperometric signals.

A. Correlation coefficient of spectral power fluctuations at individual frequencies between LFP and amperometric signals, averaged across five experiments (mean \pm s.e.m.). For illustration purpose, p-values smaller than 10^{-6} are set as 10^{-6} . **B.** Average power spectral density (PSD) for LFP and amperometric signals in the three different states (baseline, pinch and carbachol injection), normalized by the total power in that state (n=3 for baseline/pinch, mean \pm s.e.m.; n=2 for carbachol injection, individual black lines). **C.** Spectral indices calculated for baseline and pinch episodes were significantly different, in both LFP and amperometric recordings (**, $p < 0.001$). Each line connects a pair of corresponding baseline and pinch episodes (six experiments, 17 trials). Amp, amperometry.

Figure 5

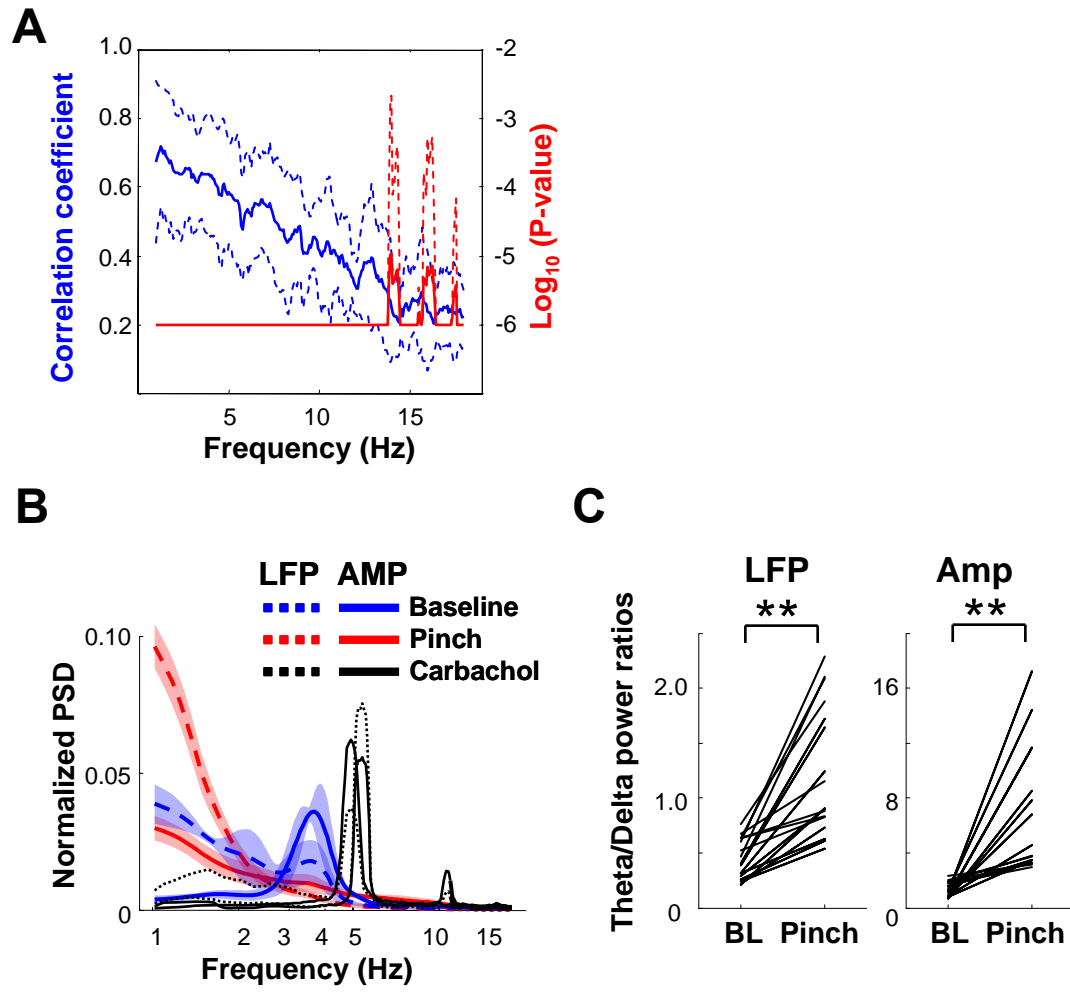


Figure 6. Physiological and pharmacologically-induced frequency signatures preserved in amperometry HFC signals recorded in free-moving rats.

A. Example spectrograms of simultaneously recorded LFP and amperometry HFC during waking (WK), slow-wave sleep and rapid-eye-movement sleep (REM) in a free-moving rat (matched color scales). Note the similar spectral patterns in all sleep-wake states. **B.** Normalized PSDs of LFPs recorded in MEA-implanted rats (upper, 5 rats, 5 sessions) and of HFC signals recorded in amperometric sensor-implanted rats (lower, 3 rats, 7 sessions). Lines and shaded area, mean \pm s.e.m. **C.** An example spectrogram of HFC signals showing a pronounced increase in theta power after amphetamine injection. **D.** Normalized PSDs of the HFC before and after amphetamine injection in **C**. Amp, amperometry.

Figure 6

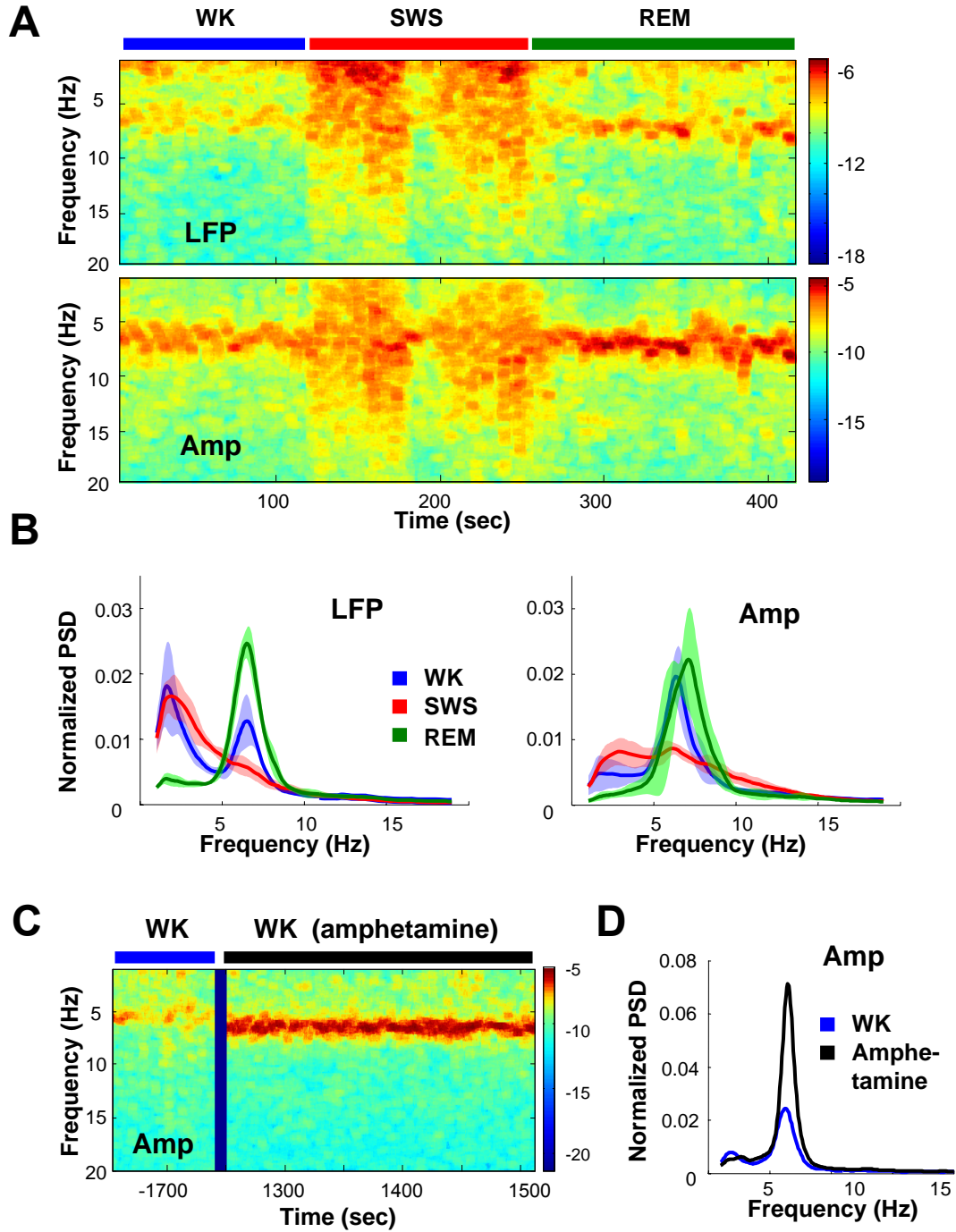


Figure 7. Amperometry HFC not affected by sensor modifications intended for neurochemical detection.

A-B. Amperometry HFC not reflecting choline fluctuations. **A.** Choline concentration increased by tail-pinch (purple arrow), reflected by signal increase on the choline sensor site (blue), but not on the self-reference site (cyan). Black traces, low frequency (<1Hz) signals. **B.** Low frequency (<1Hz) signals on the two sites were very weakly correlated (*upper*). In contrast, amperometry HFC (>1Hz) on the two sites were almost proportional (*lower*). **C.** Similar LFP-like HFC signals also appeared on bare sensors. *Left*, raw amperometric signal on all four bare sites (black traces, signals < 1Hz). The lack of exclusion layer lead to very large baseline oxidation currents compared to those on the choline sensor in **A**. The baseline oxidation current decreased when the probe was moved (blue arrow) from the hippocampus to the overlaying cortex, reflecting a change in local chemical composition. *Right*, HFC signals on the bare probes had amplitude comparable to that on the choline sensor in **A**. The oscillation pattern of HFC signals also changed from delta to theta band upon pinch (purple arrow). **D.** Comparison of amperometry HFC amplitude with baseline oxidation current. Each data point was obtained from a same recording site. Diagonal line indicates unity. Note that although the baseline current varied almost two orders of magnitude, the amplitude of the HFC remained stable regardless of enzyme coating and/or exclusion layer. **E.** Individual values (black dots) and box-and-whisker plot for HFC amplitude at different amperometric voltages.

Figure 7

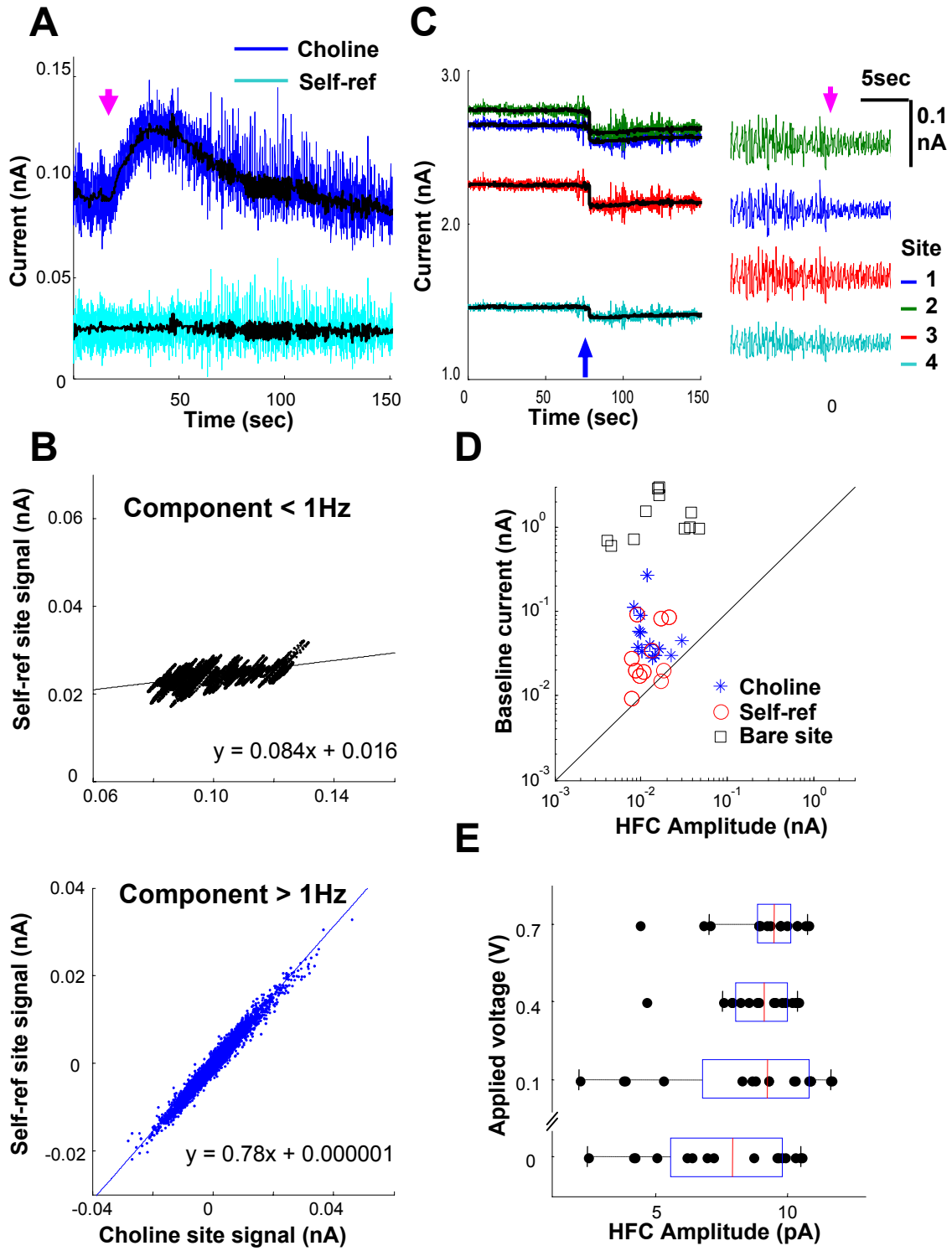


Figure 8. Noise reduction and LOD improvement for *in vivo* amperometric signals, and sensor response time *in vitro*.

A. Noise reduction. *Left to right.* 1, Baseline decay removed first. 2, Choline channels referenced to the sentinel channels, and sentinel channels referenced to each other; all referencing were corrected with effective electrode area (numbers in the middle, normalization factors for area). 3, Signals converted to choline concentrations (nM) with *in vitro* sensitivity values; dotted lines, $\pm 3x$ standard deviation (SD). **B, C.** Limit-of-detection (LOD) *in vivo*, taken as $3xSD$ during baseline, for all the trials. Local-fit, choline/sentinel signal smoothed by local-fitting algorithm. Without fitting, the majority (75%) of LODs were below 100nM; with fitting, the majority were below 10nM. **D** Example of flow-injection analysis of choline sensor response time. This sensor was made together with other ones that were used *in vivo*. The flow injection system provides very fast switching between test solution (choline, 20 μ M or H₂O₂ 8.8 μ M), and regular buffer. Pink lines, start and end of flow injection; red and blue traces, signals on choline or sentinel channels. The delay for H₂O₂ response is considered to be caused by flow time. This delay discounted, choline sensor responded to choline in less than 2 sec.

Figure 8

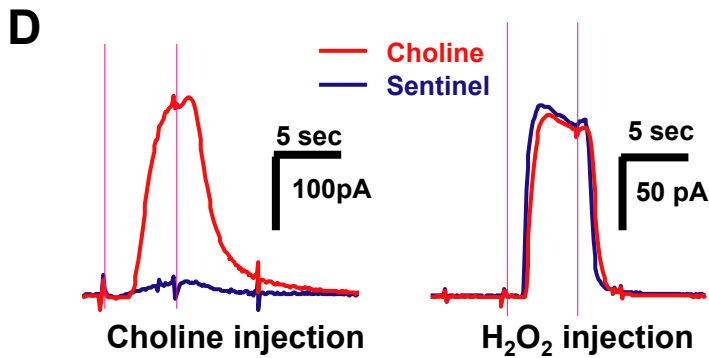
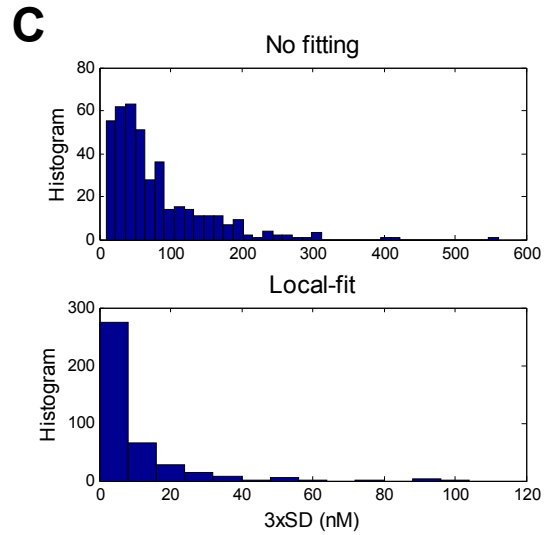
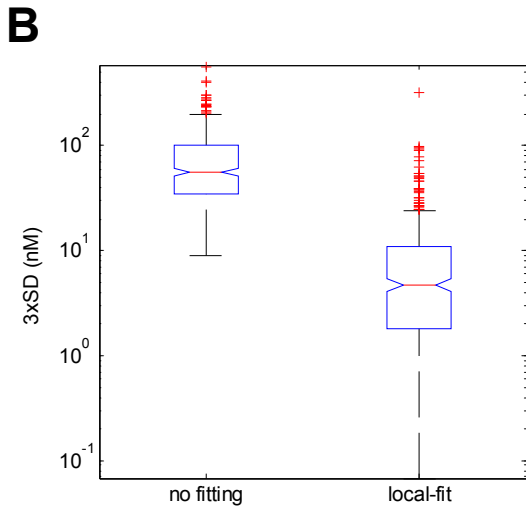
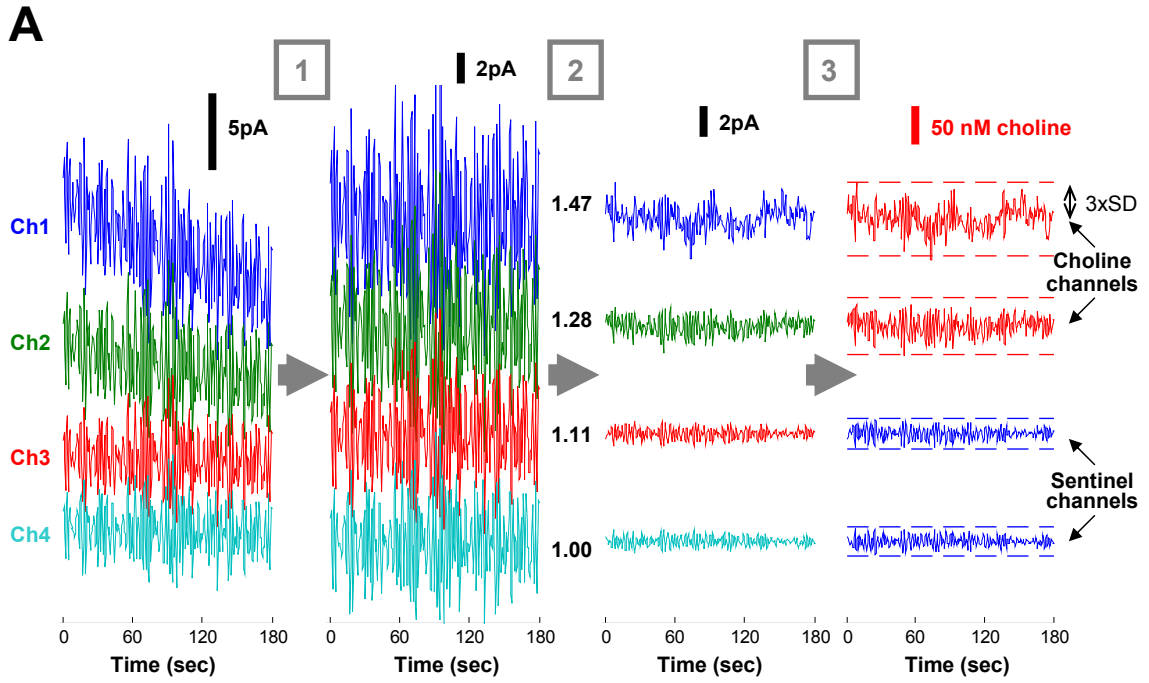


Figure 9. Phasic choline increase coupled to theta oscillations induced by tail pinch.

A. An example of phasic choline increase coupled to theta oscillations induced by tail-pinch (between pink lines). Red and blue traces, choline and sentinel signals; black lines, local-fit of the two signals. Horizontal dotted lines indicate $\pm 3 \times \text{SD}$ of baseline fluctuations. Pseudocolor spectrogram (lower) shows theta oscillations caused by pinch.

B. Phasic choline increases averaged from ten rats, each from the depth that showed maximal choline increase in an individual rat (more details about depth distribution in Figure 11). For each trial included (29 trials total), choline increase exceeded its baseline fluctuation ($3 \times \text{SD}$). Pink line, pinch start; solid lines and shading, average $\pm \text{SEM}$; Sentinel(Time), sentinel signals in the same pinch trials but at other depths; Sentinel(Depth), sentinel channels at the same depth which showed choline increase but in other trials in the same rat.

C. Choline increase quantified (averaged for 120sec after pinch) for all trials in B. Black dots, values from individual trials; **, $p < 0.001$.

Figure 9

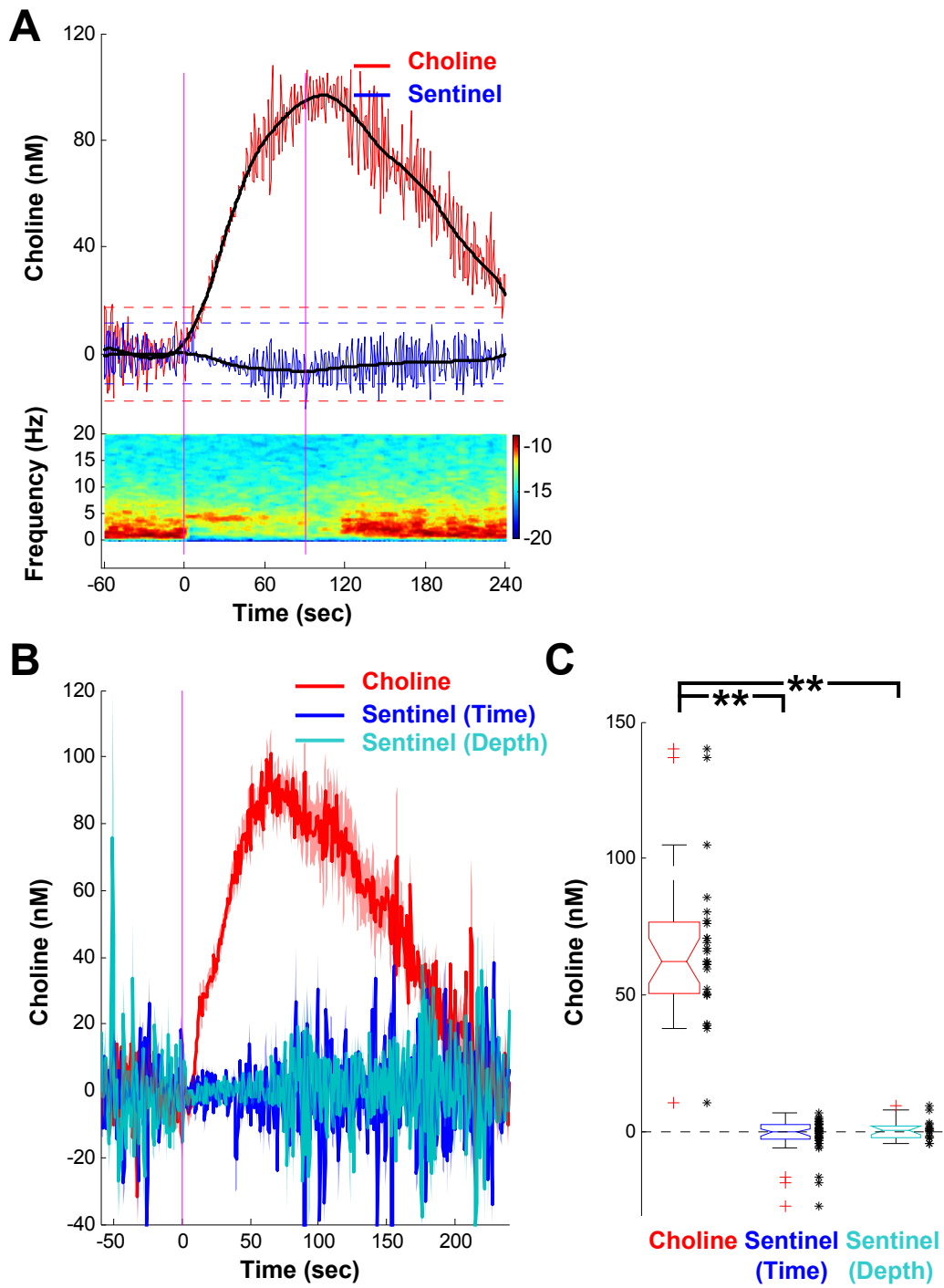


Figure 10. Phasic choline increase coupled to spontaneous theta oscillations.

Choline increases tightly accompanying spontaneous as well as pinch-induced theta. Overlaying gray boxes indicate three pinches. Red and blue traces, choline and sentinel; black trace, theta index calculated from spectrogram; gray trace in the bottom, HFC of amperometric signal. Spectrogram calculated from HFC also shows the spontaneous and induced theta. Arrows indicate spontaneous choline / theta with amplitude comparable to induced ones.

Figure 10

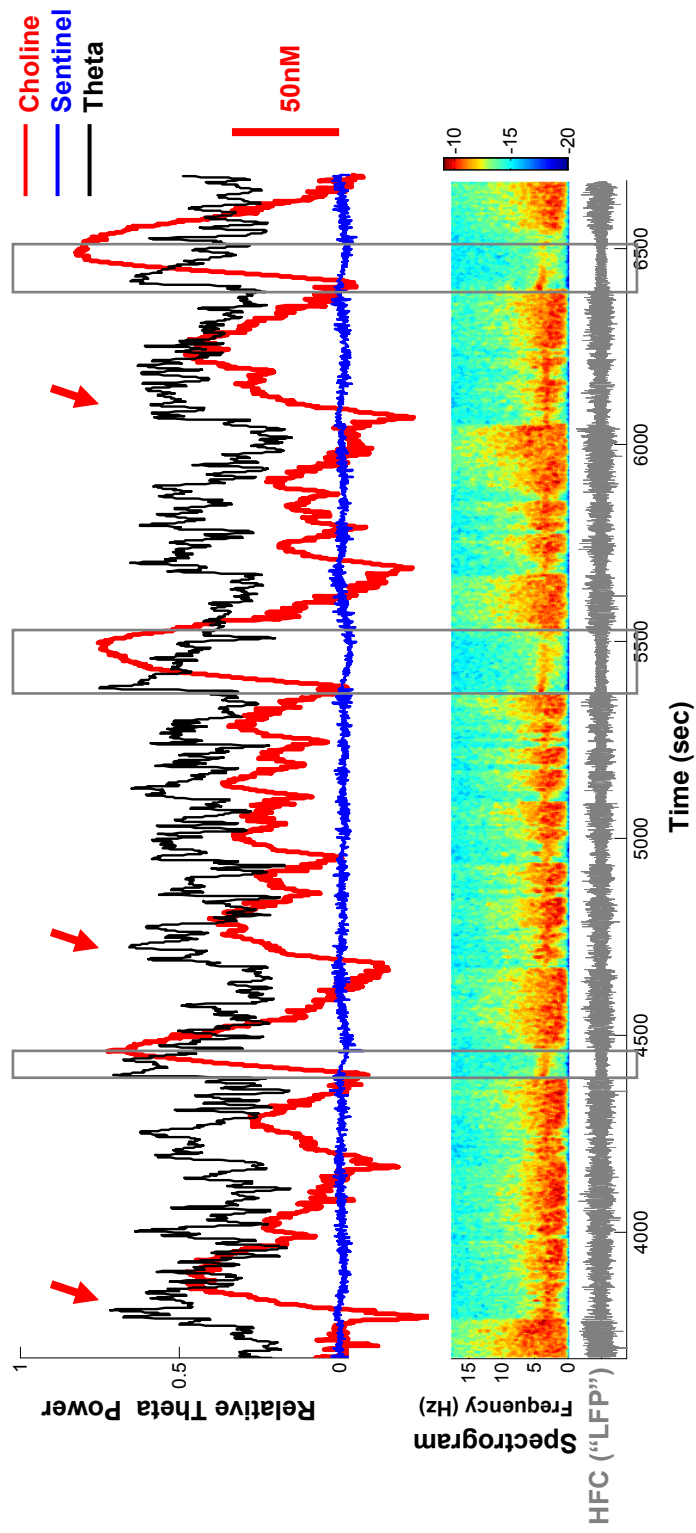


Figure 11. Maximal phasic choline increase observed around CA1 pyramidal layer.

A. An example of theta amplitude and phase changes at different depths of the hippocampus. HFC signals were color-coded for the four sensor sites. Numbers on the left, depth below dura surface. Note the different theta amplitude and phase (phase reversal emphasized by the dotted lines) across sites. As the sensor was lowered 200 μ m, theta amplitude and phase on each site (*right*) assumed the value of its immediate neighbor before being lowered (*left*). **B.** Averaged theta depth profile (mean \pm s.e.m., 5 rats), aligned according to the midpoint of theta phase reversal (defined as depth 0). **C-E.** Example of phasic choline increases in one rat. **C.** HFC theta depth profile for the recording session in **A.** Depth 0, phase reversal; horizontal box, putative pyramidal layer. **D.** Choline and sentinel signals induced by pinch. Pink line, pinch start. **E.** Choline increase quantifications (120sec average) at different depths, maximal observed at +0.3mm. **F.** Summary of depth-distribution of choline increase from ten rats. Histograms show varying choline increase distributions at different depths. Maximal choline increase around 0.3-0.6mm above phase reversal. Red and blue lines indicate median values at each depth, with a peak at 0.3-0.4mm for choline. *, $p < 0.05$, compared to distributions at other depths; increases at 0.3-0.4mm were marginally larger than at 0.5-0.6mm, $p = 0.08$, two tails.

Figure 11

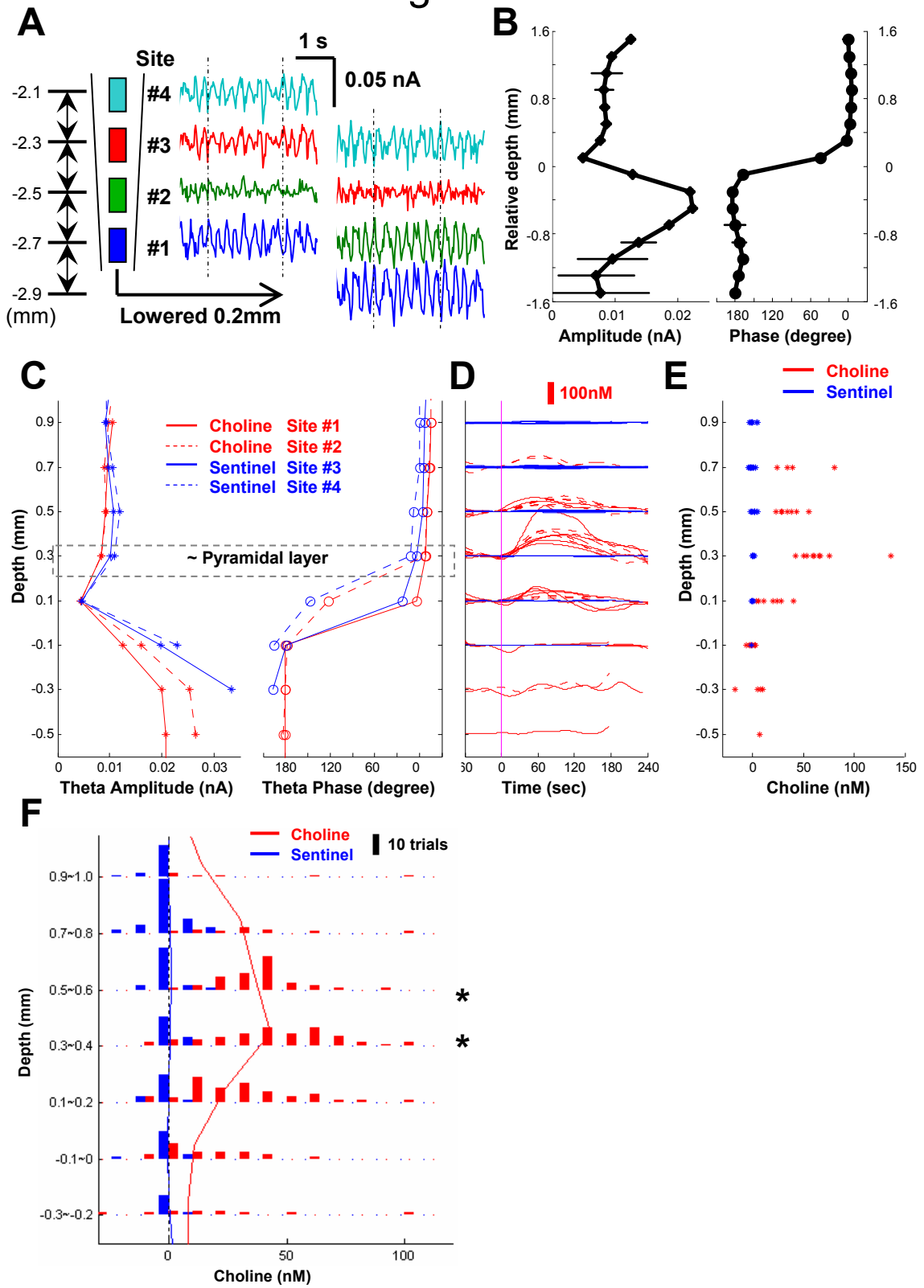


Figure 12. Phasic choline increase often lags theta initiation.

A. An example of slower choline increase compared to concomitant theta oscillations. Vertical blue lines indicate the time choline signal or theta index reached 80% of its maximal value (T_{80} , or rise time). Oblique blue lines indicate slopes for the signals to rise from 30% to 70% of maximum. Inset on right, magnified view of rapid rise of theta index (indicated by the box and black bar on the left). **B.** Summary of rise time (*left*) and slope (*right*) for paired choline signal and theta index. Each pair (one point) from one trial with significant choline increase; red points from the trials displayed in Figure 9B-C. Dotted lines indicate unity. Rise time for theta (theta initiation) was usually very short (<5sec), much faster than choline rise (both T_{80} and slope, $p < 0.001$). **C.** Cross-correlation between choline signal and theta index. Red curves, trials in Figure 9B-C; black curves, all trials with choline increase; solid lines and shading, average \pm SEM. Blue arrow indicate the lag time with the maximal correlation (30~70sec, theta leading). **D.** Summary of correlation lag time and rise time difference (ΔT_{80}) for all trials in B. Dotted line indicate unity.

Figure 12

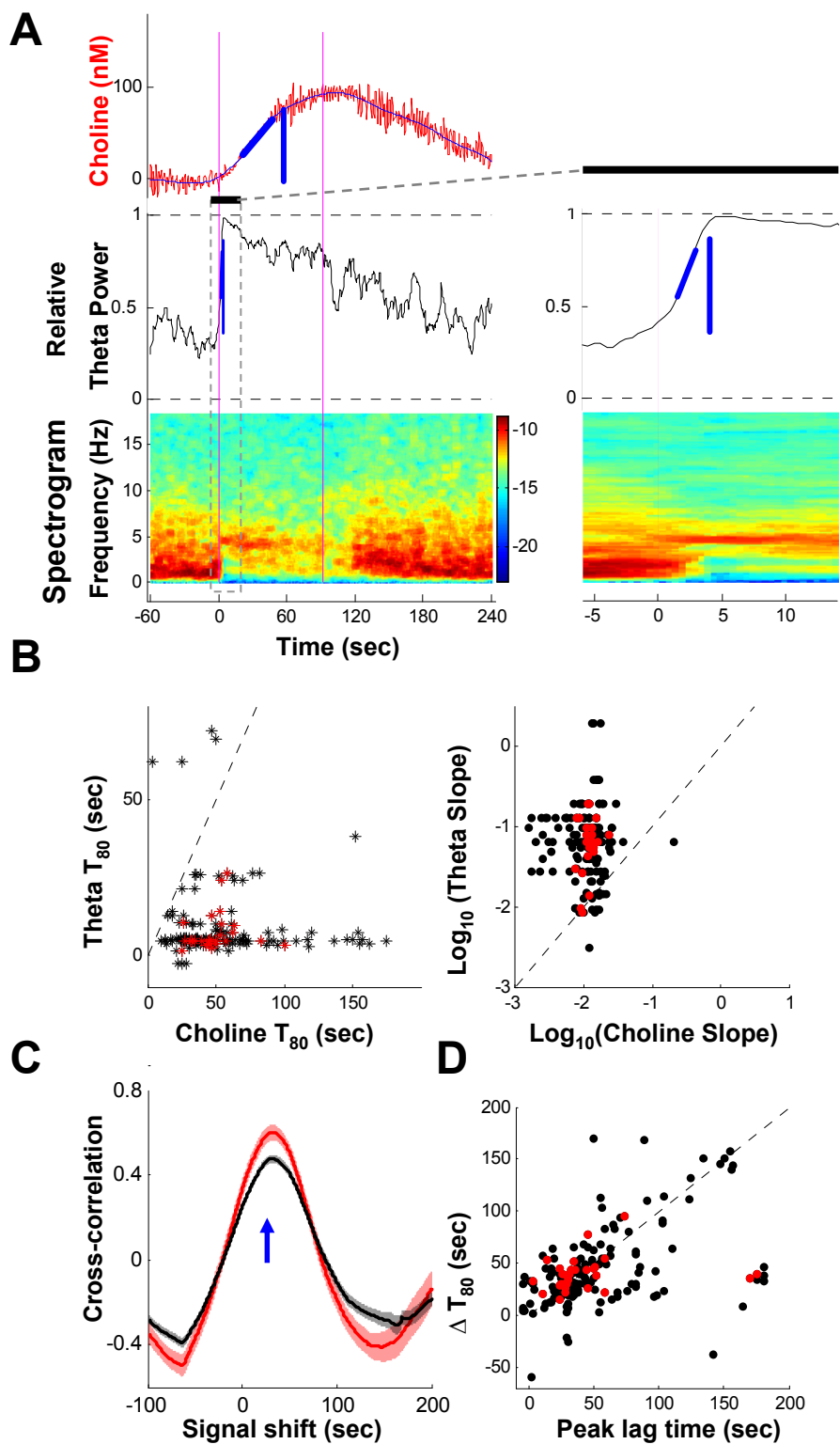
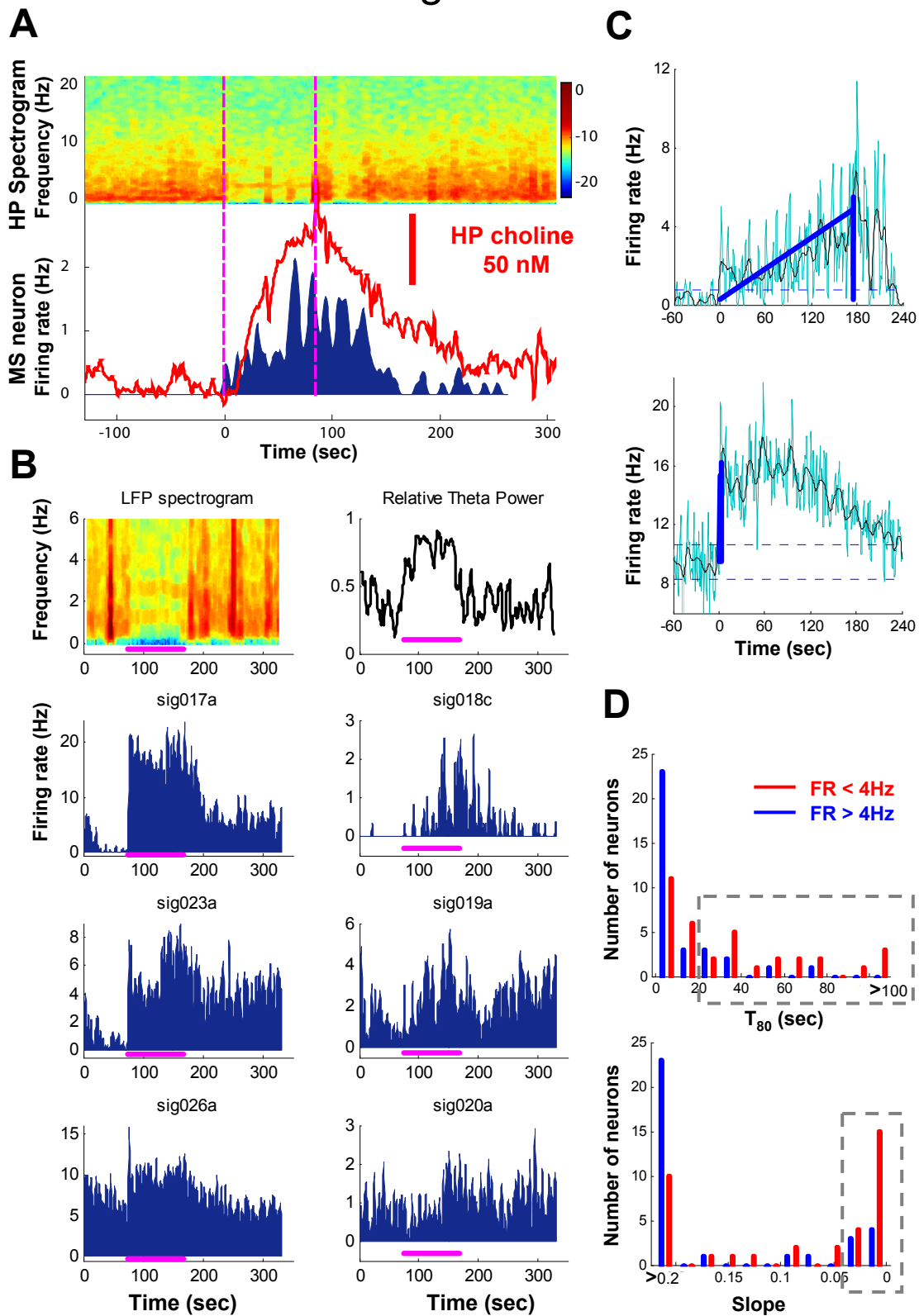


Figure 13. A subpopulation of low-frequency MSvDB neurons has slow firing rate increase matching the slow choline increase.

A. Firing rate change of a single MSvDB neuron matching simultaneously-recorded choline signal, both rising slowly, while theta initiation was much faster (spectrogram on top). Pink lines, pinch. **B.** Six MSvDB neurons (single units) recorded simultaneously during one pinch trial (pink bar). Three neurons on left had high average firing rate (>4Hz), and increased their firing rate rapidly upon pinch, while the three low-frequency MSvDB neurons (on the right) increased their firing over tens of seconds. **C.** Example of two simultaneously-recorded neurons with rise time (T_{80} , vertical blue line) and slope (0-70% maximal, oblique blue line) calculated. **D.** Summary for all neurons (single units) with significant increase of firing during pinch-induced theta episode, grouped according to their average firing rates (>4Hz or <4Hz). High-frequency neurons tended to have rapid rise, matching the rapid theta initiation. In contrast, a substantial proportion of low-frequency neurons (grey rectangles, 51%) tended to increase their firing much slower, consistent with the relative slow increase of choline signals in Figure 12.

Figure 13



Chapter 3 Putative medial septal cholinergic neurons promote hippocampal arousal and theta oscillations

3.1 Introduction

The subcortical structure, medial septum - vertical limb of the diagonal band of Broca (MSvDB), is an integral part of the septohippocampal system. It is important for many types of hippocampal dependent memories and theta oscillations in the hippocampus. Early studies have revealed that lesion or inactivation of MSvDB recapitulates many memory deficits of hippocampal lesion (Mahut 1972; Winson 1978; Gray and McNaughton 1983; Mizumori, Perez et al. 1990). Furthermore, MSvDB is considered the key pace-maker of hippocampal theta oscillations (Stumpf, Petsche et al. 1962; Macadar, Roig et al. 1970; Morales, Roig et al. 1971; Winson 1978; Andersen, Bland et al. 1979; Buzsaki, Leung et al. 1983; Bland and Bland 1986; Mizumori, Perez et al. 1990). MSvDB sends out cholinergic, GABAergic and recently discovered glutamatergic projections to hippocampus (Lewis, Shute et al. 1967; Kohler, Chan-Palay et al. 1984; Kiss, Patel et al. 1990; Hajszan, Alreja et al. 2004; Gritti, Henny et al. 2006). Among the three, cholinergic neurons in MSvDB are shown to be important for normal theta oscillations, and hippocampal-dependent learning and memory functions, which were revealed by studies using cholinergic specific lesion (Lee, Chrobak et al. 1994; Bassant, Apartis et al. 1995; Steckler, Keith et al. 1995; Dougherty, Turchin et al. 1998; Pizzo, Thal et al. 2002; Parent and Baxter 2004; Fontan-Lozano, Troncoso et al. 2005). However, the *in vivo* behavior of MSvDB cholinergic neurons and the mechanism of their functions remain unclear, especially as their firing properties are almost not known.

To address the above questions, the first step is to record from the MSvDB cholinergic neurons. This has remained an unresolved issue, since there is no easy way to identify which of the neurons recorded *in vivo* are cholinergic neurons. Neuronal recordings *in vivo* have revealed that many neurons in the MSvDB spike rhythmically or at least in correlation with theta oscillations (Stumpf, Petsche et al. 1962; Morales, Roig et al. 1971; Feder and Ranck 1973; Apostol and Creutzfeldt 1974; Gaztelu and Buno 1982; Ford, Colom et al. 1989; Stewart and Fox 1989). The chemical identity of these neurons recorded in the MSvDB has been debated for a long time. Early studies grouped neurons as cholinergic or GABAergic, based on their spike waveform and responses to pharmacological intervention, and suggested that both cholinergic and GABAergic neurons were rhythmic firing and could pace theta oscillations (Bland 1986; Stewart and Fox 1989; Brazhnik and Fox 1997). These studies were in contradiction with some *in vitro* studies which suggest that cholinergic neurons cannot fire rhythmically because their intrinsic properties limit their bursting ability (Griffith and Matthews 1986; Markram and Segal 1990; Sotty, Danik et al. 2003). Recent *in vivo* studies which recorded from identified non-cholinergic neurons also seem to reach a consensus that GABAergic neurons are responsible for the pacing of theta oscillations (Serafin, Williams et al. 1996; Simon, Poindessous-Jazat et al. 2006; Varga, Hangya et al. 2008; Hangya, Borhegyi et al. 2009). One recent *in vivo* study recorded from identified MSvDB cholinergic neurons and suggested that they fire at very low frequency and do not fire in relation with theta (Simon, Poindessous-Jazat et al. 2006).

These controversial results raised more questions about the behavior of MSvDB cholinergic neurons *in vivo*, and the exact role they play, especially in normal behaving animals (Simon, Poindessous-Jazat et al. 2006). However, although juxtacellular

recordings have been applied successfully in unanesthetized, head-fixed animals, major difficulty remains in the identification of MSvDB cholinergic neurons in free-moving animals. A viable alternative may still be to look for neurons that match plausible firing properties of MSvDB cholinergic neurons in normal behaving animals.

Besides the suggestion that MSvDB cholinergic neurons are slow-firing, there are some other hints about how they might behave under different behavioral states and respond to external stimuli. Hippocampal ACh level has been shown to be high during REM sleep and waking, but low during slow-wave (SW) sleep (Marrosu, Portas et al. 1995; Bianchi, Ballini et al. 2003). It is likely that cholinergic neurons, as the source of hippocampal ACh (Lewis, Shute et al. 1967; Mesulam, Mufson et al. 1983; Dutar, Bassant et al. 1995), would have similar firing rate changes across sleep-waking cycles. In another line of research, cholinergic neurons have been suggested to respond transiently to sensory stimuli, such as auditory stimulus (Miller and Freedman 1993).

Armed with these pieces of knowledge, we recorded neuronal activities in the MSvDB from behaving rats, and identified a subpopulation of slow-firing MSvDB neurons that had these properties. We further looked at their firing properties and their influences on hippocampal LFPs.

3.2 *Material and methods*

3.2.1 *Electrodes, animals and surgery*

Multi-electrode assembly or array (MEA) was constructed similarly to earlier studies (Nicoletis, Dimitrov et al. 2003; Lin and Nicoletis 2008). On each assembly, two 29-gauge stainless-steel cannulae were secured, with tips separated by 0.8mm

(horizontal) and 0.5 mm (vertical). As a bundle, 8 or 16 35- μ m tungsten wire electrodes were threaded together through each cannula. The bundles could be advanced by microdrives with precision over the course of the experiments. The total range of advancement was 2 mm in length. Wires spread slightly from the cannula tip after being pushed out, covering a semi cone-shaped area for about 1-1.5 mm in diameter at the end (Figure 14A). Multi-electrode array was arranged in a 4x4 form (250 μ m spacing). Two of the four rows, aiming at dentate gyrus (DG), were 0.7mm longer than the rest, which aimed at CA1.

Animal use and procedures were approved by the Duke IACUC and performed in accordance with NIH guidelines. Eight adult male Long-Evans rats (300-500g) were used in the experiments.

Surgeries for electrode implantation has been described earlier (Nicoletis, Ghazanfar et al. 1997). Animals were anesthetized with ketamine (100mg/kg) and xylazine (5mg/kg) and positioned in a stereotaxic frame. Atropine (0.02mg) was used to reduce airway secretion. Stainless steel screws were secured above frontal cortex and cerebellum, serving as grounds. Craniotomies were opened above the MSvDB region (AP +1.5- 0 mm, ML 0.5-1.5 mm relative to Bregma) and hippocampus unilaterally (AP - 4.0mm, ML 2.5mm, \sim 1x1 mm) (Paxinos and Watson 2005). MEA with two movable electrode bundles was lowered into MSvDB with an angle of 9.5° on the coronal plane, targeting two locations in MSvDB: AP+1.1/+0.3mm, ML 0mm, -6.2/-5.7mm below dura. A 4x4 array was lowered into one hemisphere to record from CA1 (-2.2mm below dura) and dentate gyrus (DG, -2.9mm below dura). Dental acrylic was used to cover and secure the implant with the help of anchoring screws. Rats were allowed to recover for at least 14 days after surgery before recordings.

3.2.2 Behavior task, auditory stimuli and electrophysiological recording

3.2.2.1 Undisturbed sleep-waking

Animal behavior was monitored on-line with a camera and recorded on video tapes. Rats were allowed to freely move around or sleep for 1~1.5 hr in the recording session, in the light/sound attenuated chamber they had been habituated to and the same one they would perform the behavioral task. To minimize disturbance during sleep, sleep-waking states were monitored remotely using online detection algorithm based on LFP spectral features (Gervasoni, Lin et al. 2004).

3.2.2.2 Behavioral task and auditory stimuli

In each recording session, rats performed a variant of the Go/NoGo behavioral task for 1~1.5 hr. The apparatus (Med Associates Inc, VT), behavioral training and task details have been described elsewhere (Lin and Nicolelis 2008). Three cues, an 80dB 6kHz tone, an 80dB white noise sound or a light (on), each lasting 2 sec, were presented in a random order during the task, with inter-trial interval (ISI) randomly varied between 6-18 sec (6, 8,10,14,18 sec). Each animal was assigned to respond to one of the cues within 5 sec of the cue onset to get reward (~ 0.4mL 10% sucrose). After they retrieved their reward, or if they did not respond, a new trial (new ITI) would start. If they licked during the ITI, the trial would be reset. There was no punishment to respond to the other two cues, or not to respond to the rewarding cue. For each type of auditory stimulus, it could be either a rewarding cue, a distracter when the other auditory cue was associated with reward, or non-relevant when the light cue was associated with reward.

3.2.2.3 Electrophysiological recording

Electrical signals were amplified with TBSI 2x or 1x headstages (Triangle BioSystems, Inc. Durham, NC, USA). Neuronal and local field potential (LFP) signals were filtered at 154-8.8kHz and 0.4-240Hz, digitized at 40kHz and 2kHz, respectively, and recorded with Multichannel Acquisition Processor (Plexon Inc, Dallas, TX). Single units were identified online based on spike waveform to aid off-line processing of single unit data (Figure 14D-F). LFP signals were also transmitted online to a remote computer to monitor the sleep-waking states of the animal.

3.2.3 Data analysis

3.2.3.1 Single unit isolation (spike sorting)

Spike waveforms were processed with offline sorter (Plexon Inc, Dallas, TX) to obtain single units. Effort was used to ensure the isolation of single units (Figure 14D-F), with signal-to-noise ratio larger than 3 and minimal amount (<0.1%) of “spike collision” (spikes occurred within the action potential refractory period, set as 1.2ms). The timestamps of the single units and LFP signals were further analyzed in Matlab (The MathWorks, Natick, MA).

3.2.3.2 Sleep-waking analysis and SIA definition

Sleep states were characterized as described earlier (Gervasoni, Lin et al. 2004). Spectral features were obtained to determine the behavioral state of the animal, as three gross categories, waking (WK), slow-wave (SW) sleep and rapid-eye-movement (REM)

sleep. Firing rates of individual neurons were calculated for the whole recording session (average) and individual sleep-waking states (Figure 15A). Instantaneous firing rates were calculated by binning spikes into each second and smoothed.

Small-amplitude irregular activity (SIA) epochs were further determined in the SW sleep episodes, based on methods described elsewhere (Jarosiewicz and Skaggs 2004). Root-mean-square amplitude of hippocampal LFP was calculated and smoothed for 0.5 sec bins. An amplitude threshold was set at a local minimal in the amplitude distribution around the 20th percentile of the distribution. Individual SIA epochs were defined as a continuous period with 80% of the amplitude below amplitude threshold, and no gaps (large amplitude) longer than 1.5 sec (Figure 17A). The remaining part of the SW sleep was defined as large-amplitude irregular activity (LIA) epochs.

3.2.3.3 Firing property indices for individual neurons

The REM index for each neuron was defined as the ratio between firing rates of REM and SW sleep.

Response to auditory stimuli was characterized using peristimulus time histograms (PSTH) with 5 ms bins. The auditory response index (Aud index) was defined as the ratio between averaged PSTH values during 15-35ms after and 300-5 ms before the stimulus onset (Figure 16B). Unless specified, the Aud index was calculated for the white noise stimulus. Aud index > 1 represents excitatory response, while index <1 represents inhibitory ones.

Histograms similar to PSTH were calculated for individual neurons, with spikes aligned to SIA onset at 100 ms bins (Figure 17B). Z-scores of firing associated with SIA onset were calculated, defined as the difference between averaged PSTH values during

-1 ~ + 0.5 sec around SIA onset, and baseline time -4 ~ -1.5 sec, divided by the standard deviation of PSTH values during the baseline time. The ratio between averaged PSTH values around SIA onset and the baseline was also calculated. The SIA index was subsequently defined as the product of the z-score and the ratio. SIA index > 1 represents an excitatory association, while index < -1 suggests inhibition. SIA index between -1 and 1 suggests no clear firing rate changes, and were treated as 0 for log transformed value. Except for these values, log transform of SIA index was performed on the absolute value, with original signs assigned to the log value (SIA index > 1 became Log index > 0; SIA index < -1 became Log index < 0).

K-means clustering, a standard algorithm in MatLab program was used to cluster neurons based on the log transformed indices. This algorithm partitions data points into defined number of clusters, and with iteration, minimizes the summed Euclidean distance to cluster centeroids.

3.2.3.4 Spectral analysis

Spectral analyses were performed with the Chronux package based on multitaper spectral methods (Dr. Partha Mitra and www.chronux.org). For different frequency ranges, slightly different moving windows were used: 0-20Hz, 2 sec window with 0.5 sec moving steps; 10-50Hz, 0.6 sec / 0.2 sec; 30-300Hz, 0.5 sec / 0.25 sec. To calculate spike-triggered or event-triggered spectrograms, spectrograms around individual spikes/events were aligned and averaged. For SIA onset related plots, spikes occurring at [-1 +1] sec of SIA onset were used; for plots during the waking state, spikes occurring [-1 +1] sec around behavioral events (cues, licks etc) were excluded to prevent potential confounding factors.

3.2.3.5 Theta related analysis

One of the DG LFPs was filtered between 4.5-9Hz for theta oscillations and theta phase were calculated using Hilbert transform on the filtered signal. Phase of individual spikes was calculated as the Hilbert phase at the time of the spike. Phase preference of each neuron was calculated with 20 sec windows / 10 sec moving steps, to reflect the fluctuation in theta appearance, or collapsed for all REM episodes. Phase-locking strength and p-values were calculated with circular statistics (Rayleigh test, MatLab toolbox from Velasco 2009). Rhythmicity index was calculated based on auto-correlogram in theta-dominated periods (like REM sleep) (Jobert, Bassant et al. 1989; Kitchigina, Kuttyreva et al. 2003).

3.3 Results

In behaving animals, we recorded from MSvDB single units (neurons), and in the following reports, we focused on the neurons with an average firing rate below 4Hz, generally regarded as the slow-firing neurons (Simon, Poindessous-Jazat et al. 2006).

3.3.1 Slow-firing¹ neurons often have higher firing rate in REM sleep

First we investigated the state-dependent firing property. The concentration of hippocampal ACh is higher during the waking state and lower during SW sleep, with the highest level during REM sleep (Marrosu, Portas et al. 1995; Bianchi, Ballini et al. 2003). Since MSvDB cholinergic neurons are the source of hippocampal ACh release (Lewis, Shute et al. 1967; Mesulam, Mufson et al. 1983), their firing patterns may match such

ACh fluctuation. This seemed to be the case for many of the slow-firing neurons we recorded from. The example MSvDB neuron shown in Figure 15A fired around 1Hz during awake, and almost ceased firing during SW sleep. Its firing rate reached a very high level (5Hz) during REM sleep. The whole population showed a similar pattern: relatively high during waking (WK, 1.14 ± 1.17 Hz, mean \pm s.d.), lowest during SW sleep (SW, 0.76 ± 1.14 Hz) and highest during REM sleep (REM, 2.98 ± 2.35 Hz). Figure 15B of their normalized firing rate demonstrated the state-dependent firing difference (Friedman Test, $p < 0.001$ for all three states; and $p < 0.001$ between each two states, Wilcoxon signed rank test).

Particularly, we compared the firing rates in REM to SW or to WK (Figure 15 C and D). Many neurons had much higher firing rate in REM compared to in SW. We defined a REM index as the ratio between the two to reflect this property. We also categorized the neurons into REM+ and REM- categories with a threshold set at REM index = 8 at one local minimum in the histogram (Figure 15E). Slightly more than half (52%) of the neurons were REM+.

3.3.2 Some slow-firing neurons have transient auditory responses

Since earlier reports have shown that MSvDB neurons respond to auditory stimulus, and the slow-firing ones among the responsive neurons might be cholinergic (Miller and Freedman 1993), we investigated in our recording the responses of the neurons to auditory stimulus, particularly the 2 sec white noise sound, which seemed to induce stronger neuronal response than the 6kHz pure tone (data not shown). Indeed, we found neurons with auditory responses, which was very transient firing (single spikes or short bursts) at about 15~35ms after stimulus onset (example in Figure 16A). To

characterize such auditory responses, we defined an auditory response index (Aud index), and grouped the neurons to Aud+ and Aud -, with a cutoff point at 5 (Figure 16C). More than half (57%) of the neurons were Aud+.

3.3.3 Activities of REM+/Aud+ neurons coupled to SIA epochs in SW sleep

Since MSvDB neurons had relatively low firing during SW sleep, we investigated the details of their firing during this state. Particularly, we identified transient arousal epochs, the small-amplitude irregular activity (SIA) epoch (Figure 17A) (Jarosiewicz and Skaggs 2004), and studied how these transient states were associated with the neuronal activities in MSvDB. We found that some MSvDB neurons had relatively high firing rate during SIA or slightly before the SIA onset (example in Figure 17B). For most of such neurons, the increased spiking started 1 to 0.5 sec before the SIA onset, suggesting that these neurons may promote the appearance of the SIA epochs. These neurons also tended to fire much less during the slow-wave epochs (LIA, large-amplitude irregular activity), which accounts for most of the SW sleep.

To characterize this association with the SIA onset, an SIA index was calculated for each MSvDB neuron. SIA+ or SIA- groups were defined with a cutoff threshold at 3. Interestingly, most of the neurons that were REM+ and Aud+ were also SIA+ (71 out of 81, 88%), while the majority (78 out of 109, 72%) of the remaining neurons were SIA- (Figure 17C), suggesting the three properties we have investigated may be tightly related.

3.3.4 A distinctive population of MSvDB neurons baring all three firing properties - putative cholinergic neurons

When all slow-firing MSvDB neurons were plotted on a 3-D plot of the three indices, the group baring all three properties seemed to be separated from the remaining neurons (Figure 18A). To confirm this observation, we used the un-supervised k-means clustering algorithm on all the MSvDB slow-firing neurons to separate them into two groups based on these three indices. The resulted two clusters matched very well with our two categories of REM+/Aud+/SIA+ (82%) and the remaining neurons (Figure 18A). This result suggests that the REM+/Aud+/SIA+ neuron group is a distinctive MSvDB subpopulation, and this subpopulation can be categorized based on these three properties. In fact, clustering with any two of these properties were quite similar to clustering with all three (data not shown). Since the REM+ and Aud+ properties had been independently indicated for cholinergic neurons, this subpopulation may putatively be cholinergic neurons.

These results also suggest that the three properties we investigated here might be intrinsically related. We tested such relationship by checking the correlation between any two of the three. Very clear correlations could be seen for all three pairs, when all the neurons were pooled together (Figure 18 B-D, $p < 0.001$, significance tested with non-parametric Spearman rank correlation). When correlations were tested within groups (REM+/Aud+/SIA+ and other neurons), most of them were not significant, except between REM and Aud indices for the remaining neurons ($p < 0.001$, Spearman rank correlation). All these results corroborate the idea that this subpopulation of putative cholinergic neurons may have firing properties intrinsically associated with arousal or desynchronization of the hippocampus.

3.3.5 Putative MSvDB cholinergic neurons promote hippocampal activation in a state-dependent manner

With this putative cholinergic subpopulation identified from the slow-firing MSvDB neurons, we further investigated how their firing could impact hippocampal LFP activities, by analyzing the spike-triggered spectrograms. As an example showed in Figure 19, during REM and WK, the firing of putative cholinergic neurons was usually associated with increased theta oscillations at higher frequencies (7-10Hz), and sometimes with 2x harmonics. The peak of such increase tended to be later than the spike, suggesting that the firing of these neurons promoted the increase of theta power in higher theta range. Increase in high gamma range (about 80~130Hz) was also seen, often in REM sleep. These increases seemed to last for no more than 2 sec. They also decreased the power in frequency band < 6Hz. Putative non-cholinergic neurons were generally not associated with such changes.

In SW sleep, the firing of these neurons around the SIA epoch onset ([-1 1] sec) was associated with a lasting decrease of power in the broad frequency range in 0-25 Hz for seconds, which corresponds to the decrease of LFP amplitude in SIA. A transient increase of power in 25-50Hz happened just after the spike of putative cholinergic neurons. The weak power reduction seen with the putative non-cholinergic were attributable to alignment to SIA epoch onset (data not shown).

Similar spectrogram patterns were found for all the putative cholinergic neurons (Figure 20). A lot more neurons in this group modulated hippocampal activities than the putative non-cholinergic neurons.

3.3.6 Putative MSvDB cholinergic neurons are not rhythmic-firing, and have mild phase-locking to theta oscillations

Since most neuronal studies in MSvDB focused on theta-related or rhythmic neurons, while the few identified cholinergic neurons were said to be not related the theta oscillations (Simon, Poindessous-Jazat et al. 2006), we tested theta related properties of the subpopulation we discovered. Almost none of these putative neurons were rhythmic, even during the highly theta-dominated REM episodes (Figure 21C). Although most of them were phase-locked to theta oscillations, (Figure 21D), their level of phase preference were relatively low, compared to the fast-firing group, or the non-cholinergic neurons (Figure 21E).

3.4 Conclusion

In this study, we have demonstrated that a subpopulation of slow-firing MSvDB neurons have distinctive properties, such as higher firing during REM sleep and low firing during SW sleep (Figure 15), and transient responses to auditory stimuli at 15-35 ms (Figure 16). These neurons often fire during the SIA epochs and/or slightly before the SIA onset, a transient arousal state during SW sleep (Figure 17). These three properties seem to be intrinsically related, distinguishing this group of neurons as a subpopulation very different from other slow-firing MSvDB neurons (Figure 18). Furthermore, the firing of these neurons promotes high theta and gamma oscillations during waking and REM sleep, and suppress slow-waves during SW sleep (Figure 19, Figure 20). They often have mild phase-locking in relation to theta oscillations, and most of them are not rhythmic-firing (Figure 21). All these properties make this subpopulation an excellent candidate of cholinergic neurons in MSvDB, and suggest that MSvDB cholinergic

neurons *in vivo* may be a general neuronal network that promotes theta states and arousal / activation of hippocampus.

3.5 Discussion

3.5.1 Evidence that support the putative cholinergic neuron hypothesis

There has been almost no direct evidence on the firing properties MSvDB cholinergic neurons. Only one recent study suggested that both under urethane anesthesia and without anesthesia, these neurons fire at low rate and have no clear relation with theta oscillations (Simon, Poindessous-Jazat et al. 2006). Unfortunately, the few neurons reported in that study made it very difficult to make conclusions about the firing properties of cholinergic neurons, except that they are probably slow-firing. The slow-firing property is supported by the results in Chapter 2, which showed that a substantial subpopulation of MSvDB slow-firing neurons have firing rate changes matching the dynamics of phasic ACh release, revealed by amperometry.

Beyond slow-firing, properties of cholinergic neurons remain completely uncharacterized under unanesthetized (free-moving or behaving) conditions. Given such reality, we had to postulate the potential properties from pertinent properties of the cholinergic system reported in the literature.

Since MSvDB is arguably the sole ACh source for the hippocampus (Lewis, Shute et al. 1967; Mesulam, Mufson et al. 1983; Dutar, Bassant et al. 1995), and ACh level has been shown to vary according to sleep-waking states (Marrosu, Portas et al. 1995; Bianchi, Ballini et al. 2003), we postulate that cholinergic neurons may have corresponding firing rate changes, being low firing during SW sleep, higher during

waking and possibly highest during REM sleep. The individual firing rates of the particular subpopulation of neurons we identified, with some variability, accord with the general notion of ACh level changes during different sleep-waking states (Figure 15).

MSvDB neurons are known to have transient sensory responses, especially responses to auditory stimulus (Zin, Conforti et al. 1977). An early study looked carefully into the hippocampal projecting cells in MSvDB that have these sensory responses, and measured the conduction velocity of action potentials along their projection axons (Miller and Freedman 1993). They reported that neurons with transient positive (~20ms) responses had low conduction rate, and concluded that they might correspond to the cholinergic neurons with little-to-none myelination on their axons (Bialowas and Frotscher 1987; Nyakas, Luiten et al. 1987), while neurons without such response had higher conduction rate, which might be GABAergic neurons with thick myelination on their axons. These auditory responsive neurons seem to be exactly the same type of neurons that showed transient auditory responses in our experiments. Therefore, it is tentative to postulate that our Aud+ neurons may similarly be cholinergic neurons.

More interestingly, this subpopulation of neurons in our experiments were associated with the onset of SIA epochs, and seemed to participate in driving the SIA onset. Although SIA generation mechanism is not known, it seems to have at least a cholinergic component. Knock-out mice with deletion of the $\beta 2$ subunit of nicotinic receptors showed decreased frequency of SIA occurrence (Lena, Popa et al. 2004), which is in line with our hypothesis that these neurons we observed were cholinergic neurons.

3.5.2 A distinctive subpopulation of neurons in MSvDB

Earlier studies tended to focus on higher-firing neurons in MSvDB. Most of these studies used glass electrodes (sharper tip), and recorded in anesthetized animals during which the experimenters were able to manipulate very finely the distance between the electrode tip and the recorded neuron, to approach it as much as possible. In this case, small neurons should have the same chance to be recorded from, compared to large neurons, but higher-firing neurons should have a higher probability to be recorded (Simon, Poindessous-Jazat et al. 2006). In our studies using multielectrode assemblies (larger tip, 35 μ m tungsten wires), we may have picked up larger neurons more often. Furthermore, since we do not have online adjustment to approach recorded neurons, waveforms of neurons with higher firing rate are more likely to be mingled with background noise. This results in fewer higher-firing single units identified, in contrast to many earlier studies using glass pipette electrodes and happened to focus on higher-firing, theta-related neurons in MSvDB. These methodological considerations made our recordings prone to identify slow-firing neurons.

The subpopulation of slow-firing neurons we report here have distinctive properties, including higher firing in REM, transient response to auditory stimuli and association with SIA and/or SIA onset. These properties, although not seem to be directly related, might have intrinsic connections, since the property indices seem to be grossly correlated across all the slow-firing neurons. Categorization based on these properties distinguished this group from other slow-firing MSvDB neurons (Figure 18).

These properties we describe here have rarely been investigated in MSvDB neurons. Most of the early recordings focused on neuronal activities related to theta oscillations, and very rarely studied the particular characteristics we have focused on.

Especially for the SIA associated firing, there are no neuronal studies in the MSvDB, and very few studies in other brain regions as well (Jarosiewicz, McNaughton et al. 2002; Jackson, Dickson et al. 2008). The results in our experiments may point to, at least for SIA in the hippocampus, a potential SIA generation pathway.

In contrast to our results and the results of identified MSvDB cholinergic neurons, the cholinergic neurons in the caudal basal forebrain regions, specifically, substantia innominata (SI), magnocellular preoptic nucleus (MCPO) and nucleus basalis magnocellularis (NBM), seem to have related but distinguishable firing properties (Lee, Hassani et al. 2005). They, like the subpopulation of MSvDB neurons we report here, have highest firing rate in REM sleep and lowest firing rate in SW sleep, although they seem to have slightly higher firing rates on average. However, they were reported to be mostly rhythmic-bursting and phase-locked to theta oscillations, which is different from our subpopulation (almost no rhythmicity), or the identified cholinergic neurons (Simon, Poindessous-Jazat et al. 2006). These differences between putative cholinergic neurons in MSvDB and basal forebrain may be caused by the different intrinsic properties of these neurons, which have been reported in *in vitro* preparations (Griffith and Matthews 1986; Markram and Segal 1990; Khateb, Muhlethaler et al. 1992; Sotty, Danik et al. 2003; Steriade 2004). Such difference would be verified with future studies on these characteristics of the cholinergic MSvDB neurons identified with immunohistochemistry.

3.5.3 New insights on the function of MSvDB cholinergic neurons.

Lesion studies have shown that a normal network of MSvDB cholinergic neurons are required for maintaining theta amplitude and stability in unanesthetized animals (Lee, Chrobak et al. 1994; Bassant, Apartis et al. 1995), and participate in learning and

memory (Steckler, Keith et al. 1995; Dougherty, Turchin et al. 1998; Pizzo, Thal et al. 2002; Parent and Baxter 2004; Fontan-Lozano, Troncoso et al. 2005), but the exact function of these neurons remains a mystery, especially with the recent discovery that they are probably slow-firing (Simon, Poindessous-Jazat et al. 2006). Our results suggest that during behavioral states in which theta is permitted, the firing of these neurons promotes an increase of the power of higher frequency theta and gamma oscillations (Figure 20). Such effect was fast and short-lasting (within 0-2 sec of an individual spike). Compared to muscarinic effects which usually happen slower, on the level of ~ 10 sec (Hasselmo and Fehlau 2001), the short-lasting effect here may be mediated by nicotinic receptors. Indeed, nicotinic mechanism has been shown to be involved in enhancing theta power (Siok, Rogers et al. 2006). The activation could be mediated by nicotinic receptors in the hippocampus. Alternatively but not mutually exclusive, such effect may be mediated by nicotinic receptors in theta-pacing GABAergic neurons in the MSvDB.

In behavioral states in which theta oscillations are not favored, such as SW sleep, the firing of these neurons seems to promote the appearance of SIA epochs. Slow activities were interrupted, and a transient burst in the beta / low gamma band (~ 20-50Hz) appeared (Figure 20), with short-lasting arousal of the animal (Jarosiewicz and Skaggs 2004). Interestingly, SIA epochs are associated with ripple bursts and silence of most pyramidal cells, except the ones that signify the location where the animal falls asleep (Jarosiewicz, McNaughton et al. 2002; Jarosiewicz and Skaggs 2004). It would be very interesting to see how the firing of these putative MSvDB cholinergic neurons are associated with or even promote these hippocampal neuronal activities.

In all, the association and promotion of SIA epochs, higher-frequency theta and gamma oscillations, suggest that these neurons might be a generalized final hippocampal arousal or activation network, which may relay activation input from other areas. Possible inputs of such activation signal include pedunculopontine tegmental nucleus (PPT), medial raphe, amygdala, locus coeruleus, hypothalamus (Zin, Conforti et al. 1977; Aston-Jones and Bloom 1981; Quirk, Repa et al. 1995; Jackson, Dickson et al. 2008).

Finally, the properties of these putative cholinergic neurons fit the role of septohippocampal ACh in promoting synaptic plasticity and learning and memory. They respond to external stimuli, and promote theta oscillations, the presence of which is known to be a favorable network state for synaptic plasticity (Larson, Wong et al. 1986; Pavlides, Greenstein et al. 1988). The short-lasting increase of theta power caused by the firing of these neurons could be a favorable short-term tag for plasticity (Vertes 2005). The putative release of ACh, which will wander around in hippocampus and act on muscarinic receptors to cause a relatively long-lasting effect, could promote signaling pathways that lead to activation of kinases (Giovannini, Pazzagli et al. 2005) and IEGs (Wirtshafter 2005 and Chapter 4). Through these sequential effects, the activity of these putative cholinergic neurons may be able to substantiate their function in synaptic plasticity and memory consolidation.

Figure 14. Recording site and neuronal spike sorting

A-C. Schematic and examples of the recording site demonstrated with histology and immunohistochemistry. **A.** The cannula implant and estimated target area (blue shade) in MSvDB. Blue dotted rectangle, area in B. **B.** Histology image. The empty space was created because of cannula implantation (arrow). Bundled electrodes spread from the tip of the cannula (arrow head). Scale bar, 500 μ m. Orange dotted rectangle, area in C. **C.** ChAT staining demonstrating cholinergic neurons in MSvDB, dispersed in the area being recorded. Scale bar, 200 μ m. **D-F.** Representative single neuron recording from one individual electrode in MSvDB. **D.** In this recording session, three single units were identified based on their spike waveform (assigned colors as yellow, green and cyan). Scale bars, 100 μ V (vertical) and 200 μ sec (horizontal). **E.** The waveform template for each unit, and corresponding inter-spike-interval (ISI) of each neuron. There was no ISI below 1.2ms, suggesting that each of them was a single unit. Gray, noise waveforms. Scale bars, 100 μ V (vertical) and 200 μ sec (horizontal). **F.** Features of their waveform separated these units as distinctive clusters in the 3-D feature space, away from the noise cluster (gray). Scale bars, 100 μ V (all three dimensions).

Figure 14

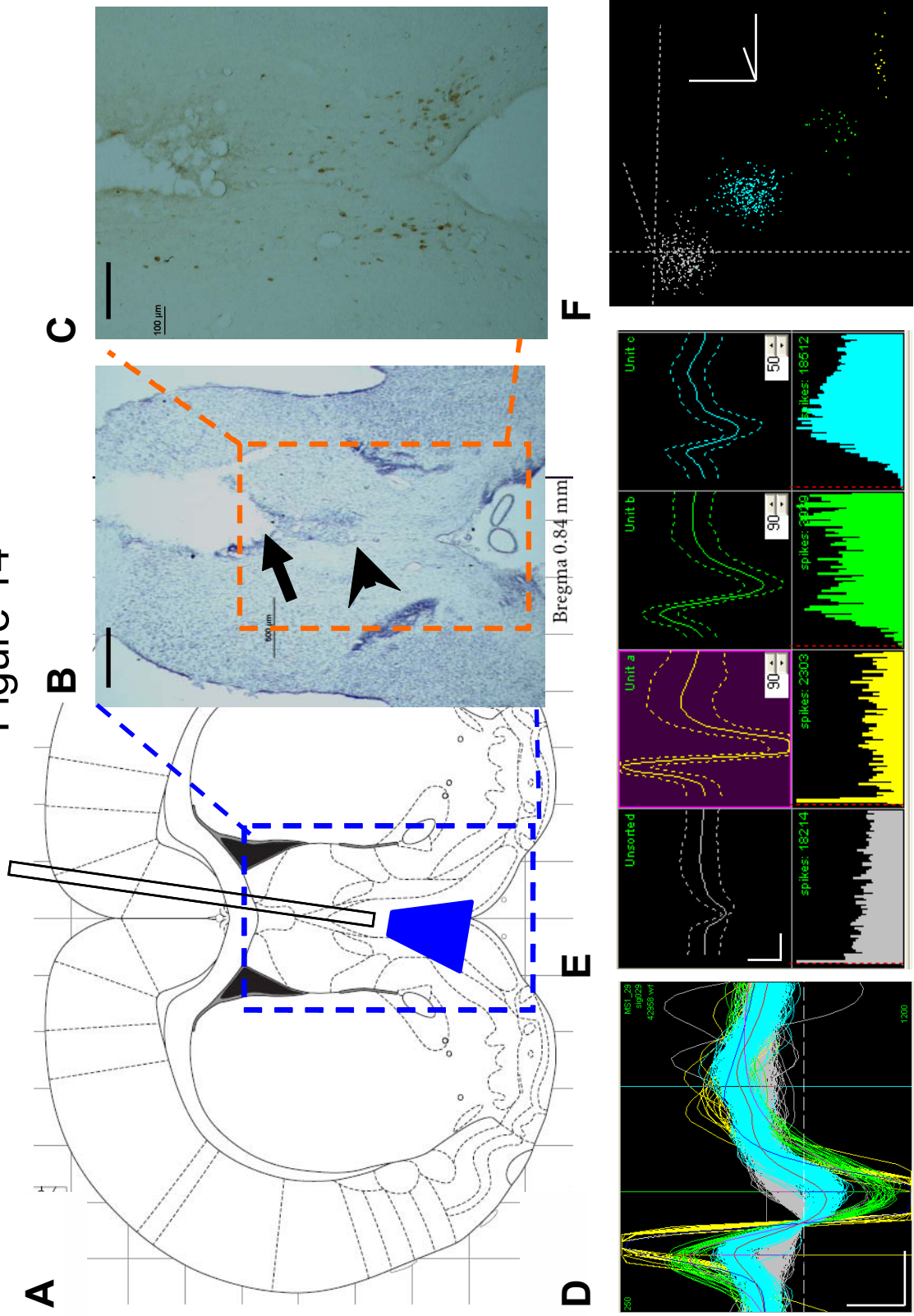


Figure 15. Slow-firing neurons often have higher firing rate in REM sleep

A. A representative slow-firing MSvDB neuron, with firing rates changing across waking (WK), SW and REM sleep. **B.** Box plot of firing rate for all the slow-firing neurons, normalized to their individual average firing rate. Dotted line indicating 1. Firing rate was highest in REM, lowest in SW, and intermediate in WK (***, $p < 0.001$, Wilcoxon signed rank test). **C** and **D.** 2-D plots of firing rate comparison for individual neurons, between REM and SW (**C**), REM and WK (**D**). Black, putative cholinergic neurons defined in Figure 18; blue, other neurons; blue lines indicate unity. For the majority of neurons, firing rates during REM were higher shown in both plots. **E.** Histogram of REM index for individual neurons. Neurons were grouped into REM+ and REM-, with a cutoff at REM index=8 (local minimum). 98 of the slow-firing neurons were grouped as REM+.

Figure 15

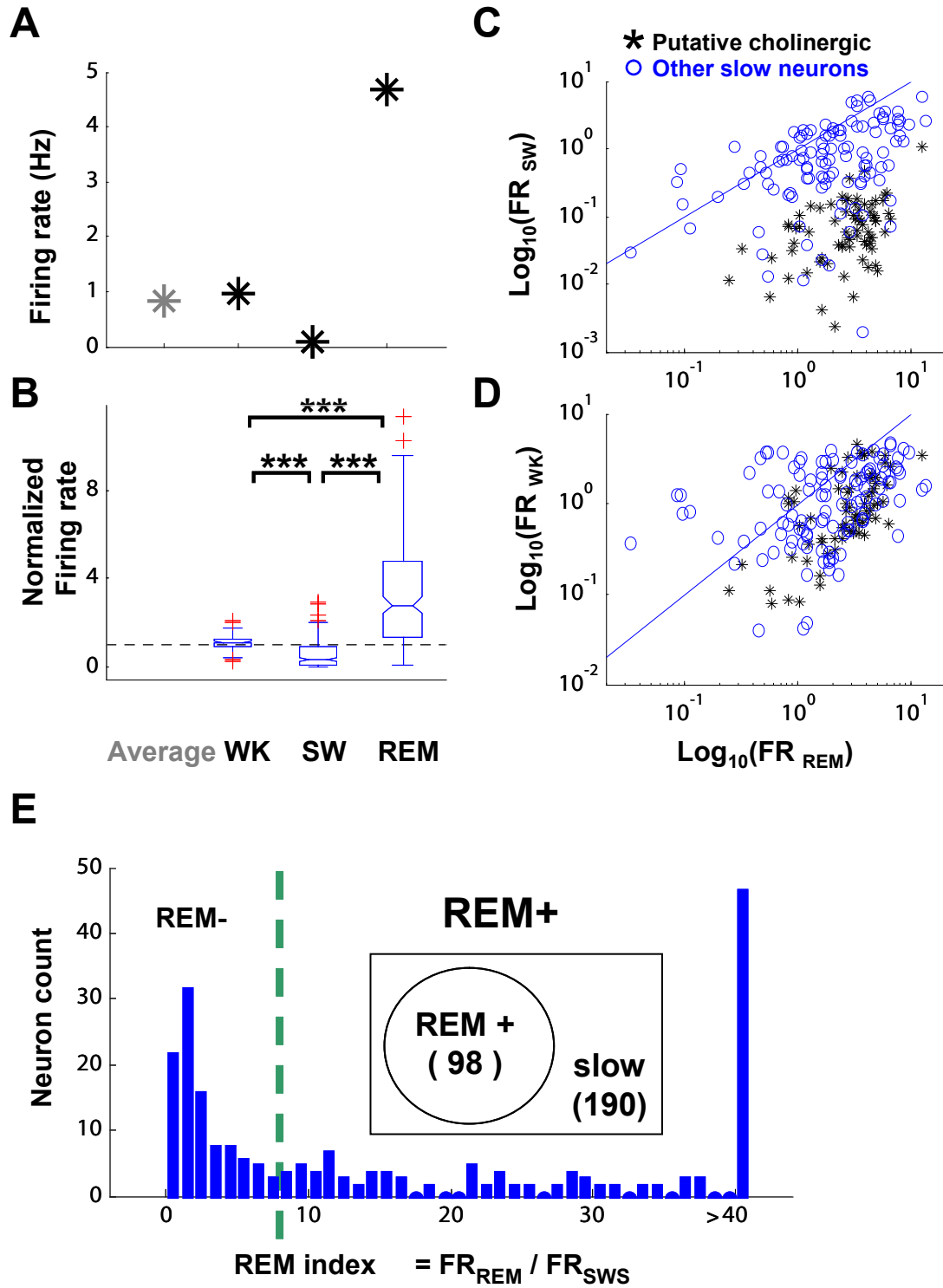


Figure 16. Many slow-firing neurons have transient auditory responses

A. Example of a neuron with transient auditory response. Gray bar on the top indicates a 2 sec auditory stimulus (an 80Hz white noise sound). Raster plot in the middle shows the trial-by-trial firing this neuron (black dot, single spike), aligned to the onset of the auditory stimuli (time = 0). Peristimulus histogram (PSTH) in the bottom summarizes the response of this neuron, showing a very strong but transient response, tightly locked at 15-30ms after the stimulus onset. B. Pseudocolored PSTHs of all slow-firing MSvDB neurons, sorted according to the auditory response index (Aud index). The example in A is # 53 on this plot (black arrow). Two gray bars below indicate the peak (15~35ms) and baseline (-300 ~ -5 ms) periods used to calculate Aud index. C. Histogram of Aud index for individual neurons. Neurons were grouped into Aud+ and Aud-, with a cutoff at Aud index=5. 108 of the slow-firing neurons were grouped as Aud+.

Figure 16

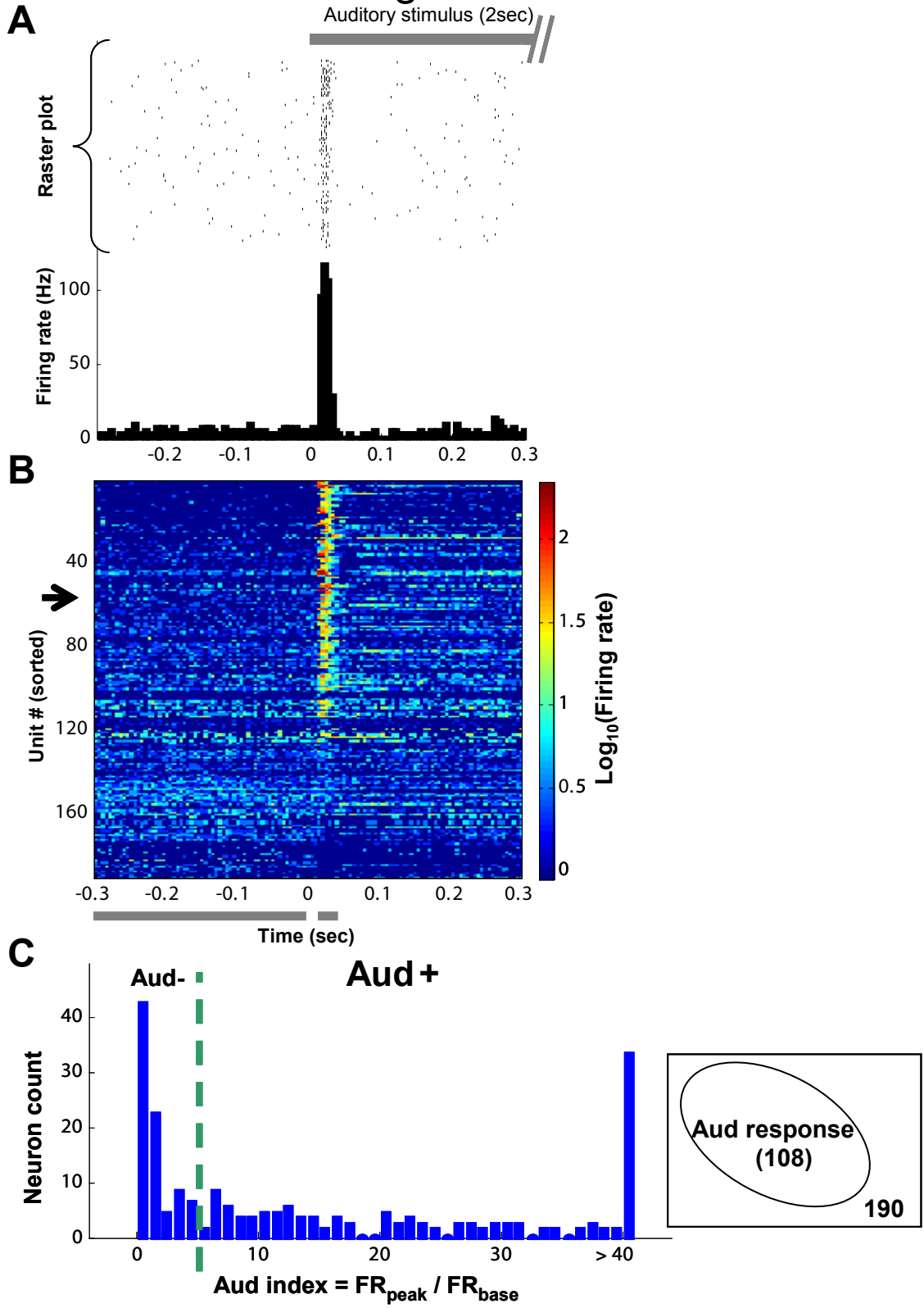


Figure 17. Activities of REM+/Aud+ neurons coupled to SIA epochs in SW sleep.

A. Example of an SIA epoch, defined by the reduced amplitude of LFP. Blue, LFP in DG; upper red line, root-mean-square amplitude of LFP; lower red line, smoothed amplitude; dotted magenta lines, beginning and end of the SIA epoch. **B.** Example of the firing of two neurons in relation to SIA onset, recorded in the same SW sleep session. *Left and middle panels*, raster plots of spikes (black) around SIA or LIA onset (aligned, time = 0 at onset). Magenta or blue dots, beginning and end of individual SIA or LIA epochs. Epochs sorted according to length, and the part beyond 10 sec not shown here. *Right panels*, averaged firing rate around the onset of SIA or LIA. Two gray bars above indicates the peak (-1~+0.5 sec) and baseline (-4 ~ -1.5 sec) periods used to calculate SIA index. The neuron in the upper panels had transient firing around SIA onset, and inhibition around LIA onset, while the neuron in the lower panels did not show firing rate changes associated with SIA or LIA. **C.** Histogram of SIA index for two groups of neurons, REM+/Aud+ and the remaining. Most REM+/Aud+ neurons had higher SIA index, while most remaining neurons had low SIA index. Neurons were further grouped into SIA+ and SIA-, with a cutoff at SIA index=3. **D.** 102 of the total slow-firing neurons are grouped as SIA+.

Figure 17

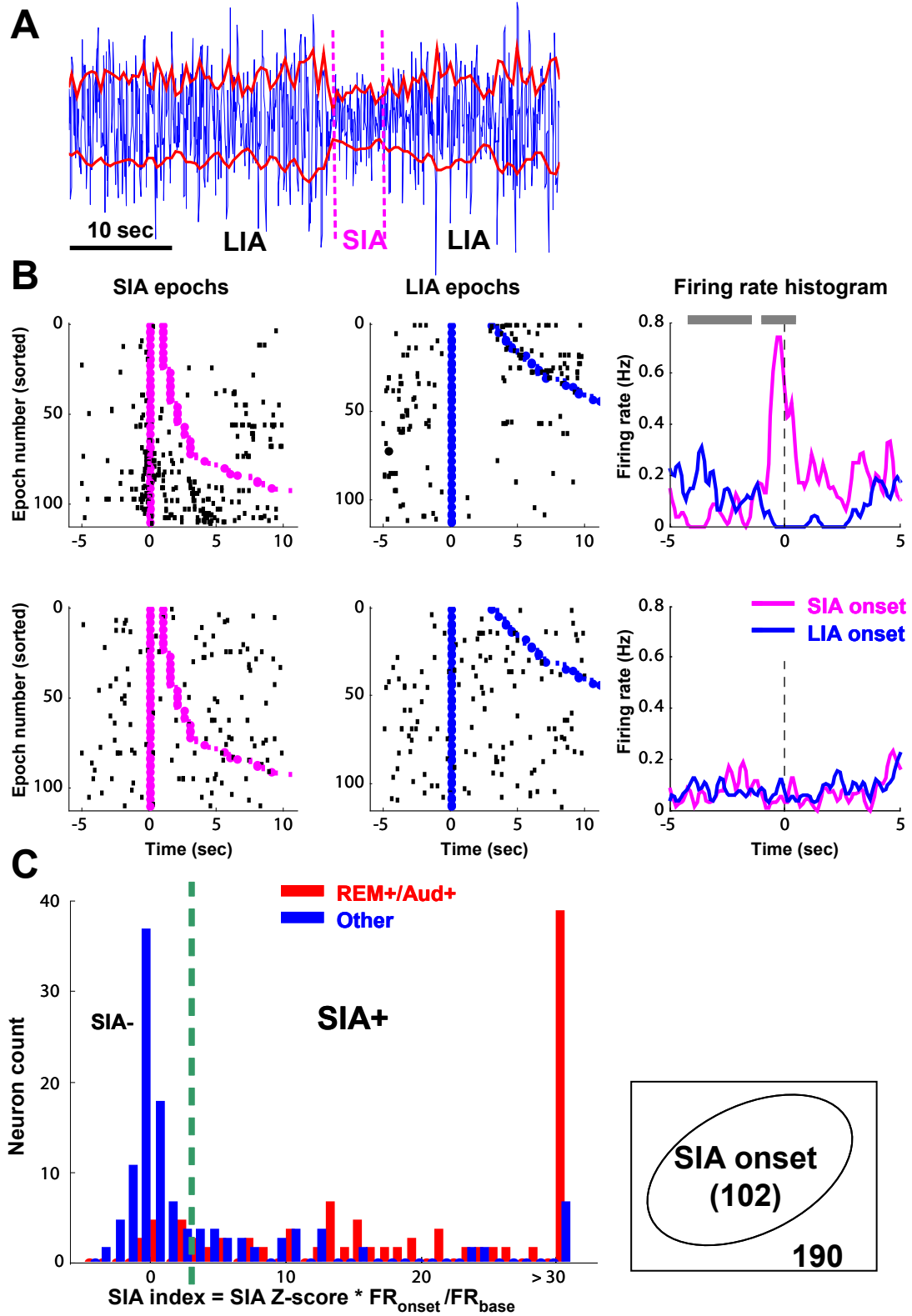


Figure 18. Putative cholinergic neurons are distinctive from other neurons.

A. REM+/Aud+/SIA+ neurons formed a distinctive population. *Left*, 3-D plots of the three log-transformed indices from one viewing angle. Black stars, REM+/Aud+/SIA+; blue stars, other MS slow-firing neurons. *Right*, the same 3-D plot with another viewing angle, turned 90 degree on the x-y plane. Circles, clustering results from unsupervised k-means algorithm. The two clusters were very consistent with the division on the left, suggesting that REM+/Aud+/SIA+ neurons are distinctive from the remaining neurons. **B-D.** Correlation between indices on 2-D views of plots in **A**. Black and blue dots, REM+/Aud+/SIA+ and the remaining neurons; black and blue lines, correlation calculated in the respective group; red lines, correlation for all neurons. Solid lines indicate significant correlation (all red lines, and blue line in left panel, $p < 0.001$; significance tested with non-parametric Spearman rank correlation); dotted lines indicate no significant correlation. **E.** Diagram showing the distribution of neurons among the REM+/-, Aud+/- and SIA+/- groups.

Figure 18

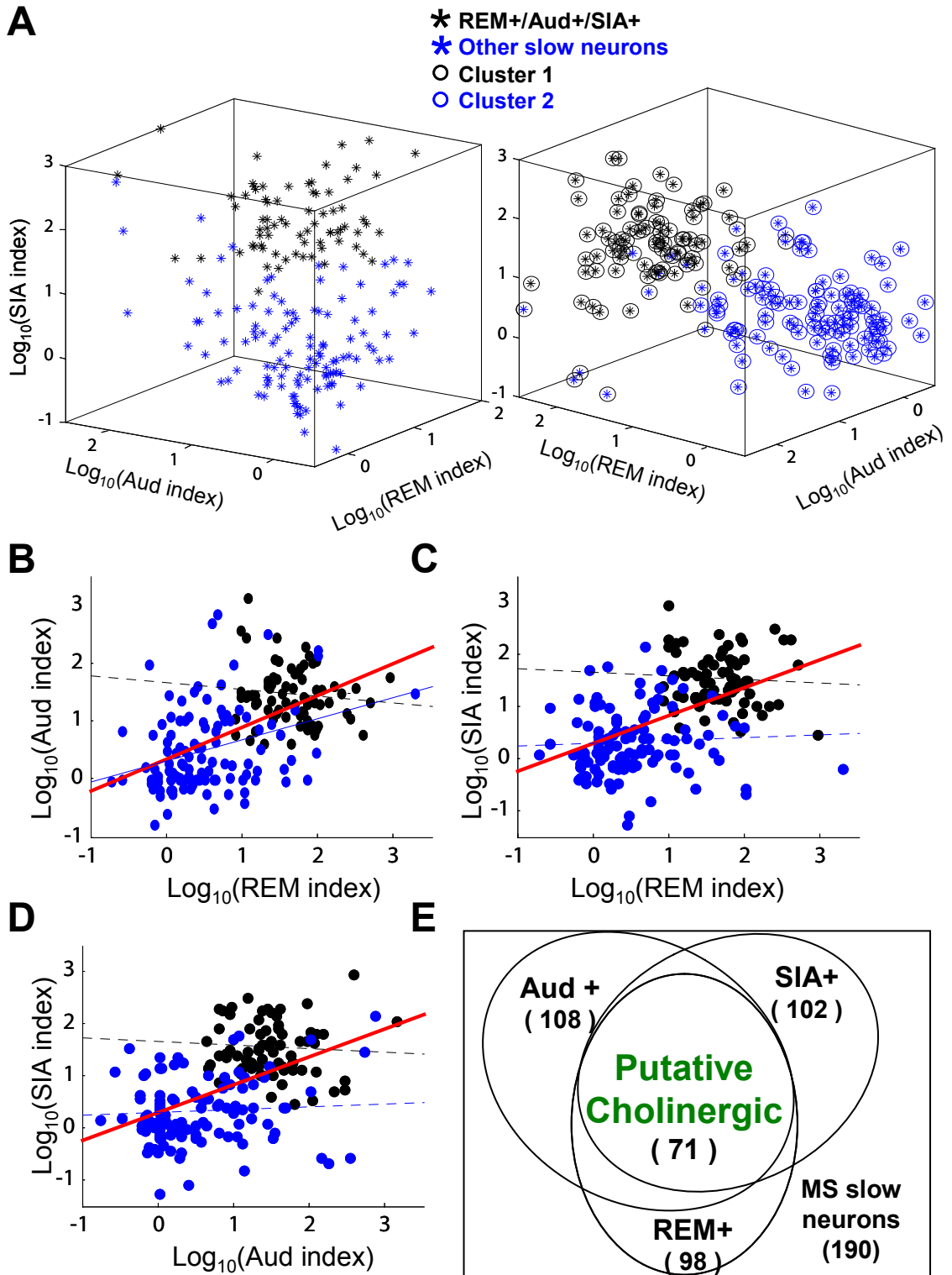


Figure 19. Putative cholinergic neurons promote hippocampal activation (example).

A-C. Example of averaged spectrograms around spikes of a putative cholinergic and a putative non-cholinergic neuron recorded in the same session. Three frequency ranges (0-20, 10-50, 30-300Hz) were displayed separately. Spectrograms were aligned to the spikes of individual neurons (time 0, black vertical line in the center). Black horizontal bar on lower left indicates the baseline period. For normalization, average log power during the baseline period at each frequency was subtracted, and pseudocolors indicate the power increase or decrease. During REM and WK, the firing of putative cholinergic neurons promoted increase of theta power, and sometimes increase in power in high gamma range in REM sleep. Their firing was also associated to decrease in power in frequency bands <6Hz. In SW sleep, the firing of these neurons around the SIA onset was associated with a marked decrease of power in lower bands, and a transient increase of power in 25-50Hz. Firing of putative non-cholinergic did not lead to comparable spectral changes.

Figure 20. Putative cholinergic neurons promote hippocampal activation (population).

A-C. Significance plots for spectrograms of all putative cholinergic and non-cholinergic neurons. Significance based on Z-score values calculated with baseline. Heat-plots indicate the percentage of neurons beyond Z-score threshold, for positive (left two columns) and negative (right two columns) Z-scores, corresponding to power increase and decrease. The pattern is similar to individual example.

Figure 20

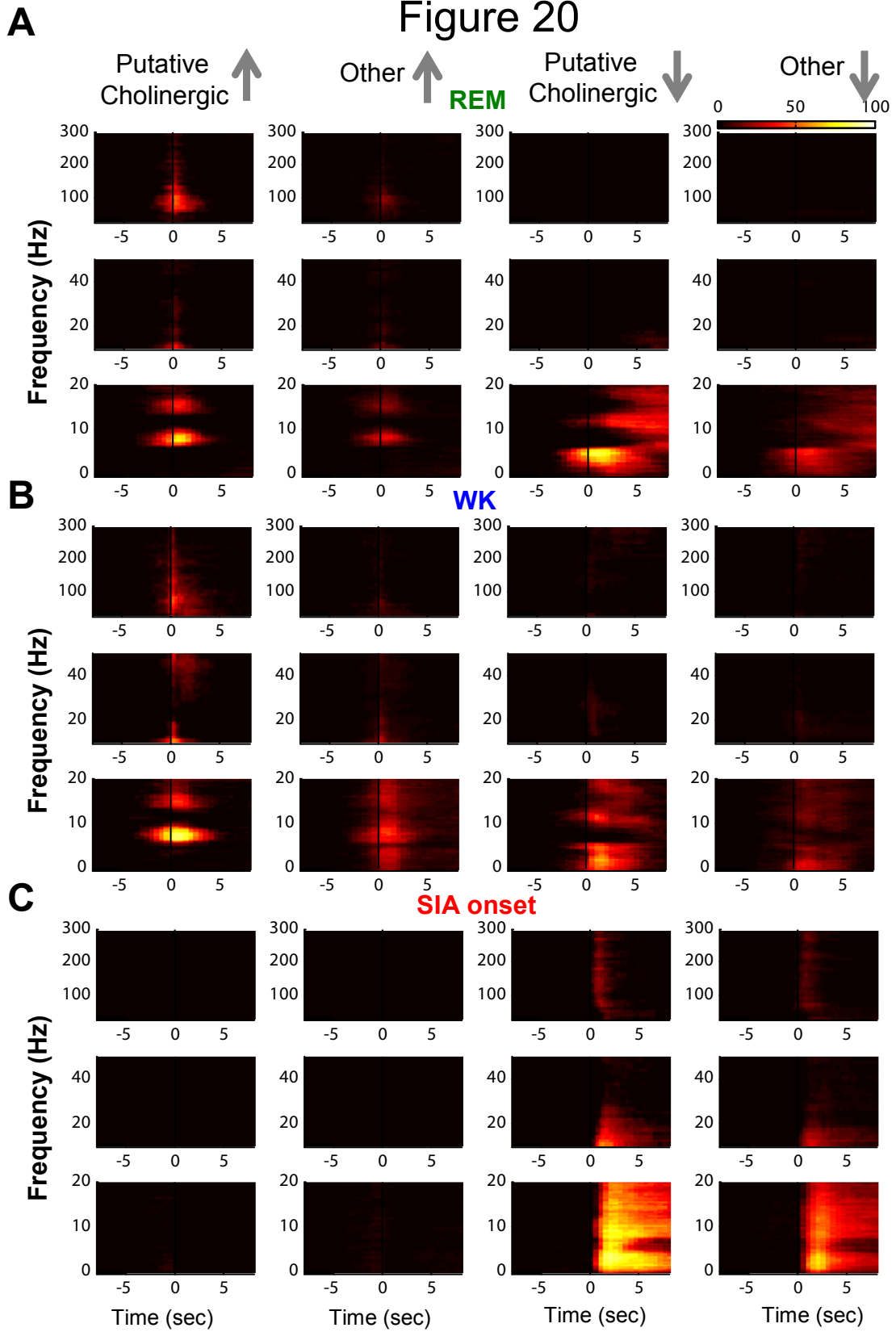
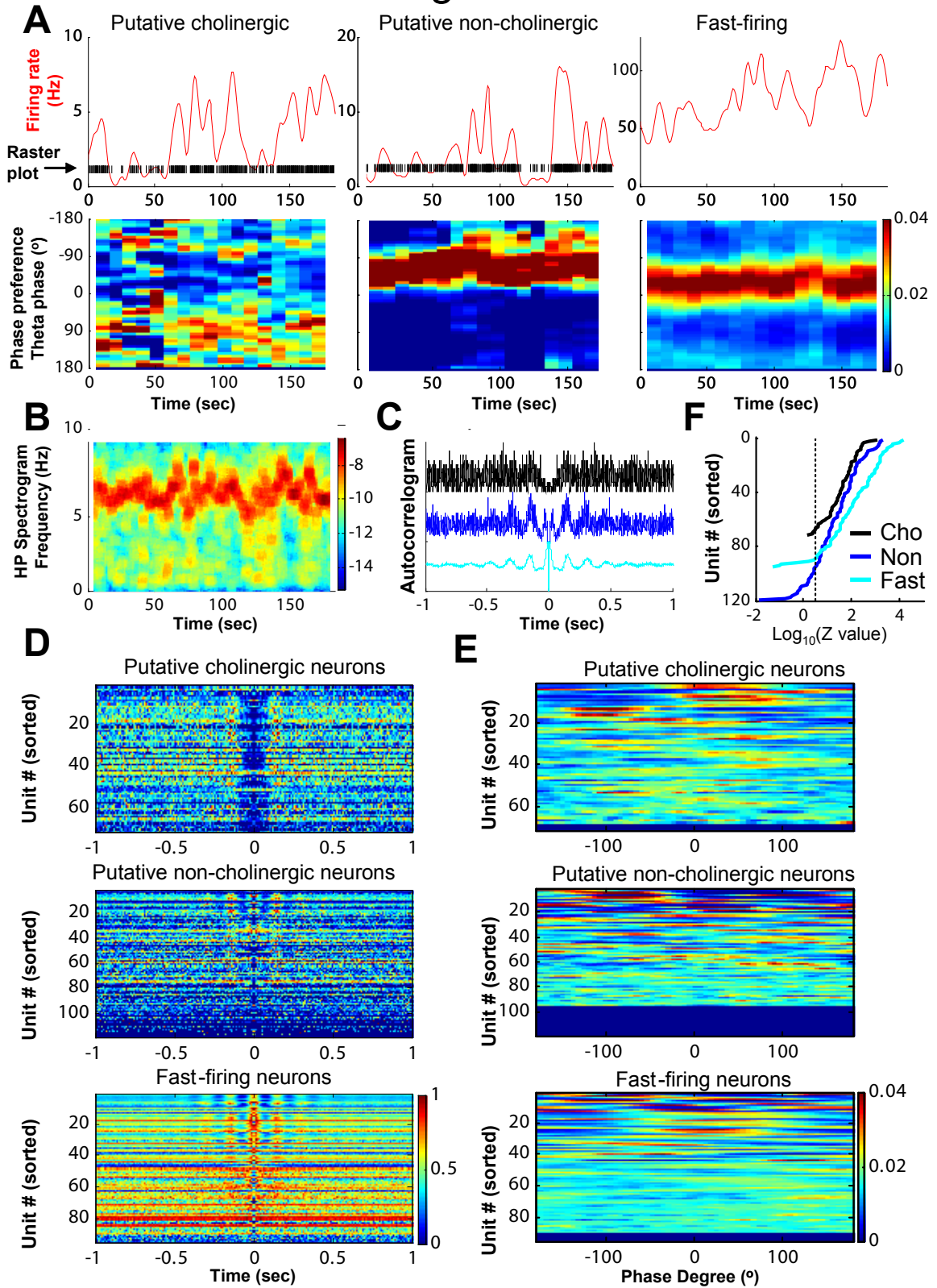


Figure 21. Firing properties of putative cholinergic neurons

A-B. Example of theta-related properties of three neurons recorded in the same REM episode. **A.** *Upper panels*, spike raster (black, not plotted for fast-firing neuron) and smoothed instantaneous firing rate (red traces). *Lower panels*, phase preferences of individual neurons, calculated for every 20 sec. **B.** Spectrogram of hippocampal LFP during the REM episode. **C.** Autocorrelation during REM episode. This putative cholinergic neuron was not rhythmic-firing, while the putative non-cholinergic neuron and the fast-firing neuron were. **D.** Population plots of autocorrelation during REM sleep of the three groups of neurons: slow-firing putative cholinergic and non-cholinergic neurons, and fast-firing neurons. Units sorted according to rhythmicity index. Many fast-firing neurons were rhythmic firing, but almost no putative cholinergic neurons were. **E.** Population plots of phase-locking during REM sleep of the three groups of neurons. Units sorted according to phase-locking strength (Rayleigh test critical value Z). Non-significant ($p > 0.05$) neurons were displayed as null in the bottom. **F.** Sorted phase-locking strength (Z values) for the three groups in **E**. Dotted line indicates significant phase-locking (to the right of the line, $p < 0.05$). Among phase-locked neurons, Z values were generally small for the putative cholinergic neurons, compared to the other two groups.

Figure 21



Chapter 4 Cholinergic modulation promotes immediate-early-gene upregulation induced by novel sensory experience: implication for learning and memory

4.1 Introduction

It is widely accepted that cholinergic systems are highly involved in learning and memory (Hasselmo and Bower 1993; Jerusalinsky, Kornisiuk et al. 1997; Gold 2003; Parent and Baxter 2004; Hasselmo 2006). Pharmacological studies in humans and animals indicate that systemic blockade of cholinergic activity produces amnesia (Pazzagli and Pepeu 1965; Caine, Weingartner et al. 1981), and patients with cholinergic deficits such as in Alzheimer's disease have memory deficits (Coyle, Price et al. 1983). Moreover, local blockade of hippocampal or cortical cholinergic signaling impairs learning and memory (Izquierdo, da Cunha et al. 1992; Warburton, Koder et al. 2003). Selective lesion of cholinergic projection neurons in MSvDB and basal forebrain with immunotoxin impairs learning and memory (Pizzo, Thal et al. 2002; Winters and Bussey 2005). On the other hand, boosting ACh transmission reverses pre-existing memory deficits (Davis and Mohs 1982; Levy, Kong et al. 1991; Hersi, Rowe et al. 1995), and even improves memory (Izquierdo, da Cunha et al. 1992).

However, the mechanism whereby ACh exerts its mnemonic functions remains to be elucidated, although the modulation of neural activity and neural plasticity by ACh has been postulated (Jerusalinsky, Kornisiuk et al. 1997; Gold 2003; Hasselmo 2006).

Learning behaviors, as simple as novel sensory experience, not only induce ACh release (Aloisi, Casamenti et al. 1997; Giovannini, Rakovska et al. 2001), but also

induce immediate early gene (IEG) expression (Hess, Lynch et al. 1995; Kelly and Deadwyler 2002; Montag-Sallaz and Montag 2003). IEGs are genes whose expression is induced by certain external stimuli but independent of *de-novo* synthesis of other proteins (Dragunow, Currie et al. 1989). Molecular neurobiology studies have shown that these IEGs (e.g. Zif-268, BDNF and *Arc*) are downstream to signaling pathways underlying synaptic plasticity. Interfering with their normal function with antisense nucleotides (Guzowski 2002) or by gene knock-out (Jones, Errington et al. 2001; Plath, Ohana et al. 2006) severely impairs synaptic plasticity and memory consolidation.

The fact that both ACh release and IEG expression are upregulated by learning experience indicates that the two may be tightly related. *In vitro* studies suggest that cholinergic muscarinic signaling regulates IEG expression (Trejo and Brown 1991; Ding, Larsson et al. 1998; Hirabayashi and Saffen 2000), and cholinergic agonist has been found to induce IEG expression *in vivo* (e.g. Fos protein (Hughes and Dragunow 1993)). Therefore, one possible way that ACh contributes to learning and memory functions may be by promoting IEG expression to facilitate memory consolidation. We hypothesize that ACh, and specifically, local ACh enhances IEG expression induced by learning experience. So far, evidence supporting this hypothesis is minimal (Wirtshafter 2005) and controversial (Fletcher, Baxter et al. 2007).

To test this hypothesis, we induced robust IEG expression using an enriched novel environment (Staiger, Bisler et al. 2000; Pinaud, Penner et al. 2001), and tested whether muscarinic antagonist would impair such induction, and if so, in which brain areas. Since *arc* (activity-regulated cytoskeleton-associated protein) is one of the IEGs that have been implicated in neural plasticity and learning and memory instead of mere reflection of neuronal activity (Lyford, Yamagata et al. 1995; Fletcher, Calhoun et al.

2006; Plath, Ohana et al. 2006; Tzingounis and Nicoll 2006; Bramham, Worley et al. 2008), *arc* was used as a representative IEG. We found strong *arc* induction in primary somatosensory (S1) cortices, as well as induction in other cortical and hippocampal areas, and such induction could be suppressed by scopolamine. We further tested if depletion of local ACh release, such as in cortex, would directly counteract the induction. To test this possibility, we produced cholinergic specific lesion in unilateral basal forebrain, the source of ACh input to the cortex.

4.2 Material and methods

4.2.1 Chemicals and materials

Scopolamine (mixed enantiomers) and methyl scopolamine (-) enantiomer, 3,3'-Diaminobenzidine (DAB) were obtained from Sigma Chemical Co. (St Louis, MO, USA). The immunotoxin, 192IgG-saporin, was purchased from Advanced Targeting Systems (San Diego, CA, USA). The rat *arc* antisense and sense cDNA were kindly provided by from Drs. Kazuhiro Wada and Erich Jarvis. Goat-anti-ChAT primary antibody, rabbit-anti-goat secondary antibody were purchased from Millipore (Billerica, MA, USA). ABC reagents were purchased from Vector Laboratories, INC (Burlingame, CA, USA).

4.2.2 Novel enriched environment exploration and drug treatment in mice

Thirty-five adult male mice (2-8 months) were used in the pharmacological study. Mice were individually housed with food and water ad lib. They were handled and habituated everyday for 6 consecutive days in their home cages in the room where the

behavioral experiment was conducted on the 6th day. Habituation constituted at least 3 hrs during the dark cycle and behavioral experiments were conducted during the dark cycle too. During this time, the room was only lit with a dim red light.

On the 6th day, a novel enriched environment (EE) was prepared in a plastic box (60cm x 30 cm x 25cm) with plenty of novel toys/objects of various shapes/textures/sizes (20~30 objects). Groups and behavioral/pharmacology assignments were specified in Figure 22. For the last four groups assigned drug or saline, they were injected intraperitoneally (I.P.) 5 minutes before the behavioral session. Scop-Novel mice were given 2mg/kg (body weight) scopolamine, with effective dose of 1mg/kg of the active enantiomer. Mice in mScop-Novel group were given 1mg/kg (body weight) of the pure active enantiomer of methyl scopolamine (peripheral muscarinic antagonist). Mice in “Saline” groups (Sal-Novel and Sal-HC) were given equivalent volume of saline.

Each mouse in the “Novel” groups were allowed to explore the novel environment/objects freely for 30 min (except Sal-Novel group), after which they were sacrificed. Mice in Sal-Novel group were exposed to the environment for certain time (2.5, 5, 10, 20, 30min) and put back to their home-cages, until they were sacrificed 30 min after the beginning of the novelty exploration. All exploration behaviors were recorded with an infrared camera.

“HC” control mice were briefly handled 30 min before being directly sacrificed from their home-cages. “Sal-HC” controls were injected with saline 35 min before sacrifice, to control for the potential arousing effect of IP injection on IEG induction as opposed to novelty.

4.2.3 Immunolesion of rats and novel enriched environment

Seven adult rats (3-5 month) were subjected to cholinergic specific lesion with immunotoxin. After anesthetized (ketamine, 100mg/kg, xylazine 5mg/kg, atropine 0.02mg), rats were positioned in a stereotaxic frame. Small craniotomies were drilled over targeted basal forebrain regions bilaterally at AP -1.0mm, ML \pm 2.5mm relative to Bregma (Paxinos and Watson 2005). Immunotoxin diluted to appropriated concentrations was injected unilaterally at depth -7.5mm below dura through a 30-gauge needle (2 rats: 65ng; 2 rats: 130ng; 3 rats: 260ng), and saline into the contralateral basal forebrain site. The injection volume was kept to be 1 μ L at each injection site for all animals. After injection, craniotomies were covered with dental acrylic and the skin was sutured. Two weeks were given for the rats to recover from surgery and the cholinergic lesion to be complete (Heckers, Ohtake et al. 1994).

All rats were handled and habituated after recovery, similar to the mice. Each of them were exposed to a large novel EE (120 cm x 80 cm x 70 cm) with plenty of novel objects of various shapes/textures/sizes (20~30 objects). After 30 min of exposure, the rats were sacrificed.

4.2.4 *In situ* hybridization and immunohistochemistry

After euthanasia of the animal, brains were promptly removed, frozen with embedding medium in dry ice, before stored at -80°C . Serial frontal sections (10 μm) were taken across the brain regions of interest (+0.5 ~ -2.5mm, in mouse; +1.0 ~ 4.0mm in rat; relative to Bregma) and thaw-mounted on RNase-free glass slides (Superfrost Plus; VWR Scientific, West Chester, PA). 20 μm sections were collected every 120 μm and stained with cresyl-violet for identification of anatomical structures.

Procedures for *in situ* hybridization has been described elsewhere (Ribeiro, Mello et al. 2002; Wada, Sakaguchi et al. 2004). ³⁵S-labeled riboprobes (antisense and sense RNA for *arc*) were transcribed from rat *arc* cDNA, with ³⁵S- labeled UTP. Before hybridization, sections were fixed in 3% paraformaldehyde, washed in phosphate-buffered saline, acetylated, washed in SSPE buffer, dehydrated, and then covered with hybridization solution containing ³⁵S-labeled riboprobe. Sections were incubated 12hrs at 65 °C, washed, dried and then exposed to a high-resolution phosphor screen for 48-72 hr. Images were then scanned on a Storm Phosphorimager System (Amersham Biosciences, Sunnyvale, CA). Absence of sense-strand hybridization signal was used as a control for specificity. Phosphorimager densitometric quantifications were performed to quantify gene expression levels for subsequent analyses, using ImageQuant software (Molecular Dynamics). Statistics were performed with SPSS software (SPSS Inc., Chicago, IL, USA).

Immunohistochemistry were performed on 20 µm rat sections containing the basal forebrain region (0 ~ -3mm, relative to Bregma). Sections were fixed in 3% paraformaldehyde, washed in phosphate-buffered saline, and stained with goat-anti-ChAT primary antibody(1:500), rabbit-anti-goat secondary antibody, ABC reagents and visualized with DAB. The number of ChAT+ neurons in the basal forebrain areas were counted for the lesioned and control hemispheres.

4.3 Results

4.3.1 Novel sensory experience induced *arc* upregulation in both somatosensory cortex and hippocampus

Novel environment (usually empty arena) has been shown to induce strong IEG upregulation in rats (Filipkowski, Rydz et al. 2000; Staiger, Bisler et al. 2000; Vazdarjanova, McNaughton et al. 2002; Wirtshafter 2005). First, we wanted to demonstrate that a novel environment with a large number of novel objects would induce *arc* expression in mice too. We tested this with naïve mice habituated to the experiment room. Figure 23 shows that this type of novel enriched environment (EE) was very effective in inducing *arc* expression in both cortex and hippocampus. Particularly, somatosensory cortex and motor cortex showed 2~2.5 fold *arc* activation in animals exposed to the novel EE, compared to animals stayed in their home-cages (Figure 23B, $p < 0.001$, two-tail t-test), while there was no induction in thalamus, the input stage of the sensory information. In somatosensory cortex, two clear bands of induction were seen in superficial and deeper layers respectively, matching the expression in layer IV and VI according to anatomical location (Hughes and Dragunow 1993; Filipkowski, Rydz et al. 2000; Bisler, Schleicher et al. 2002). In hippocampus, CA1 area had highest level of *arc* activation (~ 2 fold, $p < 0.01$), CA3 had mild upregulation ($p < 0.05$), while *arc* in dentate gyrus (DG) was not activated (Figure 23C). The cortical input/output of the hippocampus, perirhinal cortex, also had ~ 2 fold activation. These results established that novel EE, which provides a large amount of novel tactile information, can be a potent setting to induce *arc* upregulation in mouse, similar to rats.

4.3.2 Central but not peripheral scopolamine suppressed *arc* induction

To test whether blocking of cholinergic muscarinic transmission would suppress *arc* upregulation induced by the novel tactile information, we injected scopolamine, a muscarinic antagonist, 5 min before the mice were exposed to novel EE. The control groups received appropriate drug/saline 5 min before exposed to novel EE (Figure 22).

Some scopolamine treated mice did not explore as much as the Novel mice. To control for this potential confounding effect, exposure time to the novel EE in Sal-Novel mice were limited, ranging from 2.5 ~ 20 min, except for one Sal-Novel mice which was allowed the full 30 min in the novel EE. Despite exposed various amount of time (and shorter than the Scop-Novel group, 511 ± 402 and 1133 ± 339 sec, mean \pm s.d.), *arc* upregulation in Sal-Novel mice did not differ across exploration time ($p > 0.1$, Pearson correlation), so the expression levels were collapse for all Sal-Novel mice.

Like mice without saline injection, Sal-Novel mice also had robust cortical and hippocampal *arc* activation. However, *arc* levels in mice received scopolamine showed marked suppression, for all the areas had *arc* upregulation in Sal-Novel mice (Figure 24B, $p < 0.01$ in CA3, all other areas $p < 0.001$, Bonferroni multiple comparison test). These results suggest that *arc* induction was suppressed by systemic muscarinic antagonist.

To confirm that this effect was a result of central cholinergic antagonism, but not a peripheral effect, we tested the peripheral muscarinic antagonist, methyl scopolamine, which does not cross the blood brain barrier. This antagonist did not impair *arc* induction, compared to the Sal-Novel group (Figure 24B, except in CA1 area). These results

suggest that central, but not peripheral blockade of muscarinic receptors could suppress *arc* upregulation induced by novel tactile information.

When the reduced *arc* expression in Scop-Novel mice were compared to the HC mice with or without saline injection, the expression level were mostly not significantly different (LSD multiple comparison test (should use some other), $p > 0.6$ in almost all areas, except for Scop-Novel vs HC, in S1BF, $p = 0.02$, and motor cortex, $p = 0.03$). These results suggest that in the limit of our experimental error, the novel information induced *arc* upregulation was almost completely blocked by the central muscarinic antagonism. All these results suggest that central cholinergic transmission is an essential component that promotes IEG upregulation induced by novel information.

4.3.3 Specific lesion of basal forebrain cholinergic neurons constrains *arc* induction in somatosensory cortex

To further investigate whether the impairment of *arc* induction was a result of impairment of local cholinergic mechanism, we tried to deplete local ACh release by specifically lesioning the cholinergic neurons that are the source of ACh. We took advantage of the bilaterally organized basal forebrain area, which are known to be the source of ipsilateral cortices (Woolf 1991), and tested unilateral lesion with a within-subject control design. Rats were used because the high efficacy of the immunotoxin 192IgG-saporin on their cholinergic neurons than on mice. Rats were injected with one of three doses of the toxin (65, 130 and 260 ng in total), and saline was injected into the contralateral BF as an internal control. The cholinergic lesion was quite effective, as shown by the example in Figure 25A. The hemisphere injected with toxin usually had

10~30% of ChAT+ neurons compared to the saline control hemisphere, confirming evident to severe loss of cholinergic neuron depending on the toxin dose (Figure 25C).

After recovery, rats were habituated and exposed to novel EE. We compared the *arc* expression level in the lesioned hemisphere to that in the control hemisphere. In animals with relatively mild lesion, the reduction of *arc* level was almost negligible, while only animals with severe lesion showed stronger reduction in the lesioned hemisphere (Figure 25C). When the *arc* expression ratio was correlated with the lesion efficacy (ratio of ChAT+ cells in lesioned and control hemispheres), a significant correlation was only seen in the S1BF *arc* levels, but not in motor cortex or CA1 area of the hippocampus (Figure 25D). These results suggest that impairment of *arc* induction was correlated the completeness of the cholinergic lesion. Therefore, local ACh release in somatosensory cortex (S1BF) contribute to IEG induction. However, such induction in somatosensory cortex seemed to be affected only by severe cholinergic depletion.

4.4 Conclusion

In this study, we hypothesized that ACh promotes IEG expression induced by novel sensory experience, and tested the prediction that interference with normal cholinergic activities would impair IEG induction. We first demonstrated that muscarinic antagonism in the central, but not peripheral, nervous system suppressed both cortical and hippocampal *arc* induction (Figure 24). Based on the results with systemic cholinergic intervention, we further demonstrated that local cortical *arc* activation could be constrained by reduction of cortical ACh release, produced by specific cholinergic lesion in the basal forebrain (Figure 25). These results suggest that normal muscarinic

cholinergic transmission ensures novel-information-induced IEG activation, and at least part of this effect is local to the site of acetylcholine release.

4.5 Discussion

4.5.1 Site of action: direct (local) or indirect?

Systematic muscarinic antagonist suppresses IEG induction almost completely (Figure 24). However, the exact site of muscarinic antagonism could not be revealed by systemic intervention. At least two scenarios could be conceived. The first and simplistic possibility is that local ACh release, such as in S1 cortex or CA1 of hippocampus, directly acts on local cells and enhances their IEG expression level. The second but indirect mechanism is that the muscarinic antagonist acts on an area (or areas) that projects to cortex or hippocampus, and the antagonist modulates the activities of that unidentified area which is not under experimental investigation. The activities of that unidentified area, in turn, influence the IEG expression in the examined target areas. However, it is not easy to test and disambiguate either of these two possibilities. The indirect pathways, of course, are difficult to look for, since it is hidden. The direct action hypothesis, nevertheless, cannot be simply tested by local infusion of muscarinic antagonist into the target areas either, since IEGs are very sensitive to local disturbance. The mere action of injection could be a confounding factor that actually promotes IEG induction (Dragunow, Goulding et al. 1990; Honkaniemi, Sagar et al. 1995). Therefore, a manipulation in a remote site is required to interfere with the cholinergic activities in the target areas. As a solution, lesion of the cholinergic projection cells could be a way to test the first possibility.

Our results suggest that the first possibility, that local ACh release promotes IEG induction, is in play (Figure 25). However, this has been controversial in the literature. Supporting evidence comes from studies with lesion or inactivation of MSvDB, or its projection to the hippocampus, which did reduce IEG induction (Fletcher, Calhoun et al. 2006; Miyashita, Kubik et al. 2009). In contrast, a further study failed to reproduce the reduction of IEG after using the cholinergic specific toxin to impair hippocampal ACh input (Fletcher, Baxter et al. 2007). Based on these results, the authors suggested that cholinergic input from MSvDB is not required for hippocampal IEG induction. This result is not entirely consistent with our result. To reconcile these results, a few methodological considerations should be noted.

First of all, we waited two weeks after lesion (Heckers, Ohtake et al. 1994), while in this earlier paper (Fletcher, Baxter et al. 2007), the authors waited two months after the toxin lesion before testing the effect on IEG induction. Although the number of cholinergic cells has been shown to not recover during this extended period of time (Heckers, Ohtake et al. 1994), compensations could have taken place. The remaining cholinergic cells might have increased their ACh output dramatically, which has been shown by microdialysis (Chang and Gold 2004), and there could also be compensatory innervation from other cholinergic sources, such as the sympathetic nerve ingrowth (Harrell, Parsons et al. 2005). All these effect could have compensated the ACh release in the hippocampus, and maintained a relatively normal IEG induction.

Second, we produced unilateral lesion in the basal forebrain region and used within-subject control, which gave us better power to resolve the effect of the lesion. In contrast, MSvDB is a midline structure and it would be very difficult to produce unilateral lesion. This earlier paper had to compare between groups (lesion and control), which

might have larger individual variability that masked the difference between the two groups.

Nevertheless, our results are not in marked contrast with this earlier paper. The cholinergic lesion in our experiments was not complete either, which is not uncommon (Waite and Chen 2001; McGaughy, Dalley et al. 2002). With mild lesion, the IEG induction was hardly affected. When expression levels of all animals were averaged together, the cholinergic impairment was mild to none. This result, together with earlier results (Fletcher, Baxter et al. 2007), suggest that cholinergic enhancement of IEG induction may require just a mild level of ACh but not the entire normal level, and only severe impairment of cholinergic activities would impair IEG induction. Alternatively, local area may not be the sole action site of ACh on IEG induction.

The indirect possibility of cholinergic action could be supported by structural substrates. Cholinergic system innervates other subcortical structures, including other neuromodulatory systems (Woolf 1991). For example, basal forebrain cholinergic neurons innervates amygdala, which is known to be involved in memory functions (Power 2004) and regulation of IEGs, possibly interacting with noradrenergic signaling (McIntyre, Miyashita et al. 2005; Sheth, Berretta et al. 2008). Furthermore, besides long-range projection, cholinergic neurons in MSvDB and basal forebrain also have local collaterals to innervate non-cholinergic neurons in the same nuclei (Woolf 1991). Such innervation may in turn, exert synergistic modulation on the IEG expression in the target areas. These potential pathways may partly explain the residual induction seen in animals with cholinergic-specific lesion.

In all, our results suggest that local action of ACh in S1 is a direct mechanism to modulate IEG induction, but possibility of indirect pathways remains open and are very

likely to exist too. Dependence on these two mechanisms may also differ for different areas (S1BF cortex vs motor cortex, or hippocampus).

4.5.2 Intracellular mechanism of local cholinergic modulation on *arc* expression

The modulation of IEG by ACh is mostly through muscarinic receptors (Hughes and Dragunow 1993; Teber, Kohling et al. 2004). Our results are consistent with this notion. Earlier studies have suggested that M1 receptor may be responsible for such activation (Hughes and Dragunow 1994). M1 receptor involvement under current behavioral condition remains to be verified with a potent and specific M1 receptor antagonist. Alternatively, M1 receptor knock-out mice, and more ideally, region-specific M1 receptor knock-out mice, could be used to confirm such hypothesis. Downstream to M1 receptors are the G-proteins and phospholipase proteins including type C (PLC), which can further activate a series of downstream signaling-kinase pathways, including extracellular regulated protein kinase (ERK) (Felder 1995; Rosenblum, Futter et al. 2000; Lanzafame, Christopoulos et al. 2003). Cholinergic modulation of learning-induced ERK activation has been demonstrated, and is critical for memory consolidation (Giovannini, Pazzagli et al. 2005). Kinases including ERK, can in turn activate transcription factors to initiate transcription of IEGs (Bozon, Kelly et al. 2003; Murphy and Blenis 2006; Girault, Valjent et al. 2007).

4.5.3 Molecular mechanism underlying cholinergic modulation of neural plasticity *in vivo*: implications for learning and memory

IEGs are speculated to be the molecular underpins of synaptic plasticity and memory consolidation. Promotion of learning-induced IEG expression substantiates the role of ACh in mnemonic functions. Our results indicate that mild impairment of cholinergic activities leaves IEG induction relatively intact. It requires a severe cholinergic impairment to produce marked suppression of IEG induction. These results parallel some controversial conclusions reached by earlier behavioral/learning studies: systemic or local pharmacological interference with muscarinic antagonist usually impairs memory consolidation, while specific lesion of septohippocampal cholinergic projection produced mild to no effect.

One possible explanation is that the role of ACh in memory consolidation may not be an indispensable factor, but a facilitator or enhancer. Novel information can be conveyed by cortical or hippocampal circuitries, which use glutamatergic transmission primarily. Memory could be formed and stored by such circuitry alone, but may suffer from inefficiency under conditions without cholinergic modulation. Conversely, having an intact cholinergic system may greatly improve the efficiency of the consolidation of such memory traces. In parallel, the induction of IEG is possibly initiated by non-cholinergic mechanisms, such as glutamatergic transmission. Having adequate cholinergic activities in the network amplifies the signaling, and helps to promote the downstream molecular cascades.

Another possibility may be that the ACh level in most experimental setup is more than enough to ensure memory consolidation, especially in experimental setups which ACh release is dramatically induced and the entire goal of the experiment is to form a

specific memory designed by the experimenter. Under more natural conditions, ACh release might be fine-tuned, and the effect on IEG induction may be more critical to consolidate memory traces from background information.

Figure 22. Schematics of mice experiments with pharmacology

Mice were assigned into groups randomly. All mice habituated for 6 days with at least 3 hrs in their home-cages in an almost-dark experiment room with a dim red light. For groups assigned with drug or saline injection, mice were injected I.P. 5 min before the exploration (or 35min before sacrifice for Sal-HC). All Novel groups were exposed to a novel enriched environment (EE) for thirty minutes except the group Sal-Novel, which was put back to their home-cages sometime during the 30 min. After the behavioral session, all mice were sacrificed and brains were removed promptly for gene expression measurement.

Figure 22

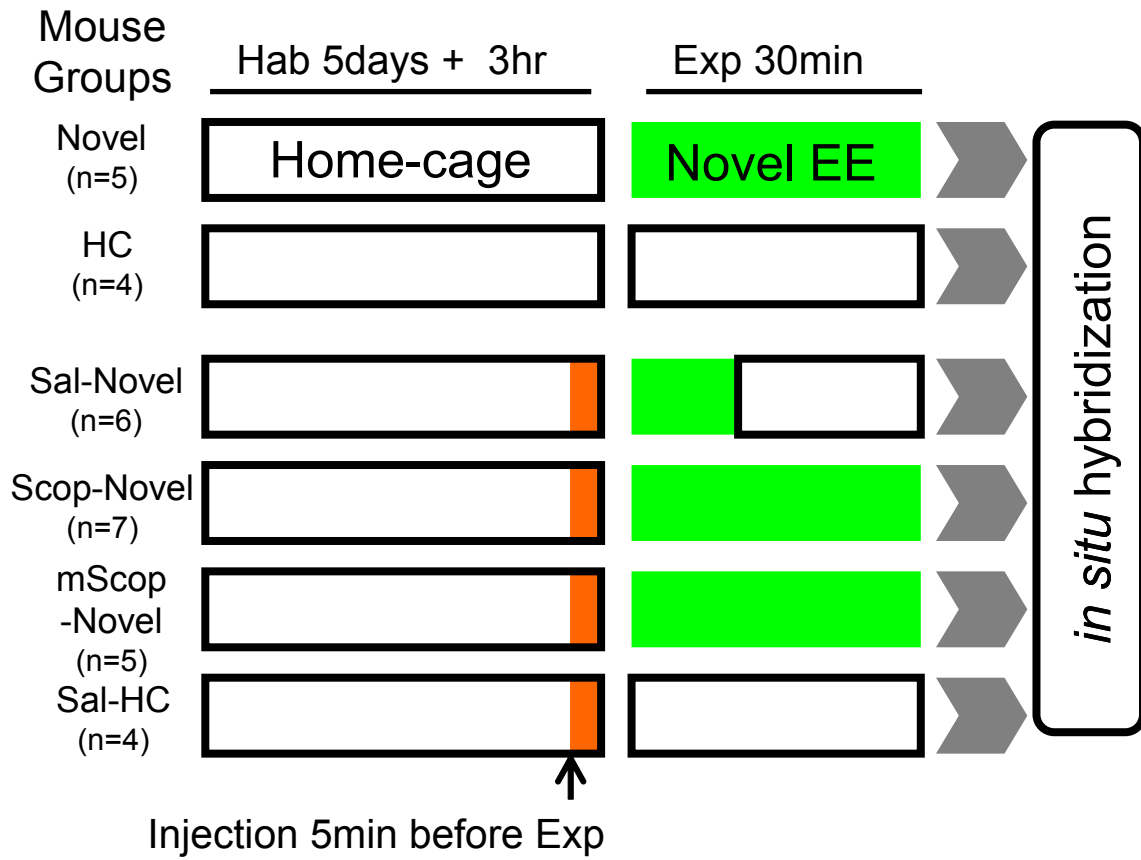


Figure 23. Novel sensory experience induces *arc* upregulation in both somatosensory cortex and hippocampus.

A. Pseudo-color image of representative *arc* expression from Novel and HC groups. Warmer colors indicate higher expression level. **B.** Novel somatosensory experience induced robust cortical and CA1 *arc* expression in mice. Expression levels in thalamus and dentate gyrus (DG) of hippocampus were not upregulated. Expression level is in units of phosphor-image density (arbitrary units). S1BF: primary somatosensory cortex, barrel field. S2: secondary somatosensory cortex. Ect/PRh: ectorhinal/perirhinal cortices. Error bar, S.E.M. ***, $p < 0.001$; **, $p < 0.01$; *, $p < 0.05$, two-tail t-test.

Figure 23

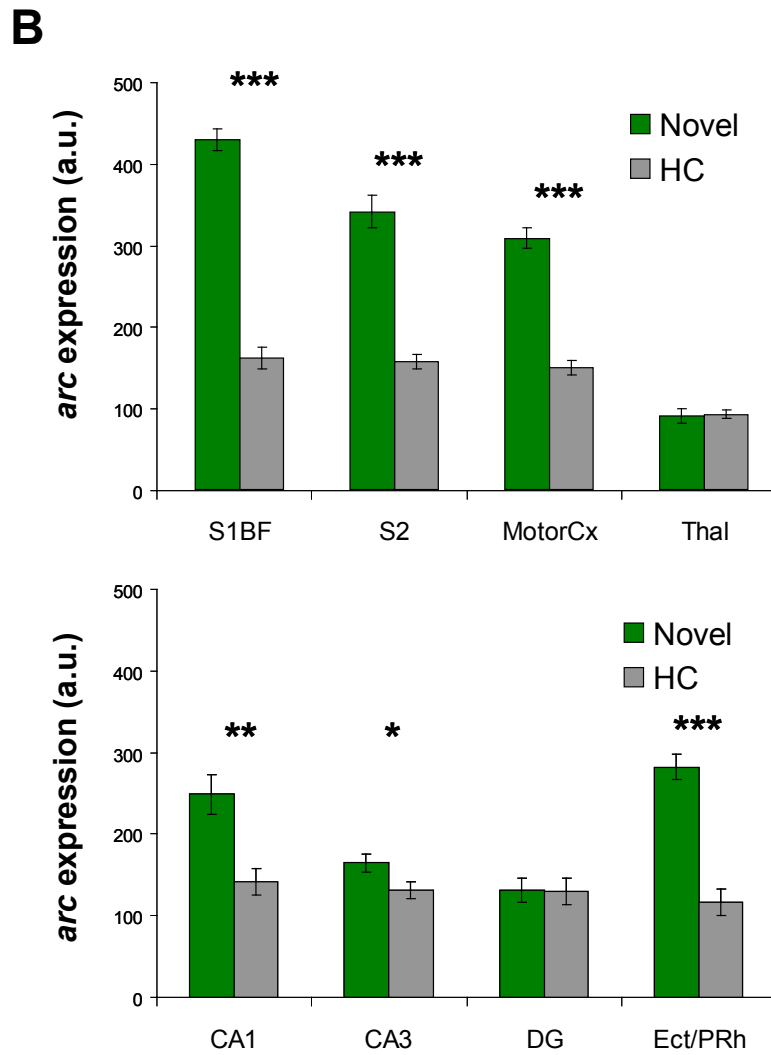
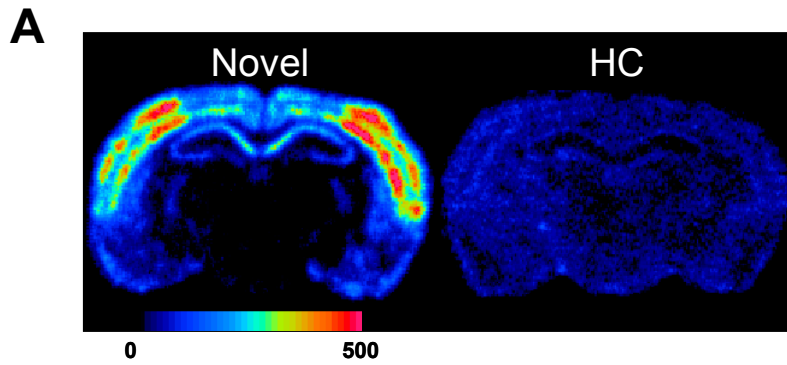


Figure 24. Central but not peripheral scopolamine suppresses *arc* induction.

A. Pseudo-color image of representative *arc* expression from different groups. **B.** All areas with *arc* upregulation in normal mice showed impairment of the upregulation after scopolamine treatment. The peripheral antagonist, methyl scopolamine, did not affect such upregulation, except in CA1 area of the hippocampus. Error bar, S.E.M. ***, $p < 0.001$; **, $p < 0.01$; o, $p > 0.05$, Bonferroni multiple comparison tests .

Figure 24

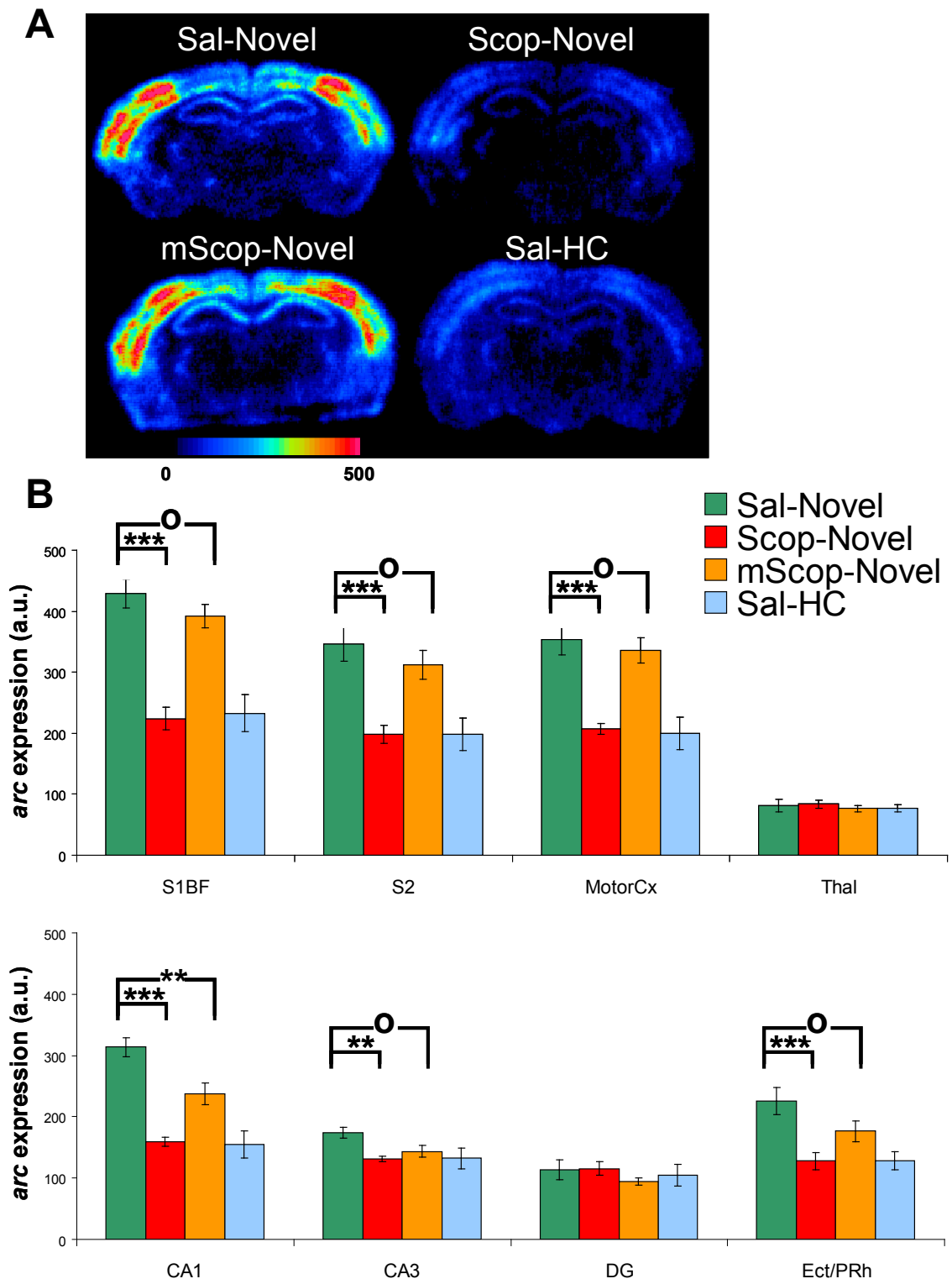
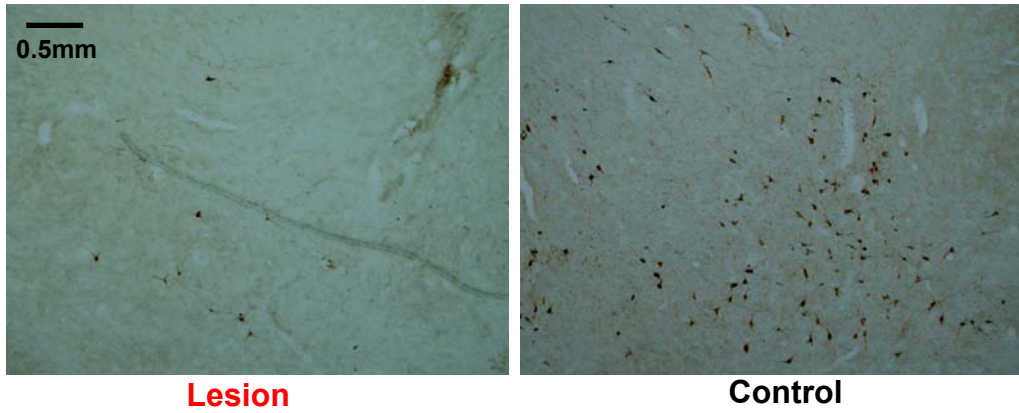


Figure 25. Specific lesion of basal forebrain cholinergic neurons constrains *arc* induction in ipsilateral somatosensory cortex.

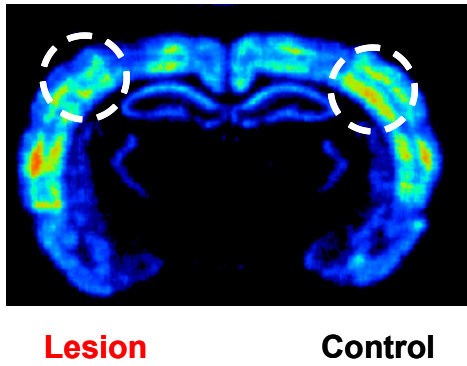
A. Representative immunohistochemistry image with cholinergic lesion demonstrated with ChAT staining. The number of ChAT+ cells were greatly reduced in the toxin injected hemisphere (*left*), compared to saline injected hemisphere (*right*). **B.** Representative unilateral reduction of *arc* expression in S1BF region. Circles indicate S1BF. **C.** Remaining ChAT+ cell number as a function of toxin dose. Higher dose resulted in more complete lesion. **D.** Correlation of remaining cholinergic function and *arc* expression. Number of ChAT+ cells, and *arc* expression were compared between lesion and control hemispheres, and correlation across animals were calculated. Only the S1BF showed significant correlation ($p=0.04$, Pearson correlation), but not motor cortex ($p=0.21$) or CA1 ($p=1.0$).

Figure 25

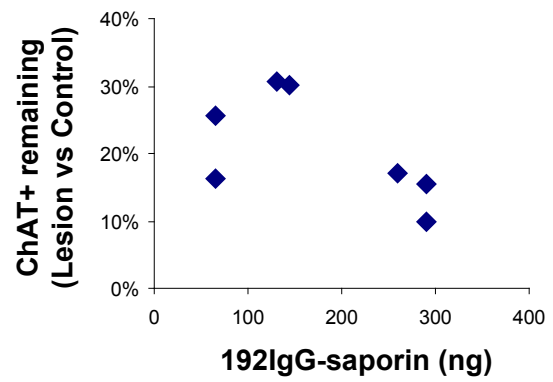
A



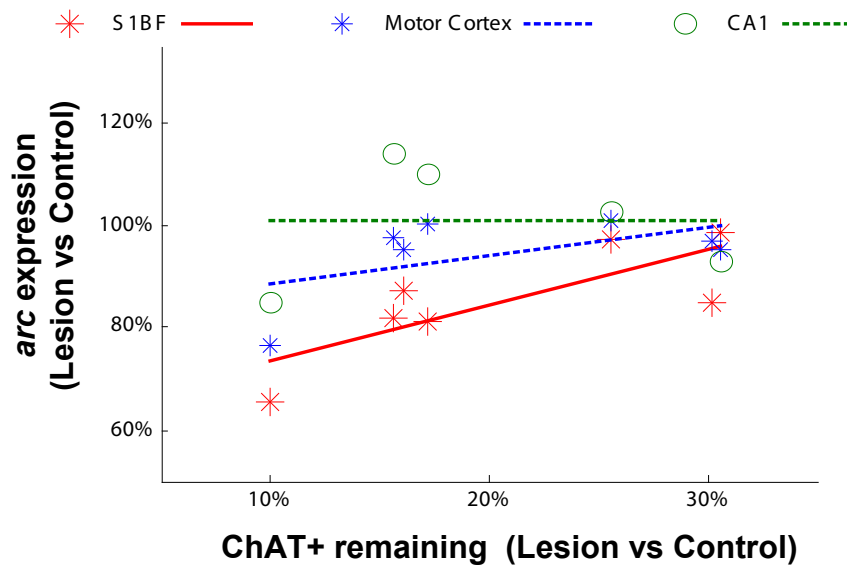
B



C



D



Chapter 5 General discussions

5.1 Conclusions

To study the mechanisms of forebrain cholinergic functioning, I monitored their dynamic activities with amperometry and electrophysiology, and further investigated their influence on hippocampal LFPs and IEG induction.

First, I developed a novel neurophysiological technique to acquire simultaneous electrophysiological and neurochemical information with amperometry. Using this technique, I discovered that phasic hippocampal ACh release was tightly coupled to the appearance of both spontaneous and induced theta oscillations. Maximal ACh release was observed around or slightly above the pyramidal layer. Interestingly, such release lagged behind theta initiation by 20-40 seconds. The slow ACh release profile was matched by the slow firing rate increase of a subset of medial-septal low-firing-rate neurons. Together, these results establish for the first time the tight *in vivo* coupling between phasic ACh release and theta oscillations on fine spatiotemporal scales. These findings also suggest that phasic ACh is not required for theta initiation, and may instead operate synergistically with theta oscillations to promote neural plasticity in service of learning and memory.

Second, I further investigated MSvDB neurons in behaving rats, and looked for putative cholinergic neurons and their functions. I identified a subpopulation of slow-firing MS neurons, which had much higher firing rate during REM sleep and often had brief responses (15~35 ms after stimulus onset) to auditory stimuli. The firing of these putative cholinergic neurons modulated hippocampal activity in a state dependent

manor. During waking or rapid-eye-movement (REM) sleep in which theta oscillations are permitted, their firing promoted higher-frequency theta and gamma oscillations. During slow-wave (SW) sleep in which theta is not favored, their firing interrupted slow-wave activities and induced a short burst of beta / lower gamma oscillations, possibly promoting the transient SIA epochs. These results suggest that putative cholinergic neurons in MSvDB may be a generalized hippocampal arousal/activation network, and they may contribute to cognitive functions through their dynamic modulation of hippocampal LFPs.

Third, I investigated a potential molecular mechanism by which cholinergic system supports neural plasticity and learning&memory. Specifically, I manipulated cholinergic transmission and tested the effect on the induction of IEGs, using *arc* as a representative IEG. I found that *arc* induction was suppressed by pharmacological blockade of muscarinic receptors, or by a cholinergic specific lesion in basal forebrain. These results suggest that cholinergic transmission, including local transmission, may substantiate learning and memory function by promoting IEG expression for memory consolidation.

To summarize, I investigated the dynamic interactions between ACh release and theta oscillations in the hippocampus, the dynamic firing of putative cholinergic neurons in MSvDB, and their influence on hippocampal local field potentials. These results suggest that cholinergic activities may operate on much faster temporal scales than traditionally assumed, in realization of its behavioral and cognitive functions. I further elucidated that forebrain cholinergic modulation promotes IEG expression induced by learning experience, which may be a molecular mechanism of cholinergic function in memory consolidation.

5.2 Cholinergic neurons in the medial septal area

Interests in neuronal activities in MSvDB grew since the early discovery of neurons that fire rhythmically at theta frequency and MSvDB was confirmed to be the pacemaker of hippocampal theta oscillations (Stumpf, Petsche et al. 1962; Macadar, Roig et al. 1970; Morales, Roig et al. 1971; Winson 1978; Andersen, Bland et al. 1979; Buzsaki, Leung et al. 1983; Bland and Bland 1986; Mizumori, Perez et al. 1990). As a result, a number of categorization schemes had been proposed, mostly based on their firing properties related to theta oscillations (Stumpf, Petsche et al. 1962; Gaztelu and Buno 1982; Ford, Colom et al. 1989). The neurons described in our studies (Chapter 3) are probably Type II neurons (Gaztelu and Buno 1982; King, Recce et al. 1998), and theta-on (Ford, Colom et al. 1989). Regardless of what traditional categories they belong to, these neurons seem to form a unique functional group that is different from MSvDB neurons being focused on traditionally.

There are very few reports with identified cholinergic neurons *in vivo*. As a result, we had to rely on other pertinent facts that hint the probable properties of cholinergic neurons. Nevertheless, we identified a subpopulation of neurons in MSvDB being cholinergic putatively, and demonstrated some of their properties that can be used in future verification studies.

If our postulation is true, that the subpopulation we recorded are cholinergic neurons, new functions of MSvDB cholinergic neurons can be proposed. During REM and waking, they promote an increase of the power of higher frequency theta and gamma oscillations. During SW sleep, they are probably promoting the transient arousal

state, SIA. Therefore, it is possible that cholinergic neurons in MSvDB form a generalized final arousal or activation network for the hippocampus.

5.3 Acetylcholine and theta oscillations

Most of the earlier studies focused on how ACh participates in the generation and modulation of theta oscillations (reviews in Bland 1986; Vanderwolf 1988; Bland and Colom 1993; Vertes and Kocsis 1997; Buzsaki 2002). Our results in Chapter 2 revealed yet another level of the tight connection between ACh and theta in the hippocampus, on much finer temporal scales.

Based on our results, an intriguing possibility can be postulated that these phasic ACh releases, working synergistically or sequentially with theta oscillations, may provide exceptional opportunities to dynamically modulate neural plasticity on much finer temporal scales than traditionally assumed. Such time course (tens of seconds – minutes), is actually consistent with the idea of promoting molecular events in support of neuronal plasticity and memory consolidation, which is corroborated with the findings in Chapter 4.

5.4 The role of acetylcholine in learning and memory functions

5.4.1 Enhancement but not required?

The role that ACh plays in learning and memory has been intensively studied over decades, especially in the septohippocampal system. Early pharmacological studies suggest that change in cholinergic transmission has parallel effect on learning and memory. Specifically, manipulations that increase hippocampal ACh release

improves performance in memory tasks (Hersi, Rowe et al. 1995; Ragozzino and Gold 1995; Scali, Giovannini et al. 1997; Scali, Giovannini et al. 1997; Nava, Carta et al. 2000; Carey, Billard et al. 2001; Kopf, Buchholzer et al. 2001; Darnaudery, Pallares et al. 2002), while decreasing hippocampal ACh leads to impaired learning and memory (Brioni, Decker et al. 1990; Hiramatsu, Mori et al. 1996; Olariu, Tran et al. 2001). Manipulations that enhance hippocampal cholinergic signaling reverse memory deficits (Howard, Gross et al. 1989; Degroot and Parent 2000; Degroot and Parent 2001). Non-specific lesions that deplete the medial septal cholinergic input to hippocampus impair memory and recapitulate many deficits produced by hippocampal lesion (Mahut 1972; Mitchell, Rawlins et al. 1982; Hagan, Salamone et al. 1988). Other than some exceptions, the majority of this type of studies favor the view that septohippocampal ACh is essential for learning and memory.

With the invention of the cholinergic specific immunotoxin, a lot of studies tried to reproduce the early results with a more specific lesion of the septohippocampal cholinergic neurons, while leaving the non-cholinergic component largely unaffected. However, the results of these studies often fail to corroborate the early view, as most of them produced no apparent deficits (Berger-Sweeney, Heckers et al. 1994; Baxter and Gallagher 1996; McMahan, Sobel et al. 1997; Kirby and Rawlins 2003), although some studies with high doses of the toxin reported significant deficits (Shen, Barnes et al. 1996; Pang, Nocera et al. 2001; Lehmann, Grottick et al. 2003). Currently, the results of this line of studies are still controversial. On one hand, non-completeness and compensatory effect might explain the lack of deficits produced by these specific lesions (Chang and Gold 2004). On the other hand, question about non-specific effect is raised when studies did show deficits produced by these toxin (Parent and Baxter 2004).

Our results in Chapter 4 showed that systematic muscarinic antagonist severely impaired the IEG induction, while mild impairment of cholinergic input left IEG induction largely intact. It seems that a severe cholinergic impairment is required to produce marked suppression of IEG induction. These results parallel the controversial results reached by earlier behavioral/learning studies.

It seems that the level of the cholinergic impairment determines whether a significant behavioral or molecular consequence would occur. One possible explanation is that the role of ACh in memory consolidation (or IEG induction) may not be an indispensable factor, but a facilitator or enhancer. Another possibility may be that in most experiments, the level of ACh is more than enough to enhance or ensure the consolidation of a specific piece of memory. Under more natural conditions, ACh release might be fine-tuned, and the effect on IEG induction may be more critical to consolidate memory traces from background information.

5.4.2 Acetylcholine and sleep-dependent memory consolidation

The participation of ACh in memory functions, and its fluctuations during in sleep-waking cycles, raise the possibility that ACh may be involved in sleep-dependent memory consolidation. Studies in the last decade or so have suggested that one of the functions of sleep may be off-line processing or consolidation of memory (Graves, Pack et al. 2001; Walker and Stickgold 2004). Since ACh level is high during REM sleep (Marrosu, Portas et al. 1995; Bianchi, Ballini et al. 2003), and putative MSvDB cholinergic neurons fire a lot more during REM sleep (Chapter 3), it is likely that such transient enhancement of ACh is involved in the memory consolidation during REM sleep (Siegel 2001). Given the evidence that ACh promotes IEG induction (Chapter 4), it

is very possible that during REM the enhanced level of ACh promotes IEG expression for the memory consolidation (Ribeiro, Goyal et al. 1999; Ribeiro, Mello et al. 2002; Ribeiro, Shi et al. 2007).

5.5 Forebrain acetylcholine functioning and common theme of the functioning of neuromodulatory systems

5.5.1 Cholinergic modulation of plasticity

Neural plasticity is considered the underlying mechanism for learning and memory, and other types of behavior that involves long term changes in the brain. The function of ACh in many behavioral and cognitive processes, are likely substantiated by the function of ACh in modulating plastic changes in the brain. So far, supporting evidence comes from two main lines of research. The first one is the involvement of cholinergic mechanism in support of LTP. These studies demonstrate that both *in vitro* and *in vivo*, cholinergic transmission promotes, or even permits LTP formation, usually in the hippocampus (Jerusalinsky, Kornisiuk et al. 1997; Segal and Auerbach 1997; Leung, Shen et al. 2003; Doralp and Leung 2008). The second line of studies focuses on the reorganization of cortical sensory representation (Kilgard and Merzenich 1998; Sachdev, Lu et al. 1998; Conner, Chiba et al. 2005; Origlia, Kuczewski et al. 2008), and some of these changes also lead to behavioral consequences (Weinberger 2003).

The participation of cholinergic system in these plastic events is supported by the organization of the cholinergic system. Cholinergic axons innervate almost all the forebrain areas (discussed in the next section), and can act through a variety of receptors (Woolf 1991). Particularly, through the G-protein coupled muscarinic receptors (Volpicelli and Levey 2004), cholinergic transmission can participate in the molecular

cascades involved in the intracellular mechanism of neuronal plasticity, and consequently modulate the expression of IEGs (Chapter 4). By modulating these molecular and cellular events, the cholinergic system can substantiate its role in neural plasticity and consequently changes in behavior, including memory consolidation.

5.5.2 A global network

The forebrain cholinergic projection systems innervate the hippocampus and the entire cortical mantle, and they are interlinked with other cholinergic systems in the brain (Woolf 1991). This suggests that the cholinergic systems, as a whole, may work as a global network that help to set the basic tones of the brain. In other words, the function of this network may be not to process specific or detailed information, but to ensure the general state or mode of the brain (or part of the brain), like arousal, attention, or learning. With the stage setup, specific information processing may then take place in the cortex or the hippocampus. This general view of global network may also apply to other neuromodulatory systems (Woolf 1996), which I will discuss in the next section.

Traditionally, such setting of global state is considered rather slow. The results in Chapter 2 and 3 suggest that the temporal dynamics of the cholinergic system may be much faster than previously assumed. Through this potent and dynamic global cholinergic network, the state of the neural network may be quickly updated, by external stimulus/requirements, and internal drives.

5.5.3 Comparison to other neuromodulatory systems

The functioning of the cholinergic system shares a lot of similar properties with other neuromodulatory systems, such as the norepinephrine, dopamine, and serotonin systems. They all originate from fairly localized subcortical structures, and innervate almost the entire brain (Nicholls and Fuchs 2001; Purves, Augustine et al. 2004). All of them can act through a number of corresponding receptors that may differentially modulate the activity of the neurons and areas that express these receptors. Almost all the receptors are metabotropic receptors, which are linked to the intracellular signaling pathways that are involved in neuronal plasticity. Indeed, all these neuromodulatory systems have been shown to consequently modulate IEG expressions too (Hughes and Dragunow 1995). In this way, all these systems have the ability to participate in the plastic changes that underlies the long term behavioral changes, including learning and memory, addiction, psychiatric disease, etc.

The dynamics of the other neuromodulatory systems have also been shown to be more temporally fine-tuned than previously thought. The locus coeruleus norepinephrine neurons can function in two modes, phasic and tonic, which may help with optimization of task performance (exploitation), or disengagement and searching for alternative behaviors (exploration) (Aston-Jones and Cohen 2005). The dopaminergic system have been shown to function in tonic and phasic modes too, the latter of which is tightly related to behaviorally-important or reward-associated events (Dreher and Burnod 2002).

There are some differences between the cholinergic systems and the other neuromodulatory systems. Comparing to all other systems, the cholinergic systems may have more complex dynamics on multiple time scales, as shown in Chapter 2 and

Chapter 3, and a seminal research paper published recently (Parikh, Kozak et al. 2007) (dopamine system may operate on multiple time scales too, see Schultz 2007).

Furthermore, the extensive forebrain cholinergic network in the medial septal – basal forebrain areas, together with other cholinergic nuclei in the caudal areas, seem to have a more complicated architecture than the other neuromodulatory systems. The cholinergic systems may therefore be able to play more diversified roles in behavior and cognitive processes. They may also have finer-tuning in spatial specificity, in other words, more localized effect in specific brain modules.

In summary, all the neuromodulatory systems, including the cholinergic systems, may participate in a relatively global manner, with certain fine-tuning capabilities, to shape the neuronal activities and plasticity in the target areas, which would subsequently affect the behavior.

In fact, the dynamic interaction between neuromodulatory systems and neural activities in the target areas is gaining research interest in recent years. However, limitations in experimental techniques have hindered the growth of the field. The technical improvement I will discuss in the next section may help to bridge the gap and promote the research in this general direction.

5.6 A novel neurophysiology method and its potential applications

5.6.1 A hidden property of voltammetry method never describe before

To our knowledge, the high frequency signal has been typically treated as general noise and routinely discarded by other researchers, and there has not been any

explicit statement that suggested the existence of LFP-originated “noise” in amperometric signals. The closest description of such *in vivo* noise speculated it to be “induced by physical motions of the animal” (Garguilo and Michael 1996). Thus, understanding the nature of such a signal component represents a fundamental contribution to the use of amperometry technique in the brain. Such knowledge will facilitate specific efforts to reduce electrophysiological noise, which will improve amperometry measurement sensitivity and/or accuracy.

On the other hand, we propose to take advantage of this signal and use amperometry to obtain both LFP and neurochemical information. As we pointed out earlier, simultaneous acquisition of both conventional LFP and amperometric signals requires the implementation of independent amperometric and electrophysiological recording systems, which is technically challenging, and is an expensive combination that is not commonly available in most research laboratories. This technical challenge clearly contributed to the scarcity of this type of research. Our discovery provides a convenient alternative to obtain both LFP and chemical information using only the amperometry system. Furthermore, these two types of signals originated from the same recording electrode, which is a clear advantage over recording these signals from two separate electrodes with two systems. These advantages make our method more practical, and may promote a wide range of new studies.

5.6.2 Further improvements to use amperometry HFC as an LFP substitute

While the spectral features of amperometry HFC and LFP were grossly similar, minor discrepancies were noted, such as differences in the relative spectral power

(Figure 5B and Figure 6B) and the diminished correlation at higher frequencies (Figure 5A). Several factors may have contributed to the discrepancies. First, the sensor and the MEA were placed in contralateral hemispheres. Even though we tried to match the recording locations, minor differences were expected. Second, the distinctive material and geometry of the active sites in amperometric sensor and multi-electrode array (MEA, the LFP recording electrodes) may have also contributed to the discrepancies. Third, the measurements were different – amperometry measures currents while regular electrophysiology measures voltages, and the voltage-current conversion may introduce waveform distortions and may depend on different filtering properties of the electrical circuitry in the amplifier (Nelson, Pouget et al. 2008).

It is important to point out that amperometry HFC is not a simple equivalent to conventional LFP. Voltage fluctuations in the brain (such as LFPs) are converted to amperometry HFC based on the impedance in the system. Since the impedance may not be readily measurable, it may be very difficult to reconstruct conventional LFPs in every aspect. Nevertheless, because impedance can be reasonably assumed to be constant in individual experiments, many aspects of the intended LFP information can be reliably retrieved, qualitatively and/or quantitatively, as demonstrated in our results.

Regarding the frequency range of LFPs, the upper limit of our amperometric recording is 40 Hz, thus we currently do not know up to which frequency range amperometry HFC would reflect LFPs. However, it is very likely that the acquisition of the signal has a much higher theoretical frequency limit. If a higher sampling frequency and proper hardware filtering are used, it may be possible to retrieve the full spectrum of LFP information. Towards the very high frequency range (1 k-50 kHz), it may even be

possible to detect action potentials of individual neurons using an amperometric sensor electrode with a reduced area comparable to the MEA.

5.6.3 Separating chemical signals from electrical signals and the validity of chemical information obtained from amperometry

The phenomenon we reported here was demonstrated with the FAST-16 amperometry setup. We cannot be completely sure, therefore, whether this high frequency component appears generically in other electrochemical systems. Theoretically, this LFP-like component would not appear if the input impedance of the amplifier is infinite, but this is generally not the case. In fact, some researchers were aware of the noise showing up on *in vivo* amperometric recordings (Garguilo and Michael 1996). It is now clear that this type of “noise” in our system originates from electrical signals in the brain. Thus, the immediate concern would be: how can one reliably retrieve chemical signals, which is the original purpose of using amperometry and other voltammetric techniques?

Without knowing this specific noise source, researchers in previous *in vivo* electrochemical studies have used generic noise-reduction and validation methods, such as filtering, self-referencing or applying alternative voltage. We revisit these methods below to highlight their respective strengths and limitations, and accommodate them in our recommendations for chemical signal separation as well as validation, in light of our new knowledge on the origin of amperometry HFC signals.

As a first approximation, we recommend a frequency separation, i.e. taking the low-frequency component as the chemical signal. We used 1Hz as the frequency cut-off to separate the “chemical” and “LFP” signals, because chemical signals in amperometric

recordings generally do not fluctuate faster than 1Hz (Garguilo and Michael 1996; Parikh, Pomerleau et al. 2004; Parikh, Kozak et al. 2007; Rutherford, Pomerleau et al. 2007). This frequency-separation method can be used reasonably well and has the extra advantage of being very convenient when the chemical dynamics are known to have little overlap with LFP in the frequency domain. However, it should be pointed out that LFP oscillations can be slower than 1Hz (Penttonen, Nurminen et al. 1999; Wolansky, Clement et al. 2006). Conversely, the onset of phasic neurotransmitter release may contain frequency component exceeding 1Hz (Dugast, Suaud-Chagny et al. 1994; Robinson, Venton et al. 2003). Therefore, since residual electrical (chemical) signal in the low (high) frequency component may be expected, when using the frequency-separation in amperometric studies, the exact cut-off frequency should be estimated and justified by the nature and the focus of the particular study.

An alternative to retrieve the chemical signal is to use a self-reference design for the sensor (Burmeister, Palmer et al. 2003; Rutherford, Pomerleau et al. 2007) so that the differential signal between the chemical-sensing site and the reference site should in theory represent a pure chemical signal. In practice, however, the reference site can never be as identical as the chemical-sensing site, because the two sites differ at least in their physical locations. Additional minor difference in effective area may also lead to difference in the amplitude of their HFC signals (reflecting LFPs), likely offset by a fixed factor as shown in Figure 7A. A simple subtraction of the two original signals will erroneously include the residual LFP-originated signal into the presumed chemical signal. To resolve the issue of size difference, we suggest combining the frequency separation and self-reference methods: the amplitude ratio of LFP information can be first estimated using only HFC signals (>1Hz), which can then be applied to correct the

low-frequency component between the two sites (see Figure 8). This combination retrieves the chemical signal with less contamination from electrical signals, and should help to improve signal-to-noise ratio for chemical measurement.

Separating out putative chemical signals is often closely related to the validation of these signals. For example, self-referencing has an important second function as a validation method. One more available validation method we would like to recommend is to directly estimate the LFP-originated amperometry HFC amplitude and frequency by recording at a certain low voltage (such as 0V) with the same electrode. This method is based on the fact that applying an alternative voltage could minimize the target chemical reactions, while the HFC amplitude is not affected by the applied voltage (Figure 7E). The disadvantage of this method is that a separate recording session is required to collect these data.

Based on the above discussion of the strengths and limitations of individual separation / validation methods, we suggest using multiple methods to retrieve chemical signals from amperometry recordings.

Without appropriate validation, and if this LFP-originated high frequency component does appear in other amperometry setups, a particular theoretical concern is the use of the “event-related average” to identify chemical responses. Small LFP-ERP (event-related potential) responses may stand out in the averaging process (Gazzaniga, Ivry et al. 2002) , and potentially be mistaken as evoked chemical responses when appropriate signal validation was not applied. In this regard, event-related amperometric studies are likely most susceptible to LFP contamination and should be interpreted with more caution regarding the validity of chemical signals, especially when appropriate validation was lacking.

5.6.4 Potential applications

Technical difficulties have limited studies on real time interaction between neuromodulators and electrophysiological activities. One solution, represented by Dr. Wightman and others, was to use a quasi-simultaneous method that switches between neuronal spike recording and fast-scan cyclic voltammetry with two recording systems (Williams and Millar 1990; Stamford, Palij et al. 1993; Cheer, Heien et al. 2005). Although this method has a similar advantage to record signals from a single electrode, it cannot be used to record continuous signals like LFPs. Our method can solve this problem in a convenient way.

Based on the methodology proposed in Chapter 2, simultaneous acquisition of both LFP and neurochemical information can now be realized in many labs using amperometry alone, without additional equipments. We believe that this technical breakthrough will contribute significantly to the future growth of *in vivo* electrochemistry by allowing a series of new experiments to be performed. Using the technique, we demonstrated for the first time that phasic acetylcholine release is coupled to the occurrence of theta oscillations on a fine temporal scale, currently not measurable by microdialysis (Chang, Savage et al. 2006). The same general strategy could be applied to study interaction between other neurochemical and brain rhythms with the method proposed here.

On a broader perspective, one approach to study the function of neuromodulatory systems is to investigate how they influence neuronal activities related to particular behaviors or disorders. Such line of investigation has been hindered because of obstacles to obtain simultaneous *in vivo* neurochemical and

electrophysiological measurement on a desirable time scale. The technical advancement proposed in our paper, with a relatively simple experimental setup, solves this issue and may contribute decisively for the expansion of research that aims at characterizing the contribution of neuromodulators to normal or pathological brain states in behavioral models or models of neurological disorders (Cheer, Heien et al. 2005; Costa, Lin et al. 2006; Dzirasa, Ribeiro et al. 2006).

5.7 Limitation and Future directions

5.7.1 Choline measurement in free-moving animals

In Chapter 2, we demonstrated for the first time the tight coupling between phasic ACh release and theta oscillations *in vivo*. However, these experiments were performed on anesthetized animals. Whether the same observation can be extended to unanesthetized animals remain to be verified.

Currently, I am working on the implementation of amperometry recording in behaving animals. So far, I have observed a couple cases in which phasic choline increase accompanied REM sleep episodes, consistent with earlier microdialysis results (Marrosu, Portas et al. 1995; Bianchi, Ballini et al. 2003).

However, a few technical improvements are required for progress. First of all, noise reduction. The noise in amperometric recording in behaving animals is much larger than in anesthetized animals. This includes movement noise, and unknown source of electrical noise. In anesthetized animals, movement noise is minimal, and the recording setup and animal can be carefully shielded from external electrical noise, so that LOD can reach very low level (Chapter 2, Figure 8 , ~ 100nM without signal

correction, and even as low as 10nM after signal correction). In behaving animals, LOD seems to be a lot more than 100nM. This seem to be similar to the *in vivo* noise level showed in another paper, but fortunately, behavioral-events-related phasic ACh release may be much larger than in anesthetized animals (Parikh, Kozak et al. 2007).

Secondly, locating maximal ACh release site. As demonstrated in Chapter 2 (Figure 11), phasic ACh release in the hippocampus is maximal around the CA1 pyramidal layer, but much smaller in other layers. If this is the case for unanesthetized animals as well, it would be quite difficult to record from the exact layer of maximal ACh release, since the current implementation have the sensor fixed after implantation, which precludes the possibility to search for a maximal release site in the way described in Chapter 2 acute recordings.

Third, sensor stability. Sensor fouling occurs quite fast after being implanted into the brain and constantly in contact with brain tissue. In my pilot experiments, they seemed to fail after a few days. It is reported that using a different exclusion layer (Nafion), the sensor could last for more than one or two weeks (personal communication). However, this negatively-charged exclusion layer only expels anions, and seems to concentrate cationic interferents, such as dopamine, which could confound results obtained with Nafion-coated choline sensors.

Last but not least, calibration during or after experiment. Calibration for sensor specificity and LOD is extremely difficult after implantation, because unlike acute studies, it is almost impossible to perform post-experiment *in vitro* calibration. Therefore, given the short life of sensor, signals obtained in behaving animals have to be more carefully scrutinized to confirm the specificity, and the cholinergic nature of the results.

With improvement of these technical issues, we will be able to address questions on fast dynamics of ACh in behaving animals and what exact role they play in different types of behavioral and cognitive processes.

5.7.2 Chemical identity of neurons recorded *in vivo*

In Chapter 2, putative MSvDB cholinergic neurons were found to match the phasic ACh release profile. In chapter 3, I looked for firing properties of putative MSvDB cholinergic neurons that had not been focused on before, and identified a distinct subpopulation that may be by far the most likely candidate for cholinergic neurons. However, like most earlier studies, we could not verify the chemical identity of these neurons. A few approaches may help to verify whether these are cholinergic neurons.

First of all, juxtacellular labeling and immunohistochemical identification will be the most convincing approach to resolve this issue. However, the low yield of the recording is a technical barrier that needs to be overcome.

Secondly, it may be plausible to introduce cell-type specific expression of channel-rhodopsin into MSvDB cholinergic cells (Zhang, Aravanis et al. 2007), and identify them based on their response to locally applied light stimulation. When using such optogenetic method, extra caution should be used to make sure that light-responsive cells are the transfected cells, but not cells excited mono- or poly-synaptically by the transfected cells. The extra bonus of this method is that it enables precise control to exogenously recruit the MSvDB cholinergic cell network, and study how the activation of this network would affect hippocampal activities as well as function (such as information processing, memory consolidation, etc).

The third method that may be able to help is to apply cholinergic-specific toxin locally into MSvDB to eliminate cholinergic cells, and to see whether the neurons with properties described in our study (Chapter 3) are eliminated. Caution is needed when using this method to carefully gauge the completeness and specificity of the cholinergic lesion (Torres, Perry et al. 1994; Pizzo, Waite et al. 1999; Chang, Savage et al. 2006). Furthermore, if such cells are indeed shown to be reduced in number, it needs to be considered whether the effect is a direct reflection of the loss of cholinergic neurons, or it is secondary to the loss. Example of the latter seemed to have happened in an earlier MSvDB study. That paper concluded that the rhythmic-bursting cells were cholinergic cells because the cholinergic-specific lesion greatly reduced the appearance of these cells (Apartis, Poindessous-Jazat et al. 1998), but only later the same group identified cholinergic neurons with immunostaining and stated that all of the cholinergic cells were slow-firing and had no apparent relationship with theta oscillations, in both anesthetized and unanesthetized animals (Simon, Poindessous-Jazat et al. 2006).

5.7.3 General future directions

The dynamic cholinergic activities presented in this dissertation were recorded from animals engaged in relative simple behaviors (or in anesthetized animals). Their interaction with and influence on hippocampal activities reported here may reflect a baseline state of *in vivo* cholinergic action. Whether their engagement and their impact would follow similar manner or behave in a different pattern, during more complex cognitive processes such as during specific learning and memory tasks, requires further investigation. With the novel and the improved techniques and approaches used here, more detailed *in vivo* mechanism of cholinergic functions can be pursued.

References

- Aloisi, A. M., F. Casamenti, et al. (1997). "Effects of novelty, pain and stress on hippocampal extracellular acetylcholine levels in male rats." Brain Res **748**(1-2): 219-26.
- Andersen, P., H. B. Bland, et al. (1979). "Septo-hippocampal pathway necessary for dentate theta production." Brain Res **165**(1): 13-22.
- Andersen, P. M., R. D. Amaral, et al., Eds. (1996). The Hippocampus Book, Oxford University Press.
- Apartis, E., F. R. Poindessous-Jazat, et al. (1998). "Loss of rhythmically bursting neurons in rat medial septum following selective lesion of septohippocampal cholinergic system." J Neurophysiol **79**(4): 1633-42.
- Apostol, G. and O. D. Creutzfeldt (1974). "Crosscorrelation between the activity of septal units and hippocampal EEG during arousal." Brain Res **67**(1): 65-75.
- Arvidsson, U., M. Riedl, et al. (1997). "Vesicular acetylcholine transporter (VAChT) protein: a novel and unique marker for cholinergic neurons in the central and peripheral nervous systems." J Comp Neurol **378**(4): 454-67.
- Aston-Jones, G. and F. E. Bloom (1981). "Norepinephrine-containing locus coeruleus neurons in behaving rats exhibit pronounced responses to non-noxious environmental stimuli." J Neurosci **1**(8): 887-900.
- Aston-Jones, G. and J. D. Cohen (2005). "An integrative theory of locus coeruleus-norepinephrine function: adaptive gain and optimal performance." Annu Rev Neurosci **28**: 403-50.
- Aznavour, N., N. Mechawar, et al. (2002). "Comparative analysis of cholinergic innervation in the dorsal hippocampus of adult mouse and rat: a quantitative immunocytochemical study." Hippocampus **12**(2): 206-17.
- Bassant, M. H., E. Apartis, et al. (1995). "Selective immunolesion of the basal forebrain cholinergic neurons: effects on hippocampal activity during sleep and wakefulness in the rat." Neurodegeneration **4**(1): 61-70.
- Baxter, M. G. and M. Gallagher (1996). "Intact spatial learning in both young and aged rats following selective removal of hippocampal cholinergic input." Behav Neurosci **110**(3): 460-7.

- Berger-Sweeney, J., S. Heckers, et al. (1994). "Differential effects on spatial navigation of immunotoxin-induced cholinergic lesions of the medial septal area and nucleus basalis magnocellularis." J Neurosci **14**(7): 4507-19.
- Bialowas, J. and M. Frotscher (1987). "Choline acetyltransferase-immunoreactive neurons and terminals in the rat septal complex: a combined light and electron microscopic study." J Comp Neurol **259**(2): 298-307.
- Bianchi, L., C. Ballini, et al. (2003). "Investigation on acetylcholine, aspartate, glutamate and GABA extracellular levels from ventral hippocampus during repeated exploratory activity in the rat." Neurochem Res **28**(3-4): 565-73.
- Bigl, V., N. J. Woolf, et al. (1982). "Cholinergic projections from the basal forebrain to frontal, parietal, temporal, occipital, and cingulate cortices: a combined fluorescent tracer and acetylcholinesterase analysis." Brain Res Bull **8**(6): 727-49.
- Bisler, S., A. Schleicher, et al. (2002). "Expression of c-Fos, ICER, Krox-24 and JunB in the whisker-to-barrel pathway of rats: time course of induction upon whisker stimulation by tactile exploration of an enriched environment." J Chem Neuroanat **23**(3): 187-98.
- Bland, B. H. (1986). "The physiology and pharmacology of hippocampal formation theta rhythms." Prog Neurobiol **26**(1): 1-54.
- Bland, B. H. and L. V. Colom (1993). "Extrinsic and intrinsic properties underlying oscillation and synchrony in limbic cortex." Prog Neurobiol **41**(2): 157-208.
- Bland, B. H., S. Declerck, et al. (2007). "Septohippocampal properties of N-methyl-D-aspartate-induced theta-band oscillation and synchrony." Synapse **61**(3): 185-97.
- Bland, B. H. and I. Q. Whishaw (1976). "Generators and topography of hippocampal theta (RSA) in the anaesthetized and freely moving rat." Brain Res **118**(2): 259-80.
- Bland, S. K. and B. H. Bland (1986). "Medial septal modulation of hippocampal theta cell discharges." Brain Res **375**(1): 102-16.
- Bliss, T. V. and G. L. Collingridge (1993). "A synaptic model of memory: long-term potentiation in the hippocampus." Nature **361**(6407): 31-9.
- Blokland, A. (1995). "Acetylcholine: a neurotransmitter for learning and memory?" Brain Res Brain Res Rev **21**(3): 285-300.

- Book, A. A., R. G. Wiley, et al. (1992). "Specificity of 192 IgG-saporin for NGF receptor-positive cholinergic basal forebrain neurons in the rat." Brain Res **590**(1-2): 350-5.
- Book, A. A., R. G. Wiley, et al. (1994). "192 IgG-saporin: I. Specific lethality for cholinergic neurons in the basal forebrain of the rat." J Neuropathol Exp Neurol **53**(1): 95-102.
- Borhegyi, Z., V. Varga, et al. (2004). "Phase segregation of medial septal GABAergic neurons during hippocampal theta activity." J Neurosci **24**(39): 8470-9.
- Bozon, B., A. Kelly, et al. (2003). "MAPK, CREB and zif268 are all required for the consolidation of recognition memory." Philos Trans R Soc Lond B Biol Sci **358**(1432): 805-14.
- Bramham, C. R., P. F. Worley, et al. (2008). "The immediate early gene arc/arg3.1: regulation, mechanisms, and function." J Neurosci **28**(46): 11760-7.
- Brazhnik, E. S. and S. E. Fox (1997). "Intracellular recordings from medial septal neurons during hippocampal theta rhythm." Exp Brain Res **114**(3): 442-53.
- Brazhnik, E. S. and S. E. Fox (1999). "Action potentials and relations to the theta rhythm of medial septal neurons in vivo." Exp Brain Res **127**(3): 244-58.
- Brioni, J. D., M. W. Decker, et al. (1990). "Muscimol injections in the medial septum impair spatial learning." Brain Res **522**(2): 227-34.
- Buccafusco, J. J., S. R. Letchworth, et al. (2005). "Long-lasting cognitive improvement with nicotinic receptor agonists: mechanisms of pharmacokinetic-pharmacodynamic discordance." Trends Pharmacol Sci **26**(7): 352-60.
- Burmeister, J. J., M. Palmer, et al. (2003). "Ceramic-based multisite microelectrode array for rapid choline measures in brain tissue." Analytica Chimica Acta **481**(1): 65-74.
- Burmeister, J. J., F. Pomerleau, et al. (2008). "Ceramic-based multisite microelectrode arrays for simultaneous measures of choline and acetylcholine in CNS." Biosens Bioelectron **23**(9): 1382-9.
- Butt, A. E., G. Testylier, et al. (1997). "Acetylcholine release in rat frontal and somatosensory cortex is enhanced during tactile discrimination learning." Psychobiology **25**(1): 18-33.
- Buzsaki, G. (2002). "Theta oscillations in the hippocampus." Neuron **33**(3): 325-40.

- Buzsaki, G., L. Kellenyi, et al. (1980). "Effects of scopolamine upon hippocampal electrical activity associated with running and swimming in rats." Physiol Behav **24**(1): 191-4.
- Buzsaki, G., L. W. Leung, et al. (1983). "Cellular bases of hippocampal EEG in the behaving rat." Brain Res **287**(2): 139-71.
- Caine, E. D., H. Weingartner, et al. (1981). "Qualitative analysis of scopolamine-induced amnesia." Psychopharmacology (Berl) **74**(1): 74-80.
- Calandrea, L., P. Trifilieff, et al. (2006). "Extracellular hippocampal acetylcholine level controls amygdala function and promotes adaptive conditioned emotional response." J Neurosci **26**(52): 13556-66.
- Carey, G. J., W. Billard, et al. (2001). "SCH 57790, a selective muscarinic M(2) receptor antagonist, releases acetylcholine and produces cognitive enhancement in laboratory animals." Eur J Pharmacol **431**(2): 189-200.
- Cartling, B. (2001). "Neuromodulatory control of interacting medial temporal lobe and neocortex in memory consolidation and working memory." Behav Brain Res **126**(1-2): 65-80.
- Chang, Q. and P. E. Gold (2004). "Impaired and spared cholinergic functions in the hippocampus after lesions of the medial septum/vertical limb of the diagonal band with 192 IgG-saporin." Hippocampus **14**(2): 170-9.
- Chang, Q., L. M. Savage, et al. (2006). "Microdialysis measures of functional increases in ACh release in the hippocampus with and without inclusion of acetylcholinesterase inhibitors in the perfusate." J Neurochem.
- Cheer, J. F., M. L. Heien, et al. (2005). "Simultaneous dopamine and single-unit recordings reveal accumbens GABAergic responses: implications for intracranial self-stimulation." Proc Natl Acad Sci U S A **102**(52): 19150-5.
- Cole, A. E. and R. A. Nicoll (1984). "Characterization of a slow cholinergic post-synaptic potential recorded in vitro from rat hippocampal pyramidal cells." J Physiol **352**: 173-88.
- Colom, L. V., S. Nassif-Caudarella, et al. (1991). "In vivo intrahippocampal microinfusion of carbachol and bicuculline induces theta-like oscillations in the septally deafferented hippocampus." Hippocampus **1**(4): 381-90.

- Conner, J. M., A. A. Chiba, et al. (2005). "The basal forebrain cholinergic system is essential for cortical plasticity and functional recovery following brain injury." Neuron **46**(2): 173-9.
- Costa, R. M., S. C. Lin, et al. (2006). "Rapid alterations in corticostriatal ensemble coordination during acute dopamine-dependent motor dysfunction." Neuron **52**(2): 359-69.
- Coyle, J. T., D. L. Price, et al. (1983). "Alzheimer's disease: a disorder of cortical cholinergic innervation." Science **219**(4589): 1184-90.
- Crouzier, D., D. Baubichon, et al. (2006). "Acetylcholine release, EEG spectral analysis, sleep staging and body temperature studies: a multiparametric approach on freely moving rats." J Neurosci Methods **151**(2): 159-67.
- Dale, N., S. Hatz, et al. (2005). "Listening to the brain: microelectrode biosensors for neurochemicals." Trends Biotechnol **23**(8): 420-8.
- Darnaudery, M., M. Pallares, et al. (2002). "The neurosteroid pregnenolone sulfate infused into the medial septum nucleus increases hippocampal acetylcholine and spatial memory in rats." Brain Res **951**(2): 237-42.
- Davis, K. L. and R. C. Mohs (1982). "Enhancement of memory processes in Alzheimer's disease with multiple-dose intravenous physostigmine." Am J Psychiatry **139**(11): 1421-4.
- DeCoteau, W. E., C. Thorn, et al. (2007). "Learning-related coordination of striatal and hippocampal theta rhythms during acquisition of a procedural maze task." Proc Natl Acad Sci U S A **104**(13): 5644-9.
- Degroot, A. and M. B. Parent (2000). "Increasing acetylcholine levels in the hippocampus or entorhinal cortex reverses the impairing effects of septal GABA receptor activation on spontaneous alternation." Learn Mem **7**(5): 293-302.
- Degroot, A. and M. B. Parent (2001). "Infusions of physostigmine into the hippocampus or the entorhinal cortex attenuate avoidance retention deficits produced by intraseptal infusions of the GABA agonist muscimol." Brain Res **920**(1-2): 10-8.
- Descarries, L. (1998). "The hypothesis of an ambient level of acetylcholine in the central nervous system." J Physiol Paris **92**(3-4): 215-20.

- Descarries, L., V. Gisiger, et al. (1997). "Diffuse transmission by acetylcholine in the CNS." Prog Neurobiol **53**(5): 603-25.
- Ding, W. Q., C. Larsson, et al. (1998). "Stimulation of muscarinic receptors induces expression of individual fos and jun genes through different transduction pathways." J Neurochem **70**(4): 1722-9.
- Doralp, S. and L. S. Leung (2008). "Cholinergic modulation of hippocampal CA1 basal-dendritic long-term potentiation." Neurobiol Learn Mem **90**(2): 382-8.
- Dougherty, K. D., P. I. Turchin, et al. (1998). "Septocingulate and septohippocampal cholinergic pathways: involvement in working/episodic memory." Brain Res **810**(1-2): 59-71.
- Dragunow, M., R. W. Currie, et al. (1989). "Immediate-early genes, kindling and long-term potentiation." Neurosci Biobehav Rev **13**(4): 301-13.
- Dragunow, M., M. Goulding, et al. (1990). "Induction of c-fos mRNA and protein in neurons and glia after traumatic brain injury: pharmacological characterization." Exp Neurol **107**(3): 236-48.
- Dreher, J. C. and Y. Burnod (2002). "An integrative theory of the phasic and tonic modes of dopamine modulation in the prefrontal cortex." Neural Netw **15**(4-6): 583-602.
- Dugast, C., M. F. Suaud-Chagny, et al. (1994). "Continuous in vivo monitoring of evoked dopamine release in the rat nucleus accumbens by amperometry." Neuroscience **62**(3): 647-54.
- Dutar, P., M. H. Bassant, et al. (1995). "The septohippocampal pathway: structure and function of a central cholinergic system." Physiol Rev **75**(2): 393-427.
- Dzirasa, K., S. Ribeiro, et al. (2006). "Dopaminergic control of sleep-wake states." J Neurosci **26**(41): 10577-89.
- Everitt, B. J. and T. W. Robbins (1997). "Central cholinergic systems and cognition." Annu Rev Psychol **48**: 649-84.
- Ewing, A. G., K. D. Alloway, et al. (1983). "Simultaneous electrochemical and unit recording measurements: characterization of the effects of D-amphetamine and ascorbic acid on neostriatal neurons." Brain Res **261**(1): 101-8.
- Feder, R. and J. B. Ranck, Jr. (1973). "Studies on single neurons in dorsal hippocampal formation and septum in unrestrained rats. II. Hippocampal slow waves and

- theta cell firing during bar pressing and other behaviors." Exp Neurol **41**(2): 532-55.
- Felder, C. C. (1995). "Muscarinic acetylcholine receptors: signal transduction through multiple effectors." Faseb J **9**(8): 619-25.
- Filipkowski, R. K., M. Rydz, et al. (2000). "Tactile experience induces c-fos expression in rat barrel cortex." Learn Mem **7**(2): 116-22.
- Fletcher, B. R., M. G. Baxter, et al. (2007). "Selective cholinergic depletion of the hippocampus spares both behaviorally induced Arc transcription and spatial learning and memory." Hippocampus.
- Fletcher, B. R., M. E. Calhoun, et al. (2006). "Fornix lesions decouple the induction of hippocampal arc transcription from behavior but not plasticity." J Neurosci **26**(5): 1507-15.
- Fontan-Lozano, A., J. Troncoso, et al. (2005). "Cholinergic septo-hippocampal innervation is required for trace eyeblink classical conditioning." Learn Mem **12**(6): 557-63.
- Ford, R. D., L. V. Colom, et al. (1989). "The classification of medial septum-diagonal band cells as theta-on or theta-off in relation to hippocampal EEG states." Brain Res **493**(2): 269-82.
- Freund, T. F. and G. Buzsaki (1996). "Interneurons of the hippocampus." Hippocampus **6**(4): 347-470.
- Garguilo, M. G. and A. C. Michael (1996). "Amperometric microsensors for monitoring choline in the extracellular fluid of brain." J Neurosci Methods **70**(1): 73-82.
- Gaykema, R. P., P. G. Luiten, et al. (1990). "Cortical projection patterns of the medial septum-diagonal band complex." J Comp Neurol **293**(1): 103-24.
- Gaztelu, J. M. and W. Buno, Jr. (1982). "Septo-hippocampal relationships during EEG theta rhythm." Electroencephalogr Clin Neurophysiol **54**(4): 375-87.
- Gazzaniga, M. S., R. B. Ivry, et al. (2002). Cognitive neuroscience: the biology of the mind. New York, W. W. Norton & Company, Inc.
- Gervasoni, D., S. C. Lin, et al. (2004). "Global forebrain dynamics predict rat behavioral states and their transitions." J Neurosci **24**(49): 11137-47.

- Gillin, J. C., N. Sitaram, et al. (1982). "Acetylcholine, sleep, and depression." Hum Neurobiol **1**(3): 211-9.
- Giovannini, M. G., M. Pazzagli, et al. (2005). "Inhibition of acetylcholine-induced activation of extracellular regulated protein kinase prevents the encoding of an inhibitory avoidance response in the rat." Neuroscience **136**(1): 15-32.
- Giovannini, M. G., A. Rakovska, et al. (2001). "Effects of novelty and habituation on acetylcholine, GABA, and glutamate release from the frontal cortex and hippocampus of freely moving rats." Neuroscience **106**(1): 43-53.
- Girault, J. A., E. Valjent, et al. (2007). "ERK2: a logical AND gate critical for drug-induced plasticity?" Curr Opin Pharmacol **7**(1): 77-85.
- Gold, P. E. (2003). "Acetylcholine modulation of neural systems involved in learning and memory." Neurobiol Learn Mem **80**(3): 194-210.
- Golebiewski, H., B. Eckersdorf, et al. (1992). "Cholinergically-induced theta-like oscillations in the hippocampal formation of freely moving cats." Neuroreport **3**(5): 417-20.
- Golebiewski, H., B. Eckersdorf, et al. (1993). "Muscarinic (M1) mediation of hippocampal spontaneous theta rhythm in freely moving cats." Neuroreport **4**(12): 1323-6.
- Gotti, C. and F. Clementi (2004). "Neuronal nicotinic receptors: from structure to pathology." Prog Neurobiol **74**(6): 363-96.
- Granon, S., P. Faure, et al. (2003). "Executive and social behaviors under nicotinic receptor regulation." Proc Natl Acad Sci U S A **100**(16): 9596-601.
- Graves, L., A. Pack, et al. (2001). "Sleep and memory: a molecular perspective." Trends Neurosci **24**(4): 237-43.
- Gray, J. A. and N. McNaughton (1983). "Comparison between the behavioural effects of septal and hippocampal lesions: a review." Neurosci Biobehav Rev **7**(2): 119-88.
- Griffith, W. H. and R. T. Matthews (1986). "Electrophysiology of AChE-positive neurons in basal forebrain slices." Neurosci Lett **71**(2): 169-74.
- Gritti, I., P. Henny, et al. (2006). "Stereological estimates of the basal forebrain cell population in the rat, including neurons containing choline acetyltransferase, glutamic acid decarboxylase or phosphate-activated glutaminase and colocalizing vesicular glutamate transporters." Neuroscience **143**(4): 1051-64.

- Guzowski, J. F. (2002). "Insights into immediate-early gene function in hippocampal memory consolidation using antisense oligonucleotide and fluorescent imaging approaches." Hippocampus **12**(1): 86-104.
- Hagan, J. J., J. D. Salamone, et al. (1988). "Place navigation in rats is impaired by lesions of medial septum and diagonal band but not nucleus basalis magnocellularis." Behav Brain Res **27**(1): 9-20.
- Hajszan, T., M. Alreja, et al. (2004). "Intrinsic vesicular glutamate transporter 2-immunoreactive input to septohippocampal parvalbumin-containing neurons: novel glutamatergic local circuit cells." Hippocampus **14**(4): 499-509.
- Hangya, B., Z. Borhegyi, et al. (2009). "GABAergic neurons of the medial septum lead the hippocampal network during theta activity." J Neurosci **29**(25): 8094-102.
- Harrell, L. E., D. S. Parsons, et al. (2005). "The effect of central cholinergic and noradrenergic denervation on hippocampal sympathetic ingrowth and apoptosis-like reactivity in the rat." Brain Res **1033**(1): 68-77.
- Hasselmo, M. E. (2005). "What is the function of hippocampal theta rhythm?--Linking behavioral data to phasic properties of field potential and unit recording data." Hippocampus **15**(7): 936-49.
- Hasselmo, M. E. (2006). "The role of acetylcholine in learning and memory." Curr Opin Neurobiol.
- Hasselmo, M. E. and J. M. Bower (1993). "Acetylcholine and memory." Trends Neurosci **16**(6): 218-22.
- Hasselmo, M. E. and B. P. Fehlau (2001). "Differences in time course of ACh and GABA modulation of excitatory synaptic potentials in slices of rat hippocampus." J Neurophysiol **86**(4): 1792-802.
- Hasselmo, M. E. and L. M. Giocomo (2006). "Cholinergic modulation of cortical function." J Mol Neurosci **30**(1-2): 133-5.
- Hasselmo, M. E., J. Hay, et al. (2002). "Neuromodulation, theta rhythm and rat spatial navigation." Neural Netw **15**(4-6): 689-707.
- Heckers, S., T. Ohtake, et al. (1994). "Complete and selective cholinergic denervation of rat neocortex and hippocampus but not amygdala by an immunotoxin against the p75 NGF receptor." J Neurosci **14**(3 Pt 1): 1271-89.

- Hefti, F. and D. Felix (1983). "Chronoamperometry in vivo: does it interfere with spontaneous neuronal activity in the brain?" J Neurosci Methods **7**(2): 151-6.
- Henny, P. and B. E. Jones (2008). "Projections from basal forebrain to prefrontal cortex comprise cholinergic, GABAergic and glutamatergic inputs to pyramidal cells or interneurons." Eur J Neurosci **27**(3): 654-70.
- Hersi, A. I., W. Rowe, et al. (1995). "Dopamine D1 receptor ligands modulate cognitive performance and hippocampal acetylcholine release in memory-impaired aged rats." Neuroscience **69**(4): 1067-74.
- Hess, U. S., G. Lynch, et al. (1995). "Regional patterns of c-fos mRNA expression in rat hippocampus following exploration of a novel environment versus performance of a well-learned discrimination." J Neurosci **15**(12): 7796-809.
- Himmelheber, A. M., M. Sarter, et al. (2000). "Increases in cortical acetylcholine release during sustained attention performance in rats." Brain Res Cogn Brain Res **9**(3): 313-25.
- Hirabayashi, T. and D. Saffen (2000). "M1 muscarinic acetylcholine receptors activate zif268 gene expression via small G-protein Rho-dependent and lambda-independent pathways in PC12D cells." Eur J Biochem **267**(9): 2525-32.
- Hiramatsu, M., H. Mori, et al. (1996). "Improvement by dynorphin A (1-13) of galanin-induced impairment of memory accompanied by blockade of reductions in acetylcholine release in rats." Br J Pharmacol **118**(2): 255-60.
- Honkaniemi, J., S. M. Sagar, et al. (1995). "Focal brain injury induces multiple immediate early genes encoding zinc finger transcription factors." Brain Res Mol Brain Res **28**(1): 157-63.
- Howard, M. A., 3rd, A. Gross, et al. (1989). "Intracerebral drug delivery in rats with lesion-induced memory deficits." J Neurosurg **71**(1): 105-12.
- Hughes, P. and M. Dragunow (1993). "Muscarinic receptor-mediated induction of Fos protein in rat brain." Neurosci Lett **150**(1): 122-6.
- Hughes, P. and M. Dragunow (1994). "Activation of pirenzepine-sensitive muscarinic receptors induces a specific pattern of immediate-early gene expression in rat brain neurons." Brain Res Mol Brain Res **24**(1-4): 166-78.

- Hughes, P. and M. Dragunow (1995). "Induction of immediate-early genes and the control of neurotransmitter-regulated gene expression within the nervous system." Pharmacol Rev **47**(1): 133-78.
- Izquierdo, I., C. da Cunha, et al. (1992). "Neurotransmitter receptors involved in post-training memory processing by the amygdala, medial septum, and hippocampus of the rat." Behav Neural Biol **58**(1): 16-26.
- Jackson, J., C. T. Dickson, et al. (2008). "Median raphe stimulation disrupts hippocampal theta via rapid inhibition and state-dependent phase reset of theta-related neural circuitry." J Neurophysiol **99**(6): 3009-26.
- Jarosiewicz, B., B. L. McNaughton, et al. (2002). "Hippocampal population activity during the small-amplitude irregular activity state in the rat." J Neurosci **22**(4): 1373-84.
- Jarosiewicz, B. and W. E. Skaggs (2004). "Hippocampal place cells are not controlled by visual input during the small irregular activity state in the rat." J Neurosci **24**(21): 5070-7.
- Jarosiewicz, B. and W. E. Skaggs (2004). "Level of arousal during the small irregular activity state in the rat hippocampal EEG." J Neurophysiol **91**(6): 2649-57.
- Jerusalinsky, D., E. Kornisiuk, et al. (1997). "Cholinergic neurotransmission and synaptic plasticity concerning memory processing." Neurochem Res **22**(4): 507-15.
- Jimenez-Capdeville, M. E., R. W. Dykes, et al. (1997). "Differential control of cortical activity by the basal forebrain in rats: a role for both cholinergic and inhibitory influences." J Comp Neurol **381**(1): 53-67.
- Jobert, A., M. H. Bassant, et al. (1989). "Hemicholinium-3 selectively alters the rhythmically bursting activity of septo-hippocampal neurons in the rat." Brain Res **476**(2): 220-9.
- Johnson, M. D., R. K. Franklin, et al. (2008). "Implantable microelectrode arrays for simultaneous electrophysiological and neurochemical recordings." J Neurosci Methods **174**(1): 62-70.
- Jones, B. E. (1993). "The organization of central cholinergic systems and their functional importance in sleep-waking states." Prog Brain Res **98**: 61-71.

- Jones, M. W., M. L. Errington, et al. (2001). "A requirement for the immediate early gene Zif268 in the expression of late LTP and long-term memories." Nature Neuroscience 4(3): 289-296.
- Jouveneau, A., J. M. Billard, et al. (1994). "Cholinergic denervation of the rat hippocampus by 192-IgG-saporin: electrophysiological evidence." Neuroreport 5(14): 1781-4.
- Kahana, M. J., D. Seelig, et al. (2001). "Theta returns." Curr Opin Neurobiol 11(6): 739-44.
- Kamke, M. R., M. Brown, et al. (2005). "Basal forebrain cholinergic input is not essential for lesion-induced plasticity in mature auditory cortex." Neuron 48(4): 675-86.
- Kawagoe, K. T., J. B. Zimmerman, et al. (1993). "Principles of voltammetry and microelectrode surface states." J Neurosci Methods 48(3): 225-40.
- Keita, M. S., L. Frankel-Kohn, et al. (2000). "Acetylcholine release in the hippocampus of the urethane anaesthetised rat positively correlates with both peak theta frequency and relative power in the theta band." Brain Res 887(2): 323-34.
- Kelly, M. P. and S. A. Deadwyler (2002). "Acquisition of a novel behavior induces higher levels of Arc mRNA than does overtrained performance." Neuroscience 110(4): 617-26.
- Khateb, A., M. Muhlethaler, et al. (1992). "Cholinergic nucleus basalis neurons display the capacity for rhythmic bursting activity mediated by low-threshold calcium spikes." Neuroscience 51(3): 489-94.
- Kilgard, M. P. and M. M. Merzenich (1998). "Cortical map reorganization enabled by nucleus basalis activity." Science 279(5357): 1714-8.
- Kimura, F. (2000). "Cholinergic modulation of cortical function: a hypothetical role in shifting the dynamics in cortical network." Neurosci Res 38(1): 19-26.
- King, C., M. Recce, et al. (1998). "The rhythmicity of cells of the medial septum/diagonal band of Broca in the awake freely moving rat: relationships with behaviour and hippocampal theta." Eur J Neurosci 10(2): 464-77.
- Kirby, B. P. and J. N. Rawlins (2003). "The role of the septo-hippocampal cholinergic projection in T-maze rewarded alternation." Behav Brain Res 143(1): 41-8.

- Kiss, J., A. J. Patel, et al. (1990). "Distribution of septohippocampal neurons containing parvalbumin or choline acetyltransferase in the rat brain." J Comp Neurol **298**(3): 362-72.
- Kissinger, P. T., J. B. Hart, et al. (1973). "Voltammetry in brain tissue--a new neurophysiological measurement." Brain Res **55**(1): 209-13.
- Kitchigina, V. F., E. V. Kutyreva, et al. (2003). "Modulation of theta rhythmicity in the medial septal neurons and the hippocampal electroencephalogram in the awake rabbit via actions at noradrenergic alpha2-receptors." Neuroscience **120**(2): 509-21.
- Kohler, C., V. Chan-Palay, et al. (1984). "Septal neurons containing glutamic acid decarboxylase immunoreactivity project to the hippocampal region in the rat brain." Anat Embryol (Berl) **169**(1): 41-4.
- Konopacki, J., M. B. MacIver, et al. (1987). "Carbachol-induced EEG 'theta' activity in hippocampal brain slices." Brain Res **405**(1): 196-8.
- Kopf, S. R., M. L. Buchholzer, et al. (2001). "Glucose plus choline improve passive avoidance behaviour and increase hippocampal acetylcholine release in mice." Neuroscience **103**(2): 365-71.
- Kramis, R., C. H. Vanderwolf, et al. (1975). "Two types of hippocampal rhythmical slow activity in both the rabbit and the rat: relations to behavior and effects of atropine, diethyl ether, urethane, and pentobarbital." Exp Neurol **49**(1 Pt 1): 58-85.
- Kuhr, W. G., R. M. Wightman, et al. (1987). "Dopaminergic neurons: simultaneous measurements of dopamine release and single-unit activity during stimulation of the medial forebrain bundle." Brain Res **418**(1): 122-8.
- Lamour, Y., P. Dutar, et al. (1984). "Septo-hippocampal and other medial septum-diagonal band neurons: electrophysiological and pharmacological properties." Brain Res **309**(2): 227-39.
- Lanzafame, A. A., A. Christopoulos, et al. (2003). "Cellular signaling mechanisms for muscarinic acetylcholine receptors." Receptors Channels **9**(4): 241-60.
- Larson, J., D. Wong, et al. (1986). "Patterned stimulation at the theta frequency is optimal for the induction of hippocampal long-term potentiation." Brain Res **368**(2): 347-50.

- Lee, M. G., J. J. Chrobak, et al. (1994). "Hippocampal theta activity following selective lesion of the septal cholinergic system." Neuroscience **62**(4): 1033-47.
- Lee, M. G., O. K. Hassani, et al. (2005). "Cholinergic basal forebrain neurons burst with theta during waking and paradoxical sleep." J Neurosci **25**(17): 4365-9.
- Lehmann, O., A. J. Grottick, et al. (2003). "A double dissociation between serial reaction time and radial maze performance in rats subjected to 192 IgG-saporin lesions of the nucleus basalis and/or the septal region." Eur J Neurosci **18**(3): 651-66.
- Lena, C., D. Popa, et al. (2004). "Beta2-containing nicotinic receptors contribute to the organization of sleep and regulate putative micro-arousals in mice." J Neurosci **24**(25): 5711-8.
- Leung, L. S., L. A. Martin, et al. (1994). "Hippocampal theta rhythm in behaving rats following ibotenic acid lesion of the septum." Hippocampus **4**(2): 136-47.
- Leung, L. S., B. Shen, et al. (2003). "Cholinergic activity enhances hippocampal long-term potentiation in CA1 during walking in rats." J Neurosci **23**(28): 9297-304.
- Levy, A., R. M. Kong, et al. (1991). "Nimodipine improves spatial working memory and elevates hippocampal acetylcholine in young rats." Pharmacol Biochem Behav **39**(3): 781-6.
- Lewis, P. R., C. C. Shute, et al. (1967). "Confirmation from choline acetylase analyses of a massive cholinergic innervation to the rat hippocampus." J Physiol **191**(1): 215-24.
- Lin, S. C. and M. A. Nicolelis (2008). "Neuronal ensemble bursting in the basal forebrain encodes salience irrespective of valence." Neuron **59**(1): 138-49.
- Lockman, P. R. and D. D. Allen (2002). "The transport of choline." Drug Dev Ind Pharm **28**(7): 749-71.
- Luiten, P. G., R. P. Gaykema, et al. (1987). "Cortical projection patterns of magnocellular basal nucleus subdivisions as revealed by anterogradely transported Phaseolus vulgaris leucoagglutinin." Brain Res **413**(2): 229-50.
- Lyford, G. L., K. Yamagata, et al. (1995). "Arc, a growth factor and activity-regulated gene, encodes a novel cytoskeleton-associated protein that is enriched in neuronal dendrites." Neuron **14**(2): 433-45.

- Lysakowski, A., B. H. Wainer, et al. (1989). "An atlas of the regional and laminar distribution of choline acetyltransferase immunoreactivity in rat cerebral cortex." Neuroscience **28**(2): 291-336.
- Ma, L., M. Seager, et al. (2009). "Selective activation of the M1 muscarinic acetylcholine receptor achieved by allosteric potentiation." Proc Natl Acad Sci U S A.
- Macadar, O., J. A. Roig, et al. (1970). "The functional relationship between septal and hippocampal unit activity and hippocampal theta rhythm." Physiol Behav **5**(12): 1443-9.
- Mahut, H. (1972). "A selective spatial deficit in monkeys after transection of the fornix." Neuropsychologia **10**(1): 65-74.
- Markram, H. and M. Segal (1990). "Electrophysiological characteristics of cholinergic and non-cholinergic neurons in the rat medial septum-diagonal band complex." Brain Res **513**(1): 171-4.
- Marrosu, F., C. Portas, et al. (1995). "Microdialysis measurement of cortical and hippocampal acetylcholine release during sleep-wake cycle in freely moving cats." Brain Res **671**(2): 329-32.
- Martin, S. J., P. D. Grimwood, et al. (2000). "Synaptic plasticity and memory: an evaluation of the hypothesis." Annu Rev Neurosci **23**: 649-711.
- McGaughy, J., J. W. Dalley, et al. (2002). "Selective behavioral and neurochemical effects of cholinergic lesions produced by intrabasis infusions of 192 IgG-saporin on attentional performance in a five-choice serial reaction time task." J Neurosci **22**(5): 1905-13.
- McIntyre, C. K., L. K. Marriott, et al. (2003). "Cooperation between memory systems: acetylcholine release in the amygdala correlates positively with performance on a hippocampus-dependent task." Behav Neurosci **117**(2): 320-6.
- McIntyre, C. K., T. Miyashita, et al. (2005). "Memory-influencing intra-basolateral amygdala drug infusions modulate expression of Arc protein in the hippocampus." Proc Natl Acad Sci U S A **102**(30): 10718-23.
- McMahan, R. W., T. J. Sobel, et al. (1997). "Selective immunolesions of hippocampal cholinergic input fail to impair spatial working memory." Hippocampus **7**(2): 130-6.

- Mechawar, N., C. Cozzari, et al. (2000). "Cholinergic innervation in adult rat cerebral cortex: a quantitative immunocytochemical description." J Comp Neurol **428**(2): 305-18.
- Megias, M., Z. Emri, et al. (2001). "Total number and distribution of inhibitory and excitatory synapses on hippocampal CA1 pyramidal cells." Neuroscience **102**(3): 527-40.
- Mesulam, M. (2004). "The cholinergic lesion of Alzheimer's disease: pivotal factor or side show?" Learn Mem **11**(1): 43-9.
- Mesulam, M. M., E. J. Mufson, et al. (1983). "Central cholinergic pathways in the rat: an overview based on an alternative nomenclature (Ch1-Ch6)." Neuroscience **10**(4): 1185-201.
- Miller, C. L. and R. Freedman (1993). "Medial septal neuron activity in relation to an auditory sensory gating paradigm." Neuroscience **55**(2): 373-80.
- Milner, B., L. R. Squire, et al. (1998). "Cognitive neuroscience and the study of memory." Neuron **20**(3): 445-68.
- Mitchell, S. J., J. N. Rawlins, et al. (1982). "Medial septal area lesions disrupt theta rhythm and cholinergic staining in medial entorhinal cortex and produce impaired radial arm maze behavior in rats." J Neurosci **2**(3): 292-302.
- Mitra, P. B., H. (2007). Observed Brain Dynamics, Oxford University Press, USA
- Miyamoto, E. (2006). "Molecular mechanism of neuronal plasticity: induction and maintenance of long-term potentiation in the hippocampus." J Pharmacol Sci **100**(5): 433-42.
- Miyashita, T., S. Kubik, et al. (2009). "Rapid activation of plasticity-associated gene transcription in hippocampal neurons provides a mechanism for encoding of one-trial experience." J Neurosci **29**(4): 898-906.
- Miyashita, T., S. Kubik, et al. (2008). "Networks of neurons, networks of genes: an integrated view of memory consolidation." Neurobiol Learn Mem **89**(3): 269-84.
- Mizumori, S. J., C. A. Barnes, et al. (1989). "Reversible inactivation of the medial septum: selective effects on the spontaneous unit activity of different hippocampal cell types." Brain Res **500**(1-2): 99-106.

- Mizumori, S. J., G. M. Perez, et al. (1990). "Reversible inactivation of the medial septum differentially affects two forms of learning in rats." Brain Res **528**(1): 12-20.
- Monmaur, P. (1982). "Hippocampal theta rhythms from CA1 and dentate generators during paradoxical sleep of the rat: differential alterations after septal lesion." Physiol Behav **28**(3): 467-71.
- Monmaur, P. and P. Breton (1991). "Elicitation of hippocampal theta by intraseptal carbachol injection in freely moving rats." Brain Res **544**(1): 150-5.
- Monmaur, P., A. Collet, et al. (1997). "Relations between acetylcholine release and electrophysiological characteristics of theta rhythm: a microdialysis study in the urethane-anesthetized rat hippocampus." Brain Res Bull **42**(2): 141-6.
- Montag-Sallaz, M. and D. Montag (2003). "Learning-induced arg 3.1/arc mRNA expression in the mouse brain." Learn Mem **10**(2): 99-107.
- Morales, F. R., J. A. Roig, et al. (1971). "Septal unit activity and hippocampal EEG during the sleep-wakefulness cycle of the rat." Physiol Behav **6**(5): 563-7.
- Morris, R. G. (2003). "Long-term potentiation and memory." Philos Trans R Soc Lond B Biol Sci **358**(1432): 643-7.
- Murphy, L. O. and J. Blenis (2006). "MAPK signal specificity: the right place at the right time." Trends Biochem Sci **31**(5): 268-75.
- Musizza, B., A. Stefanovska, et al. (2007). "Interactions between cardiac, respiratory and EEG-delta oscillations in rats during anaesthesia." J Physiol **580**(Pt 1): 315-26.
- Nava, F., G. Carta, et al. (2000). "D(2) dopamine receptors enable delta(9)-tetrahydrocannabinol induced memory impairment and reduction of hippocampal extracellular acetylcholine concentration." Br J Pharmacol **130**(6): 1201-10.
- Nelson, M. J., P. Pouget, et al. (2008). "Review of signal distortion through metal microelectrode recording circuits and filters." J Neurosci Methods **169**(1): 141-57.
- Nicholls, J. G. M., A. R., Wallace, B.G. and P. A. Fuchs (2001). From Neuron To Brain. Sunderland, MA, Sinauer Associates, Inc.
- Nicolelis, M. A., D. Dimitrov, et al. (2003). "Chronic, multisite, multielectrode recordings in macaque monkeys." Proc Natl Acad Sci U S A **100**(19): 11041-6.

- Nicolelis, M. A., A. A. Ghazanfar, et al. (1997). "Reconstructing the engram: simultaneous, multisite, many single neuron recordings." Neuron **18**(4): 529-37.
- Nyakas, C., P. G. Luiten, et al. (1987). "Detailed projection patterns of septal and diagonal band efferents to the hippocampus in the rat with emphasis on innervation of CA1 and dentate gyrus." Brain Res Bull **18**(4): 533-45.
- Olariu, A., M. H. Tran, et al. (2001). "Memory deficits and increased emotionality induced by beta-amyloid (25-35) are correlated with the reduced acetylcholine release and altered phorbol dibutyrate binding in the hippocampus." J Neural Transm **108**(8-9): 1065-79.
- Origlia, N., N. Kuczewski, et al. (2008). "The role of cholinergic system in neuronal plasticity: focus on visual cortex and muscarinic receptors." Arch Ital Biol **146**(3-4): 165-88.
- Pang, K. C., R. Nocera, et al. (2001). "GABAergic septohippocampal neurons are not necessary for spatial memory." Hippocampus **11**(6): 814-27.
- Parent, M. B. and M. G. Baxter (2004). "Septohippocampal acetylcholine: involved in but not necessary for learning and memory?" Learn Mem **11**(1): 9-20.
- Parikh, V., R. Kozak, et al. (2007). "Prefrontal acetylcholine release controls cue detection on multiple timescales." Neuron **56**(1): 141-54.
- Parikh, V., F. Pomerleau, et al. (2004). "Rapid assessment of in vivo cholinergic transmission by amperometric detection of changes in extracellular choline levels." Eur J Neurosci **20**(6): 1545-54.
- Parikh, V. and M. Sarter (2006). "Cortical choline transporter function measured in vivo using choline-sensitive microelectrodes: clearance of endogenous and exogenous choline and effects of removal of cholinergic terminals." J Neurochem **97**(2): 488-503.
- Passetti, F., J. W. Dalley, et al. (2000). "Increased acetylcholine release in the rat medial prefrontal cortex during performance of a visual attentional task." Eur J Neurosci **12**(8): 3051-8.
- Pavlidis, C., Y. J. Greenstein, et al. (1988). "Long-term potentiation in the dentate gyrus is induced preferentially on the positive phase of theta-rhythm." Brain Res **439**(1-2): 383-7.

- Paxinos, G. and C. Watson (2005). **The rat brain in stereotaxic coordinates**. San Diego, Elsevier Academic Press.
- Pazzagli, A. and G. Pepeu (1965). "Amnesic properties of scopolamine and brain acetylcholine in the rat." Int J Neuropharmacol **4**(5): 291-9.
- Penttonen, M., N. Nurminen, et al. (1999). "Ultra-slow oscillation (0.025 Hz) triggers hippocampal afterdischarges in Wistar rats." Neuroscience **94**(3): 735-43.
- Pepeu, G. and M. G. Giovannini (2004). "Changes in acetylcholine extracellular levels during cognitive processes." Learn Mem **11**(1): 21-7.
- Perry, E., M. Walker, et al. (1999). "Acetylcholine in mind: a neurotransmitter correlate of consciousness?" Trends Neurosci **22**(6): 273-80.
- Petsche, H., C. Stumpf, et al. (1962). "[The significance of the rabbit's septum as a relay station between the midbrain and the hippocampus. I. The control of hippocampus arousal activity by the septum cells.]." Electroencephalogr Clin Neurophysiol **14**: 202-11.
- Pinaud, R., M. R. Penner, et al. (2001). "Upregulation of the immediate early gene arc in the brains of rats exposed to environmental enrichment: implications for molecular plasticity." Brain Res Mol Brain Res **91**(1-2): 50-6.
- Pizzo, D. P., L. J. Thal, et al. (2002). "Mnemonic deficits in animals depend upon the degree of cholinergic deficit and task complexity." Exp Neurol **177**(1): 292-305.
- Pizzo, D. P., J. J. Waite, et al. (1999). "Intraparenchymal infusions of 192 IgG-saporin: development of a method for selective and discrete lesioning of cholinergic basal forebrain nuclei." J Neurosci Methods **91**(1-2): 9-19.
- Plath, N., O. Ohana, et al. (2006). "Arc/Arg3.1 is essential for the consolidation of synaptic plasticity and memories." Neuron **52**(3): 437-44.
- Power, A. E. (2004). "Muscarinic cholinergic contribution to memory consolidation: with attention to involvement of the basolateral amygdala." Curr Med Chem **11**(8): 987-96.
- Power AE, V. A., McGaugh JL. (2003). "Muscarinic cholinergic influences in memory consolidation." Neurobiol Learn Mem. **80**(3): 178-93.
- Power, A. E., A. Vazdarjanova, et al. (2003). "Muscarinic cholinergic influences in memory consolidation." Neurobiol Learn Mem **80**(3): 178-93.

- Purves, D., G. J. Augustine, et al., Eds. (2004). Neuroscience. Sunderland, MA, Sinauer Associates, Inc. .
- Pych, J. C., Q. Chang, et al. (2005). "Acetylcholine release in hippocampus and striatum during testing on a rewarded spontaneous alternation task." Neurobiol Learn Mem **84**(2): 93-101.
- Quirk, G. J., C. Repa, et al. (1995). "Fear conditioning enhances short-latency auditory responses of lateral amygdala neurons: parallel recordings in the freely behaving rat." Neuron **15**(5): 1029-39.
- Ragozzino, M. E. and P. E. Gold (1995). "Glucose injections into the medial septum reverse the effects of intraseptal morphine infusions on hippocampal acetylcholine output and memory." Neuroscience **68**(4): 981-8.
- Ramanathan, D., M. H. Tuszynski, et al. (2009). "The basal forebrain cholinergic system is required specifically for behaviorally mediated cortical map plasticity." J Neurosci **29**(18): 5992-6000.
- Ribeiro, S., V. Goyal, et al. (1999). "Brain gene expression during REM sleep depends on prior waking experience." Learn Mem **6**(5): 500-8.
- Ribeiro, S., C. V. Mello, et al. (2002). "Induction of hippocampal long-term potentiation during waking leads to increased extrahippocampal zif-268 expression during ensuing rapid-eye-movement sleep." J Neurosci **22**(24): 10914-23.
- Ribeiro, S., X. Shi, et al. (2007). "Novel Experience Induces Persistent Sleep-Dependent Plasticity in the Cortex but not in the Hippocampus." Front Neurosci **1**(1): 43-55.
- Robinson, D. (1968). "The electrical properties of metal microelectrodes." Proceedings of the IEEE **56**(6): 1065-71.
- Robinson, D. L., B. J. Venton, et al. (2003). "Detecting subsecond dopamine release with fast-scan cyclic voltammetry in vivo." Clin Chem **49**(10): 1763-73.
- Rosenblum, K., M. Futter, et al. (2000). "ERK1/II regulation by the muscarinic acetylcholine receptors in neurons." J Neurosci **20**(3): 977-85.
- Rutherford, E. C., F. Pomerleau, et al. (2007). "Chronic second-by-second measures of L-glutamate in the central nervous system of freely moving rats." J Neurochem **102**(3): 712-22.

- Sachdev, R. N., S. M. Lu, et al. (1998). "Role of the basal forebrain cholinergic projection in somatosensory cortical plasticity." J Neurophysiol **79**(6): 3216-28.
- Safer, D. J. and R. P. Allen (1971). "The central effects of scopolamine in man." Biol Psychiatry **3**(4): 347-55.
- Sammut, S., D. J. Park, et al. (2007). "Frontal cortical afferents facilitate striatal nitric oxide transmission in vivo via a NMDA receptor and neuronal NOS-dependent mechanism." J Neurochem **103**(3): 1145-56.
- Sarter, M. and J. P. Bruno (2000). "Cortical cholinergic inputs mediating arousal, attentional processing and dreaming: differential afferent regulation of the basal forebrain by telencephalic and brainstem afferents." Neuroscience **95**(4): 933-52.
- Sarter, M., B. Givens, et al. (2001). "The cognitive neuroscience of sustained attention: where top-down meets bottom-up." Brain Res Brain Res Rev **35**(2): 146-60.
- Sarter, M., M. E. Hasselmo, et al. (2005). "Unraveling the attentional functions of cortical cholinergic inputs: interactions between signal-driven and cognitive modulation of signal detection." Brain Res Brain Res Rev **48**(1): 98-111.
- Scali, C., M. G. Giovannini, et al. (1997). "Effect of metrifonate on extracellular brain acetylcholine and object recognition in aged rats." Eur J Pharmacol **325**(2-3): 173-80.
- Scali, C., M. G. Giovannini, et al. (1997). "Tacrine administration enhances extracellular acetylcholine in vivo and restores the cognitive impairment in aged rats." Pharmacol Res **36**(6): 463-9.
- Scarlett, D., A. T. Dypvik, et al. (2004). "Comparison of spontaneous and septally driven hippocampal theta field and theta-related cellular activity." Hippocampus **14**(1): 99-106.
- Schultz, W. (2007). "Multiple dopamine functions at different time courses." Annu Rev Neurosci **30**: 259-88.
- Segal, M. and J. M. Auerbach (1997). "Muscarinic receptors involved in hippocampal plasticity." Life Sci **60**(13-14): 1085-91.
- Serafin, M., S. Williams, et al. (1996). "Rhythmic firing of medial septum non-cholinergic neurons." Neuroscience **75**(3): 671-5.

- Shen, J., C. A. Barnes, et al. (1996). "Differential effects of selective immunotoxic lesions of medial septal cholinergic cells on spatial working and reference memory." Behav Neurosci **110**(5): 1181-6.
- Sheth, A., S. Berretta, et al. (2008). "The amygdala modulates neuronal activation in the hippocampus in response to spatial novelty." Hippocampus **18**(2): 169-81.
- Siegel, J. M. (2001). "The REM sleep-memory consolidation hypothesis." Science **294**(5544): 1058-63.
- Simon, A. P., F. Poindessous-Jazat, et al. (2006). "Firing properties of anatomically identified neurons in the medial septum of anesthetized and unanesthetized restrained rats." J Neurosci **26**(35): 9038-46.
- Siok, C. J., J. A. Rogers, et al. (2006). "Activation of alpha7 acetylcholine receptors augments stimulation-induced hippocampal theta oscillation." Eur J Neurosci **23**(2): 570-4.
- Smythe, J. W., L. V. Colom, et al. (1992). "The extrinsic modulation of hippocampal theta depends on the coactivation of cholinergic and GABA-ergic medial septal inputs." Neurosci Biobehav Rev **16**(3): 289-308.
- Sotty, F., M. Danik, et al. (2003). "Distinct electrophysiological properties of glutamatergic, cholinergic and GABAergic rat septohippocampal neurons: novel implications for hippocampal rhythmicity." J Physiol **551**(Pt 3): 927-43.
- Staiger, J. F., S. Bisler, et al. (2000). "Exploration of a novel environment leads to the expression of inducible transcription factors in barrel-related columns." Neuroscience **99**(1): 7-16.
- Stamford, J. A. (1985). "In vivo voltammetry: promise and perspective." Brain Res **357**(2): 119-35.
- Stamford, J. A., P. Palij, et al. (1993). "Simultaneous "real-time" electrochemical and electrophysiological recording in brain slices with a single carbon-fibre microelectrode." J Neurosci Methods **50**(3): 279-90.
- Stancampiano, R., S. Cocco, et al. (1999). "Serotonin and acetylcholine release response in the rat hippocampus during a spatial memory task." Neuroscience **89**(4): 1135-43.

- Steckler, T., A. B. Keith, et al. (1995). "Cholinergic lesions by 192 IgG-saporin and short-term recognition memory: role of the septohippocampal projection." Neuroscience **66**(1): 101-14.
- Steriade, M. (2004). "Acetylcholine systems and rhythmic activities during the waking--sleep cycle." Prog Brain Res **145**: 179-96.
- Stewart, M. and S. E. Fox (1989). "Firing relations of medial septal neurons to the hippocampal theta rhythm in urethane anesthetized rats." Exp Brain Res **77**(3): 507-16.
- Stewart, M. and S. E. Fox (1989). "Two populations of rhythmically bursting neurons in rat medial septum are revealed by atropine." J Neurophysiol **61**(5): 982-93.
- Stumpf, C., H. Petsche, et al. (1962). "The significance of the rabbit's septum as a relay station between the midbrain and the hippocampus. II. The differential influence of drugs upon both the septal cell firing pattern and the hippocampus theta activity." Electroencephalogr Clin Neurophysiol **14**: 212-9.
- Teber, I., R. Kohling, et al. (2004). "Muscarinic acetylcholine receptor stimulation induces expression of the activity-regulated cytoskeleton-associated gene (ARC)." Brain Res Mol Brain Res **121**(1-2): 131-6.
- Torres, E. M., T. A. Perry, et al. (1994). "Behavioural, histochemical and biochemical consequences of selective immunolesions in discrete regions of the basal forebrain cholinergic system." Neuroscience **63**(1): 95-122.
- Trejo, J. and J. H. Brown (1991). "c-fos and c-jun are induced by muscarinic receptor activation of protein kinase C but are differentially regulated by intracellular calcium." J Biol Chem **266**(12): 7876-82.
- Tzingounis, A. V. and R. A. Nicoll (2006). "Arc/Arg3.1: linking gene expression to synaptic plasticity and memory." Neuron **52**(3): 403-7.
- Vanderwolf, C. H. (1969). "Hippocampal electrical activity and voluntary movement in the rat." Electroencephalogr Clin Neurophysiol **26**(4): 407-18.
- Vanderwolf, C. H. (1975). "Neocortical and hippocampal activation relation to behavior: effects of atropine, eserine, phenothiazines, and amphetamine." J Comp Physiol Psychol **88**(1): 300-23.

- Vanderwolf, C. H. (1988). "Cerebral activity and behavior: control by central cholinergic and serotonergic systems." Int Rev Neurobiol **30**: 225-340.
- Vanderwolf, C. H., R. Kramis, et al. (1977). "Hippocampal electrical activity during waking behaviour and sleep: analyses using centrally acting drugs." Ciba Found Symp(58): 199-226.
- Varga, V., B. Hangya, et al. (2008). "The presence of pacemaker HCN channels identifies theta rhythmic GABAergic neurons in the medial septum." J Physiol **586**(16): 3893-915.
- Vazdarjanova, A., B. L. McNaughton, et al. (2002). "Experience-dependent coincident expression of the effector immediate-early genes arc and Homer 1a in hippocampal and neocortical neuronal networks." J Neurosci **22**(23): 10067-71.
- Velasco, P. B. M. J. (2009). "Toolbox for circular statistics with Matlab." from <http://www.mathworks.com/matlabcentral/fileexchange/10676>.
- Vertes, R. P. (2005). "Hippocampal theta rhythm: a tag for short-term memory." Hippocampus **15**(7): 923-35.
- Vertes, R. P. and B. Kocsis (1997). "Brainstem-diencephalo-septohippocampal systems controlling the theta rhythm of the hippocampus." Neuroscience **81**(4): 893-926.
- Viswanathan, A. and R. D. Freeman (2007). "Neurometabolic coupling in cerebral cortex reflects synaptic more than spiking activity." Nat Neurosci **10**(10): 1308-12.
- Volpicelli, L. A. and A. I. Levey (2004). "Muscarinic acetylcholine receptor subtypes in cerebral cortex and hippocampus." Prog Brain Res **145**: 59-66.
- Wada, K., H. Sakaguchi, et al. (2004). "Differential expression of glutamate receptors in avian neural pathways for learned vocalization." J Comp Neurol **476**(1): 44-64.
- Waite, J. J. and A. D. Chen (2001). "Differential changes in rat cholinergic parameters subsequent to immunotoxic lesion of the basal forebrain nuclei." Brain Res **918**(1-2): 113-20.
- Walker, M. P. and R. Stickgold (2004). "Sleep-dependent learning and memory consolidation." Neuron **44**(1): 121-33.
- Warburton, E. C., T. Koder, et al. (2003). "Cholinergic neurotransmission is essential for perirhinal cortical plasticity and recognition memory." Neuron **38**(6): 987-96.

- Weinberger, N. M. (2003). "The nucleus basalis and memory codes: auditory cortical plasticity and the induction of specific, associative behavioral memory." Neurobiol Learn Mem **80**(3): 268-84.
- Wess, J. (2004). "Muscarinic acetylcholine receptor knockout mice: novel phenotypes and clinical implications." Annu Rev Pharmacol Toxicol **44**: 423-50.
- Whishaw, I. Q. (1976). "Neuromuscular blockade: the effects on two hippocampal RSA (theta) systems and neocortical desynchronization." Brain Res Bull **1**(6): 573-81.
- Whitlock, J. R., A. J. Heynen, et al. (2006). "Learning induces long-term potentiation in the hippocampus." Science **313**(5790): 1093-7.
- Wightman, R. M. (2006). "Detection technologies. Probing cellular chemistry in biological systems with microelectrodes." Science **311**(5767): 1570-4.
- Wiley, R. G., T. N. Oeltmann, et al. (1991). "Immunolesioning: selective destruction of neurons using immunotoxin to rat NGF receptor." Brain Res **562**(1): 149-53.
- Williams, G. V. and J. Millar (1990). "Concentration-dependent actions of stimulated dopamine release on neuronal activity in rat striatum." Neuroscience **39**(1): 1-16.
- Winson, J. (1976). "Hippocampal theta rhythm. I. Depth profiles in the curarized rat." Brain Res **103**(1): 57-70.
- Winson, J. (1978). "Loss of hippocampal theta rhythm results in spatial memory deficit in the rat." Science **201**(4351): 160-3.
- Winters, B. D. and T. J. Bussey (2005). "Removal of cholinergic input to perirhinal cortex disrupts object recognition but not spatial working memory in the rat." Eur J Neurosci **21**(8): 2263-70.
- Wirtshafter, D. (2005). "Cholinergic involvement in the cortical and hippocampal Fos expression induced in the rat by placement in a novel environment." Brain Res **1051**(1-2): 57-65.
- Wolansky, T., E. A. Clement, et al. (2006). "Hippocampal slow oscillation: a novel EEG state and its coordination with ongoing neocortical activity." J Neurosci **26**(23): 6213-29.
- Woolf, N. J. (1991). "Cholinergic systems in mammalian brain and spinal cord." Prog Neurobiol **37**(6): 475-524.

- Woolf, N. J. (1996). "Global and serial neurons form A hierarchically arranged interface proposed to underlie memory and cognition." Neuroscience **74**(3): 625-51.
- Woolf, N. J. (1997). "A possible role for cholinergic neurons of the basal forebrain and pontomesencephalon in consciousness." Conscious Cogn **6**(4): 574-96.
- Yoder, R. M. and K. C. Pang (2005). "Involvement of GABAergic and cholinergic medial septal neurons in hippocampal theta rhythm." Hippocampus **15**(3): 381-92.
- Zaborszky, L. (2002). "The modular organization of brain systems. Basal forebrain: the last frontier." Prog Brain Res **136**: 359-72.
- Zaborszky, L., D. L. Buhl, et al. (2005). "Three-dimensional chemoarchitecture of the basal forebrain: spatially specific association of cholinergic and calcium binding protein-containing neurons." Neuroscience **136**(3): 697-713.
- Zhang, F., A. M. Aravanis, et al. (2007). "Circuit-breakers: optical technologies for probing neural signals and systems." Nat Rev Neurosci **8**(8): 577-81.
- Zhang, H., S. C. Lin, et al. (2009). "Acquiring local field potential information from amperometric neurochemical recordings." J Neurosci Methods **179**(2): 191-200.
- Zin, R., N. Conforti, et al. (1977). "Sensory responsiveness of single cells in the medial septal nucleus in intact and hypothalamic-deafferented rats." Exp Neurol **54**(1): 7-23.

Biography

Hao Zhang

Born on March 10, 1981

Suzhou, Jiangsu, P.R.China

Education

1999-2003 B.S. in Life Sciences

Fudan University

2003-2009 Ph.D. in Neurobiology

Duke University

Publications

Zhang H, Lin S, Nicolelis MAL. Fine spatiotemporal coupling between hippocampal acetylcholine release and theta oscillation *in vivo*. (manuscript in preparation)

Zhang H, Lin S, Nicolelis MAL. A subpopulation of slow-firing medial septal neurons promote hippocampal arousal and theta oscillations: implications of putative cholinergic neurons. (manuscript in preparation)

Zhang H, Ribeiro S, Lin S, Nicolelis MAL. Cholinergic modulation promotes immediate-early-gene upregulation induced by novel sensory experience: implication for learning and memory. (manuscript in preparation)

Zhang H, Lin S, Nicolelis MAL. Acquiring local field potential information from amperometric neurochemical recordings. *J. Neuroscience Methods* 179(2):191-200.

Ribeiro S, Shi X, Engelhard M, Zhou Y, **Zhang H**, Gervasoni D, Lin S, Wada K, Lemos N and Nicolelis M (2007) Novel experience induces persistent sleep-dependent plasticity in the cortex but not in the hippocampus. *Front. Neurosci.* 1,1:43-55.

Conference Presentations

Zhang H, Lin S, Nicolelis MAL. Acetylcholine release coupled to theta oscillations on fine spatiotemporal scales *in vivo*. *Soc Neurosci Abst* 35: 193.29, 2009.

Zhang H, Lin S, Nicolelis MAL. Acquiring local field potential (LFP) information with

in vivo amperometry. *Soc Neurosci Abst* 34: 100.5, 2008.

Zhang H, Lin S, Nicolelis MAL. Acquiring local field potential (LFP) information with *in vivo* amperometry. *Integrative approaches to brain complexity*. Cambridge, UK, 2008

Zhang H, Ribeiro S, Lin S, Nicolelis MAL. Cholinergic modulation of cortical and hippocampal *arc* expression induced by novel sensory experience. *Soc Neurosci Abst* 32: 812.12, 2006.

Zhang H, Ribeiro S, Lin S, Gervasoni D, Nicolelis MAL. Influence of local administration of scopolamine on hippocampal local field potentials and neuronal activity in freely behaving rats. *Soc Neurosci Abst* 30:324.14, 2004.

Awards and Membership

2008	Cold Spring Harbor Laboratory / Wellcome Trust Conference (UK) Travel Award
2006	Marine Biological Laboratory Scholarship
2004 -	Society for Neuroscience (Student Member)